Chemical Studies on Medicinal Plants of Guangxi Zhuang Autonomous Region, China

2020

Yang   XueRong

Abbreviations

Ac	acetyl
aq.	aqueous
BuOH	butanol
COSY	correlated spectroscopy
DFT	density functional theory
DMEM	Dulbecco's modified eagle medium
DMSO	dimethyl sulfoxide
2D NMR	two dimensional nuclear magnetic resonance
ECD	electronic circular dichroism
EtOAc	ethyl acetate
ext.	extract
FBS	fetal bovine serum
fr.	fraction
GPC	gel permeation chromatography
HCl	hydrochloric acid
HMBC	heteronuclear multiple bond correlation
HPLC	high performance liquid chromatography
HRESIMS	high resolution electrospray ionisation mass spectrometry
IR	infrared spectroscopy
J	coupling constant
Me	methyl
MeOH	methanol
mmu	milli mass unit
n-	normal
NMR	nuclear magnetic resonance
NOESY	nuclear Overhauser effect spectroscopy
ODS	octadecylsilyl
OMe	methoxy
ROESY	rotating frame nuclear Overhauser effect spectroscopy
TDDFT	time dependent density functional theory
Tig	tigloyl
UV	ultraviolet

General Introduction

Medicinal plants, used for the treatments of various human disorders in traditional medicines such as traditional Chinese medicine, Kampo medicine, traditional Korean medicine, Ayurveda, and Unani, have been developed over many generations within respective societies. Up to now, traditional medicines have been used in approximately 85–90% of the world's population. The survey by World Health Organization (WHO) showed that 75% of the population in France, 30% of the population in Vietnam, and 40% of the population in Indonesia use their traditional medicines [1]. In China, 910 million people visit to the hospitals of traditional Chinese medicine, while 27 million inpatients are treated by traditional Chinese medicine [2]. Meanwhile, about 84% of physicians use Kampo medicine in daily practice in Japan [3].

Among remedies used in above mentioned traditional medicines, medicinal plants have occupied an important position for thousands of years, and have been generating huge interest among researchers due to their specialized metabolites possessing diverse structures and biological activities. With the dramatic development of scientific technologies, a variety of chemical entities derived from medicinal plants have been forming the backbone of new therapeutic agents (Table 1). Artemisinin is an antimalarial agent discovered from a Chinese traditional herbal medicine *Ar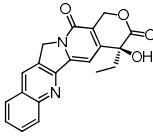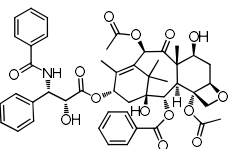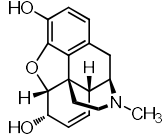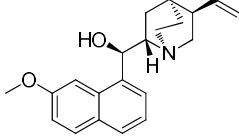temisia annua* by Tu Youyou, a laureate of 2015 Nobel Prize in Physiology or Medicine [4,5]. Thus, medicinal plants have been regarded as a significant resource for discovering new therapeutic agents and their lead compounds.

In our continuing search for specialized metabolites from medicinal plants used in various parts of the world including Japan, Uzbekistan, Mongolia, and China, we have been studying on medicinal plants of Guangxi Zhuang Autonomous Region, China. In this study, chemical constituents of five medicinal plants collected at Guangxi (*Munronia pinnata*, *Sarcandra glabra*, *Rhododendron Molle*, *Phyllanthus urinaria*, and *Macrosolen cochinchinensis*) were investigated to give new specialized metabolites, whose chemical structures were assigned on the basis of detailed spectroscopic analyses.

Table 1. Medicine plants derived natural products approved for therapeutic agent.

Medicinal plants	Drugs	Chemical Structures	Application or effects
Artemisia annua	artemisinin		antimalarial [5]
Hyoscyamus niger	(-)-hyoscyamine		muscarinic antagonist [6]
Ephedra sinica	(-)-ephedrine		adrenoceptor agonist [7]
Camptotheca acuminata	camtothecin		anticancer [8]
Taxus brevifolia	taxol		anticancer [9]
Papaver somniferum	morphine		analgesic [10]
Cinchona officinalis	quinine		antimalarial [11]

Chapter 1 Medicinal plants of Guangxi Zhuang autonomous region, China

Guangxi Zhuang autonomous region is located at southwest of China, where twelve long-dwell ethnic minority groups are living. Guangxi has unique natural conditions of karst landform (limestone area) under subtropical to tropical climate. More than 8,000 plant species including about 800 endemic species are grown in Guangxi [12].

Most of ethnic minority groups in China have developed their own traditional medicines based on their various experiences of medicinal knowledge from their unique natural conditions and customs [13]. Zhuang and Yao are two major minority groups in Guangxi. Their traditional medicines, Zhuang and Yao medicines, respectively, possessing over thousand years' history, have been mainly used for the treatments of rheumatism, snakebite, malaria, cold, cancers, and skin problems. Approximately 4,000 medicinal plant species are seen in Guangxi, accounting for more than one third of Chinese medicinal plant resources. Moreover, around 500 medicinal plants have been used as remedial agents in Zhuang medicine, while over 400 ones have been used in Yao medicine. These medicinal plants were selected mainly based on local flora, most of which were collected from the wild ecosystems [13−16].

Thus, Guangxi has rich resource of medicinal plants widely used in traditional medicines. Although some interesting bioactive natural products have been isolated from medicinal plants used in Guangxi, most of them still remain to be investigated for clarifying their biologically active constituents.
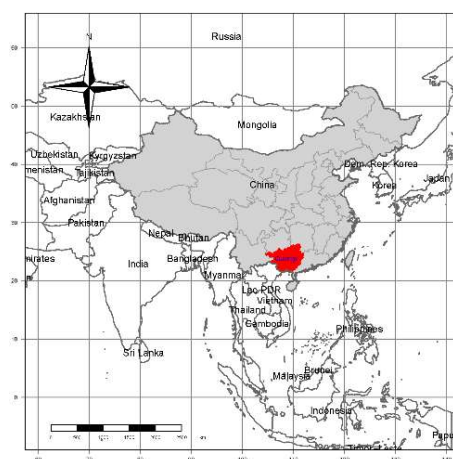
Figure 1.1. Guangxi Zhuang autonomous region (red colored).

Chapter 2 Chemical study on *Munronia pinnata* (Wall.) W. Theob.

2.1   Introduction

The genus *Munronia* (Meliaceae) are perennial herbs widely distributed in China, Sri Lanka, India, Indonesia, and the Philippines. *Munronia* plants are recognized as a rich source of limonoids with various carbon skeletons such as vilasinin, havanensin, azadirone, evodulone, nimbolinin, and prieurinin type skeletons (Figure 2.2). These limonoids exhibit a wide spectrum of biological activities including antiproliferative, antiviral, and antifungal activities [17-24].

Munronia pinnata (Wall.) W. Theob. (synonyms: *M. henryi* Harms, *M. pumila* Wight, and *M. sinica* Diels) is a small hardy and perennial herb mainly distributed in dry and savannah areas in Guangxi (Figure 2.1). This plant has been used as a traditional remedy for the treatments of tuberculosis, cough, stomachache, and sores in China. More than fifty limonoids with various skeletons such as aphanamixoid, prieurinin, nimbolinin, and evodulone type limonoids have been isolated from this species so far (Figure 2.2) [25,26]. In this study, the aerial parts of *M. pinnata* collected at Guangxi were investigated.

Figure 2.1. *Munronia pinnata* (Wall.) W. Theob.
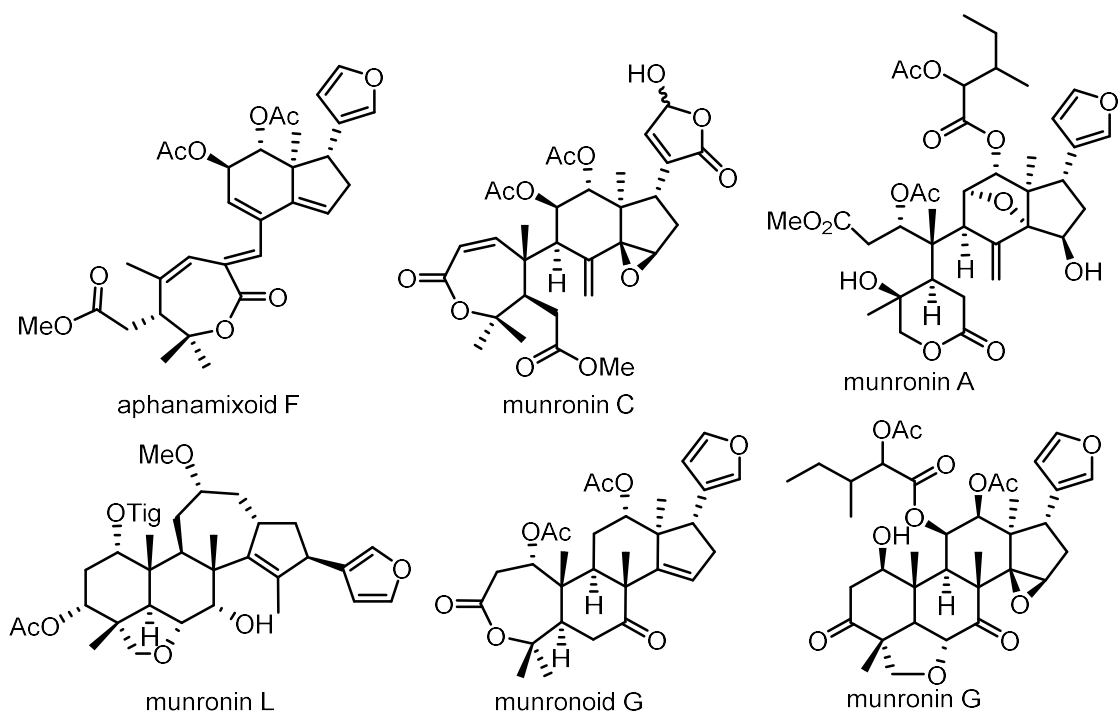
Figure 2.2. Previously isolated limonoids from *Munronia pinnata*.

2.2 Extraction and isolation

The aerial parts of *M. pinnata* (1.4 kg, dry) collected at Guangxi were air-dried and extracted with MeOH in room temperature. The MeOH extract (298 g) was partitioned between EtOAc and H_2O. Repeated chromatographic separations of the EtOAc-soluble material (116.5 g) gave nine new limonoids, munropins A–I (**1–9**), and 12 known compounds (**10–21**) (Scheme 1).

the aerial parts of *M. pinnata* (1.4 kg, dry)

| extracted with MeOH

MeOH ext. (298 g)

| partitioned between EtOAc/H$_2$O

EtOAc (116.5 g)   H$_2$O (171.5 g)

a. silica gel (*n*-hexane /EtOAc)
b. MCI gel CHP-20P (MeOH/H$_2$O)
c. GPC on HPLC (MeOH)
d. silica gel (CHCl$_3$/MeOH)
e. ODS on HPLC (MeCN/H$_2$O)

new limonoids

1 (8.4 mg)
2 (8.6 mg)
3 (2.5 mg)
4 (2.2 mg)
5 (1.5 mg)
6 (3.9 mg)
7 (2.5 mg)
8 (2.3 mg)
9 (2.2 mg)

known compounds

10 (52.5 g)	**16** (3.2 mg)
11 (45.5 mg)	**17** (25.6 mg)
12 (1.5 mg)	**18** (8.0 mg)
13 (22.0 mg)	**19** (12.3 mg)
14 (13.1 mg)	**20** (4.9 mg)
15 (11.8 mg)	**21** (9.9 mg)

Scheme 1. Isolation procedure for compounds **1**–**21**.

By comparison of spectroscopic data with the literature data, known compounds (Figure 2.3) were identified to be three limonoids, munronins C (**10**) and F (**11**) [18], and munronoid O (**12**) [27]; two diterpenes, (−)-sandaracopimaradiene (**13**) [28] and methyl-ent-4-epi-agath-18-oate (**14**) [29]; three triterpenes, piscidinol B (**15**) [30], bourjotinolone A (**16**) [31], and lanost-7-ene-3,24,25-triol (**17**) [32]; four steroids, 2β,3β,4β-trihydroxypregna-16-one (**18**) [33], 7-oxo-stigmasterol (**19**) [34], 5α,8α-epidioxy-24ξ-methylcholesta-6,22-dien-3β-ol (**20**) [35], and stigmast-4-ene-3β,6α-diol (**21**) [36].
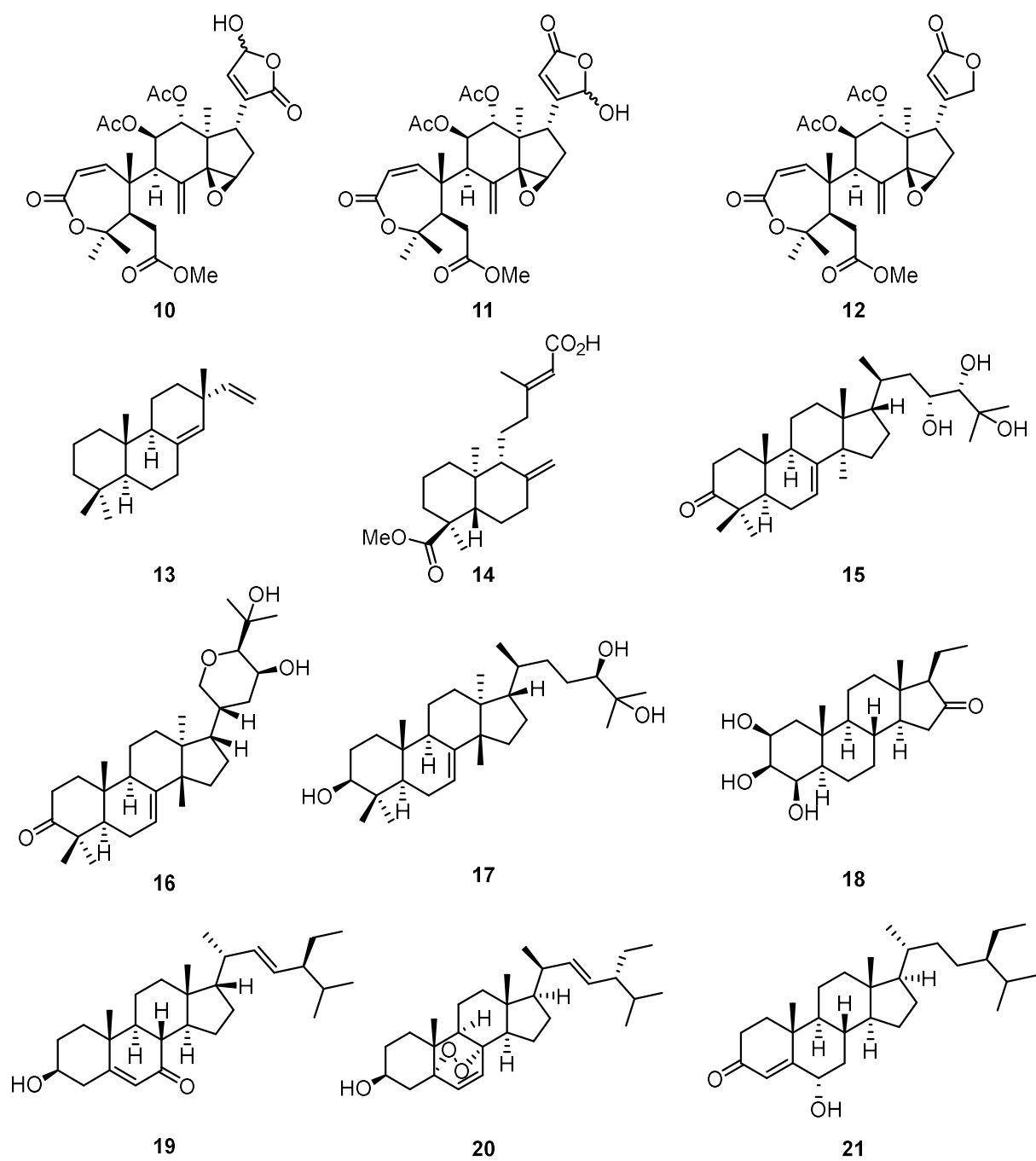
Figure 2.3. Known compounds (**10–21**) isolated from the aerial parts of *M. pinnata* in this study.

2.3 Structure elucidation of new limonoids

2.3.1 Munropins A (**1**) and B (**2**)

Munropin A (**1**), obtained as an optically active colorless amorphous solid {$[\alpha]_D^{21}$ +82 (*c* 0.10, MeOH)}, showed a sodiated molecular ion at *m/z* 608.2493 ([M+Na]$^+$, Δ +2.1 mmu) in the HRESIMS, suggesting the molecular formula of **1** to be $C_{31}H_{39}NO_{10}$. The IR spectrum displayed absorptions at 1748 and 1689 cm^{-1} due to carbonyl functionalities. The ^{1}H NMR spectrum (Figure 2.4 and Table 2.1) showed the resonances due to one trisubstituted olefin, one 1,1-disubstituted olefin, one 1,2-disubstituted olefin, six sp^3 methines, three sp^3 methylenes, and seven singlet methyls including two acetyl and one methoxy methyls. The ^{13}C NMR spectrum exhibited 31 signals including five ester or amide carbonyl, six olefinic, two oxygenated tertiary, and two quaternary carbon signals (Table 2.1).

Figure 2.4. ^{1}H NMR spectrum of **1** in CDCl$_3$ (500 MHz).

The planar structure of **1** was elucidated by 2D NMR analysis (Figure 2.5). The presence of an α-substituted α,β-unsaturated γ-lactam moiety (C-20–C-23) was revealed by ^{1}H-^{1}H COSY

cross-peaks of H-22/H$_2$-23/23-NH and HMBC correlations for H$_2$-23 with C-21 and H-17 with C-20, C-21, and C-22. This was supported by an IR absorption at 1689 cm^{-1}. The existence of an octahydroind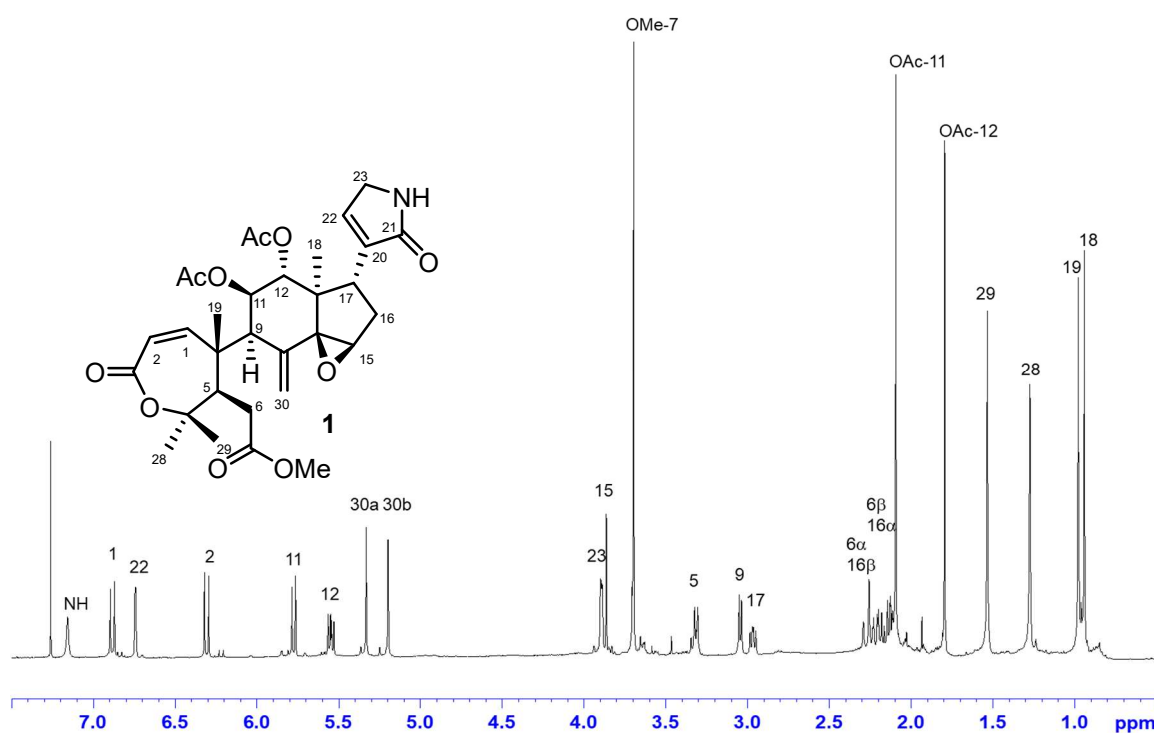ene moiety (C-8, C-9, and C-11–C-17) with a methyl group at C-13 and an exomethylene group at C-8 was indicative of ^{1}H-^{1}H COSY cross-peaks among H-9/H-11/H-12 and H-15/H$_2$-16/H-17, and HMBC correlations for H-15 with C-14, H$_3$-18 with C-12, C-13, C-14, and C-17, and H$_2$-30 with C-8, C-9, and C-14. The chemical shifts of C-14 (δ_C 72.1) and CH-15 (δ_H 3.87; δ_C 60.0) implied the presence of an epoxy group between C-14 and C-15. In the HMBC spectrum, the signals of H-11 and H-12 were correlated with acetoxy carbonyl carbons, respectively, suggesting the presence of acetoxy groups at C-11 and C-12. The structure of an α,β-unsaturated-ε-caprolactone moiety (C-1–C-5 and C-10) with three methyl groups and one methoxy carbonyl methyl group was also assigned by 2D NMR analysis. The degree of unsaturation of **1** supported the presence of the lactone ring. The connectivities among γ-lactam, octahydroindene, and caprolactone moieties were evident from HMBC correlations for H-17 with C-20 and H$_3$-19 with C-9. Therefore, the planer structure of **1** was assigned as shown in Figure 2.4.
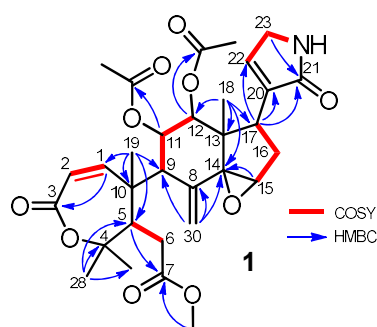
Figure 2.5. Selected ^{1}H-^{1}H COSY and HMBC correlations for **1**.

The relative configuration of **1** was elucidated by analysis of the ROESY spectrum (Figure 2.6). The β-orientations of H-12 and H-17 and the α-orientations of H-9, H-11, H-15, and Me-18 as well as the *trans*-junction of the octahydroindene ring were deduced by ROESY cross-peaks of H-12/H-17, H-11/H$_3$-18, H-16α/H$_3$-18, H-15/ H-16α, H-30a/H-9, and H-30b/H-15. In addition, the 5*R** and 10*R** configurations were indicated by ROESY correlations for H-5/H-9, H-5/H-30a, and H-2/H-12. Resemblance of 1D NMR data for **1** with those for a known prieurianin type limonoid, amooramide A (Figure 2.7) [37], supported the assignment of the relative configuration of **1**.
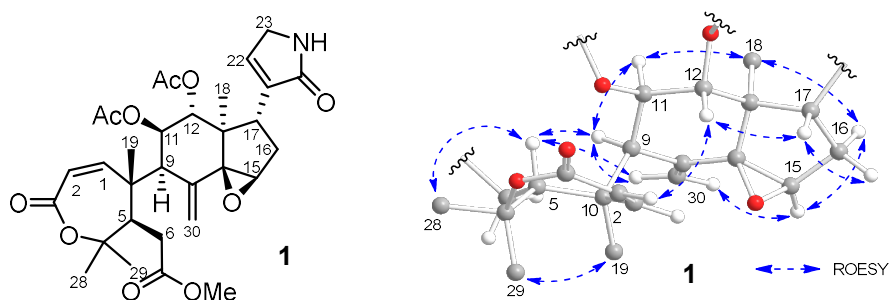
Figure 2.6. Selected NOESY correlations and relative stereochemistry for munropin A (**1**) (protons of methyl groups and substituents at C-6, C-11, C-12, and C-17 are omitted).
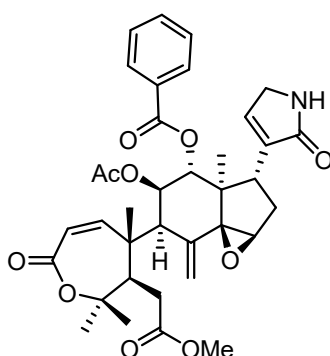
Figure 2.7. Structure of amooramide A.

The molecular formula of munropin B (**2**) was assigned to be $C_{33}H_{43}NO_{11}$ by the HRESIMS (*m/z* 652.2722 [M+Na]$^+$, Δ −1.2 mmu). The 1D NMR spectra of **2** (Table 2.1 and Figure 2.8) were similar to those of **1**, except for the resonances assignable to a nitrogen-bearing hydroxyethyl group [δ_H 3.53 (H$_2$-1') and 3.73 (H$_2$-2'); δ_C 46.3 (C-1') and 61.4 (C-2')] in **2**. HMBC correlations for H$_2$-1' to C-21 and C-23 revealed the connectivity between CH$_2$-1' and nitrogen atom of the α,β-unsaturated γ-lactam ring (Figure 2.9). Accordingly, the structure of munropin B (**2**) was elucidated as shown in Figure 2.8.

Table 2.1 ^{1}H and ^{13}C NMR data for munropins A (**1**) and B (**2**) in CDCl$_3$.

Position	1		2	
	δ_C	δ_H (*J* in Hz)	δ_C	δ_H (*J* in Hz)
1	148.4	6.89 (d, 12.5)	148.6	6.88 (d, 12.0)
2	122.4	6.31 (d, 12.5)	122.2	6.27 (d, 12.0)
3	166.9	–	167.1	–
4	83.7	–	83.8	–
5	50.8	3.32 (d, 8.9)	50.1	3.30 (d, 9.3)
6	35.5	2.28, 2.13 (each, m)	35.0	2.26, 2.19 (each, m)
7	173.7	–	173.7	–
8	137.7	–	136.6	–
9	53.4	3.05 (d, 7.1)	53.4	3.03 (d, 7.0)
10	46.7	–	46.3	–
11	71.5	5.55 (dd, 10.5, 7.1)	71.5	5.54 (dd, 11.2, 7.0)
12	74.5	5.78 (d, 10.5)	74.6	5.76 (d, 11.2)
13	45.6	–	45.6	–
14	72.7	–	71.2	–
15	60.0	3.87 (brs)	60.0	3.86 (brs)
16	31.0	2.22, 2.11 (each, m)	30.8	2.25, 2.14 (each, m)
17	38.7	2.97 (dd, 10.6, 7.4)	39.1	2.94 (dd, 11.3, 7.4)
18	13.6	0.94 (3H, s)	13.5	0.92 (3H, s)
19	22.8	0.97 (3H, s)	22.8	0.96 (3H, s)
20	136.9	–	137.1	–
21	174.5	–	172.0	–
22	141.7	6.75 (brs)	139.3	6.68 (brs)
23	46.3	3.89 (2H, brs)	52.4	3.95 (2H, brs)
28	30.3	1.28 (3H, s)	30.3	1.26 (3H, s)
29	22.8	1.54 (3H, s)	22.4	1.52 (3H, s)
30	121.2	5.33, 5.20 (each, brs)	121.3	5.33, 5.19 (each, brs)
7-OMe	52.5	3.69 (3H, s)	52.5	3.68 (3H, s)
11-OAc	170.6	–	170.6	–
	20.7	1.80 (3H, s)	20.7	1.79 (3H, s)
12-OAc	169.4	–	169.6	–
	20.5	2.09 (3H, s)	20.4	2.09 (3H, s)
1'			46.3	3.53 (2H, m)
2'			61.4	3.73 (2H, m)
N-H	-	7.16 (1H, brs)		
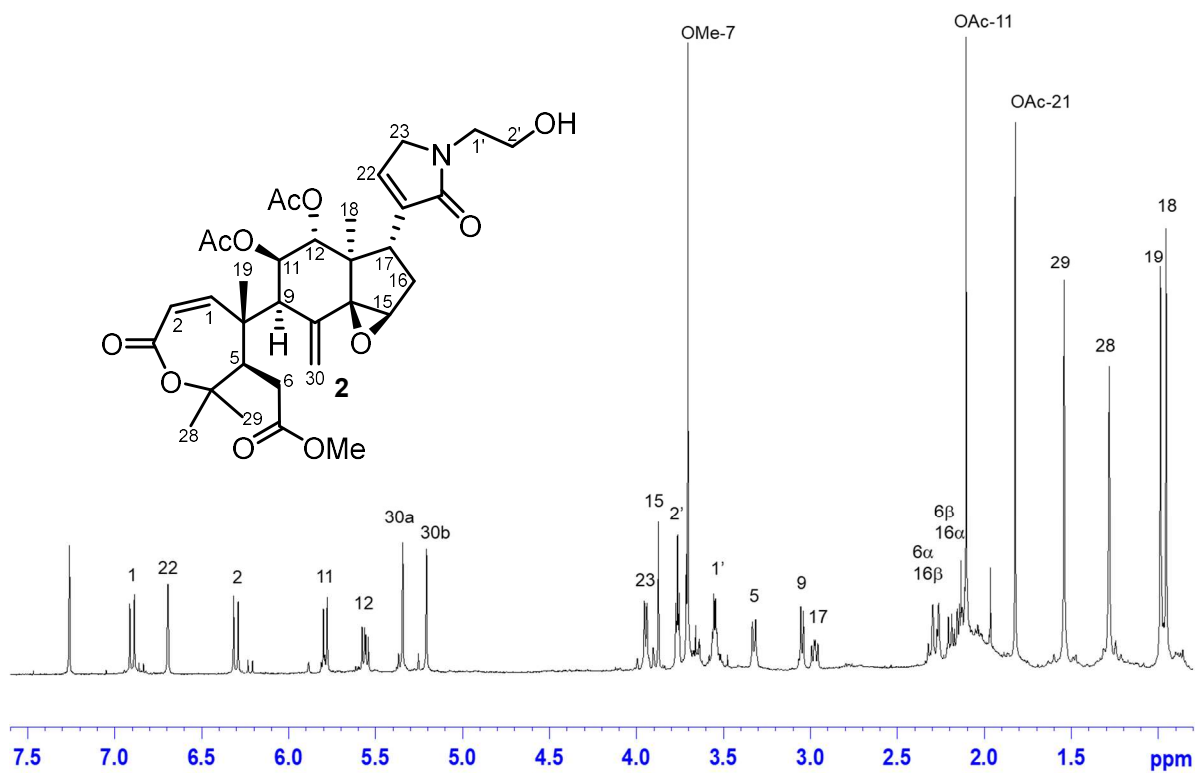
Figure 2.8. ^{1}H NMR spectrum of **2** in CDCl$_3$ (500 MHz).
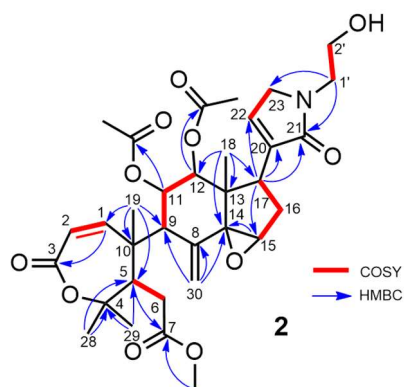
Figure 2.9. Selected ^{1}H-^{1}H COSY and HMBC correlations for **2**.

The absolute configurations of munropins A (**1**) and B (**2**) were assigned as follows. The TDDFT {CAM-B3LYP/6-31G+(d)} calculation of a possible enantiomer (5*R*,9*R*,10*R*,11*R*,12*R*,13*R*,14*S*,15*R*,17*R*) of **1** gave a calculated ECD spectrum, which corresponded to the experimental spectrum of **1** (Figure 2.10 **A**), suggesting the 5*R*, 9*R*, 10*R*, 11*R*, 12*R*, 13*R*, 14*S*, 15*R*, and 17*R* configurations of munropin A (**1**). The experimental ECD spectrum of munropin B (**2**) was similar to that of **1** (Figure 2.10 **B**), suggesting that they had the same absolute configuration. Thus, the structures of munropins A (**1**) and B (**2**) were assigned as shown in Figure 2.10.
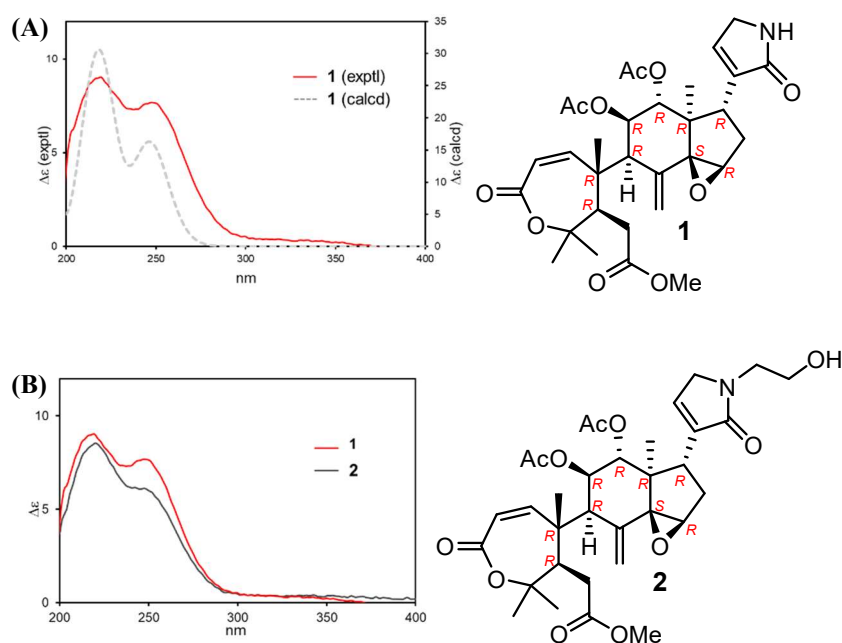
Figure 2.10. (**A**) Experimental and calculated ECD spectra of munropin A (**1**); (**B**) experimental ECD spectra of munropins A (**1**) and B (**2**).

2.3.2 Munropins C (**3**) and D (**4**)

Munropins C (**3**) and D (**4**) were obtained as optically active colorless amorphous solids $\{[\alpha]_D^{21}$ +135.0 (*c* 0.10, MeOH) for **3**; $[\alpha]_D^{21}$ +79.0 (c 0.1, MeOH) for **4**}. The HRESIMS revealed that **3** and **4** had the molecular formulae of $C_{31}H_{38}O_{11}$ and $C_{29}H_{38}O_{10}$ (*m/z* 609.2285 [M+Na]$^+$, Δ −2.7 mmu for **3**; *m/z* 569.2340 [M+Na]$^+$, Δ −2.3 mmu for **4**), respectively. The ^{1}H and ^{13}C NMR spectra of **3** and **4** (Figures 2.11 and 2.12 and Table 2.2) also resembled with those of **1**, except for the signals due to the substituents at C-17. The substituent at C-17 of **3** was assigned as an α,β-unsaturated γ-lactone by HMBC correlations for H$_2$-23 with C-21 and C-20, and H-22 with C-17, while that of **4** was elucidated to be an acetyl group by HMBC cross-peaks of H$_3$-21 to C-17 and C-20.
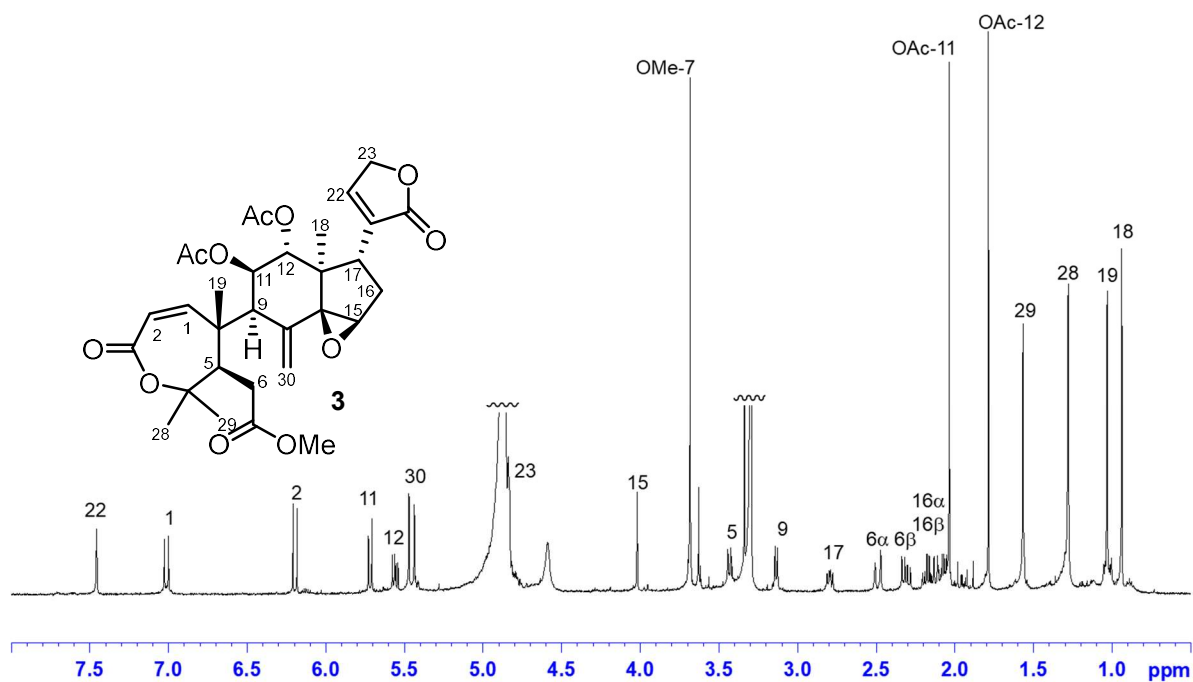
Figure 2.11. ^{1}H NMR spectrum of munropin C (**3**) in CD$_3$OD (500 MHz).
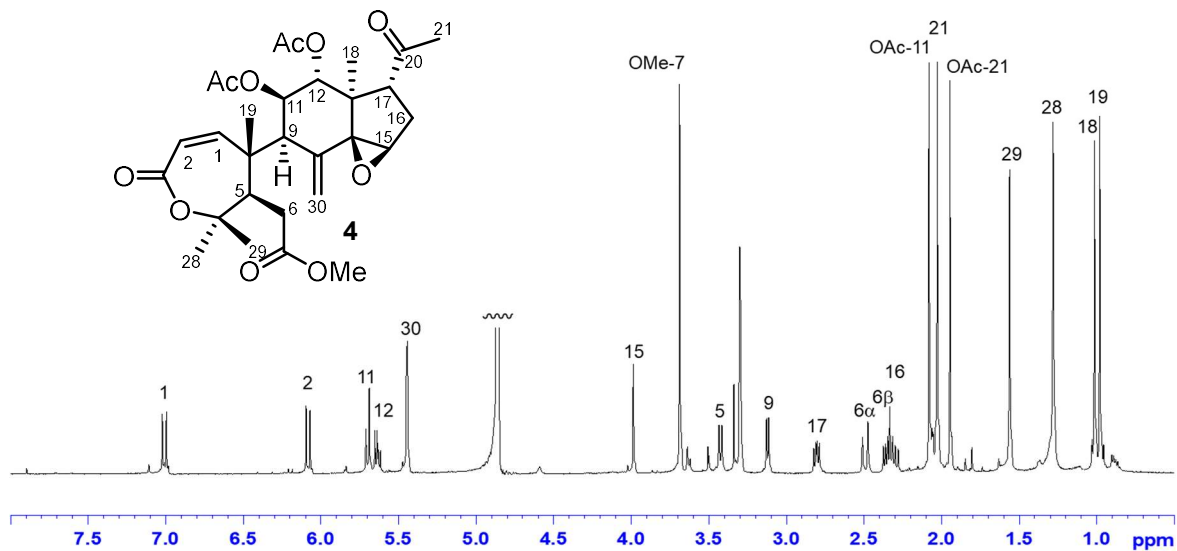
Figure 2.12. ^{1}H NMR spectrum of munropin D (**4**) in CD$_3$OD (500 MHz).

The relative configurations of munropins C (**3**) and D (**4**) were implied being the same as that of **1** by comparison of their 1D NMR data. ROESY cross-peaks of H-12/H-17, H-11/H$_3$-18, H$_3$-19/H$_3$-29, H-5/H-9 H-30a/H-9, H-30b/H-15, and H-12/H-17 observed both **3** and **4**, which were also seen in **1**, supported this assignment. The ECD spectra of **3** and **4** were calculated by TDDFT {CAM-B3LYP/6-31G+(d)} method. Comparison of the experimental ECD spectra of **3** and **4** with the calculated spectra suggested the absolute configurations of **3** and **4** as shown in Figure 2.13.

Table 2.2 ^{1}H and ^{13}C NMR data for munropins C–E (**3–5**) in CD$_3$OD.

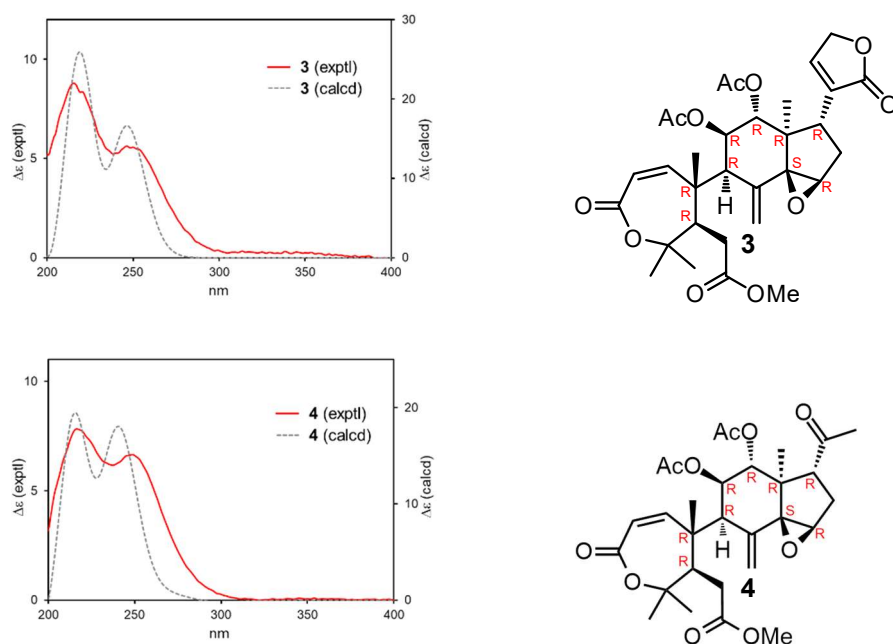| Position	3 δ_C	3 δ_H (J in Hz)	4 δ_C	4 δ_H (J in Hz)	5 δ_C	5 δ_H (J in Hz)
1	151.4	7.02 (d, 12.9)	151.9	7.01 (d, 12.7)	153.2	7.04 (d, 12.8)
2	122.6	6.20 (d, 12.9)	122.3	6.09 (d, 12.7)	121.5	6.08 (d, 12.8)
3	169.2	–	169.3	–	170.2	–
4	85.9	–	86.1	–	86.5	–
5	51.2	3.43 (d, 9.6)	51.1	3.43 (d, 9.3)	51.1	3.42 (d, 9.2)
6	35.5	2.49, 2.33 (each, m)	35.4	2.49, 2.32 (each, m)	35.5	2.49, 2.30 (each, m)
7	175.7	–	175.6	–	175.5	–
8	137.5	–	136.8	–	137.6	–
9	54.5	3.14 (d, 7.6)	54.0	3.62 (d, 7.1)	54.3	3.08 (d, 7.6)
10	47.6	–	47.6	–	47.6	–
11	73.2	5.56 (dd, 10.6, 7.6)	72.2	5.64 (dd, 10.2, 7.1)	75.4	5.42 (dd, 10.3, 7.6)
12	76.2	5.72 (d, 10.6)	76.0	6.09 (d, 10.2)	74.8	4.35 (d, 10.3)
13	46.6	–	47.1	–	47.6	–
14	72.3	–	72.1	–	72.4	–
15	61.0	4.02 (brs)	60.6	3.99 (brs)	61.1	3.94 (brs)
16	32.7	2.18, 2.13 (each, m)	31.1	2.37, 2.32 (each, m)	30.2	2.21, 2.06 (each, m)
17	39.2	2.79 (dd, 11.2, 7.1)	54.9	2.87 (dd, 10.6, 7.2)	51.2	2.88 (dd, 9.6, 6.8)
18	13.7	0.94 (3H, s)	12.9	0.98 (3H, s)	12.3	0.78 (3H, s)
19	23.2	1.04 (3H, s)	23.1	1.02 (3H, s)	23.2	0.99 (3H, s)
20	132.1	–	209.8	–	205.7	–
21	175.5	–	30.7	2.03 (3H, s)	70.5	5.25, 4.76 (each, m)
22	151.3	7.46 (3H, s)				
23	71.9	4.85 (2H, m)				
28	30.6	1.28 (3H, s)	30.6	1.28 (3H, s)	30.6	1.30 (3H, s)
29	22.7	1.57 (3H, s)	22.6	1.56 (3H, s)	22.6	1.57 (3H, s)
30	122.6	5.47, 5.44 (each, brs)	123.4	5.45, 5.44 (each, brs)	122.8	5.26, 5.23 (each, brs)
7-OMe	52.7	3.68 (3H, s)	52.6	3.69 (3H, s)	52.6	3.69 (3H, s)
11-OAc	171.7	–	172.1	–	172.2	–
	20.8	1.79 (3H, s)	20.9	1.95 (3H, s)	21.0	2.08 (3H, s)
12-OAc	171.1	–	171.4	–		
	20.7	2.04 (3H, s)	20.6	2.08 (3H, s)		
21-OAc					172.1	–
					20.3	2.17 (3H, s)

Figure 2.13. Experimental and calculated ECD spectra of munropins C (**3**) and D (**4**).

2.3.3 Munropin E (**5**)

HRESIMS analysis of munropin E (**5**) indicated the molecular formula to be $C_{29}H_{38}O_{11}$ (*m/z* 585.2314 [M+Na]$^+$, Δ +0.2 mmu). Interpretation of the 1D NMR spectra (Figure 2.14 and Table 2.2) implied that **5** was also a prieurianin type limonoid similar to **4**, whereas the signals due to an oxymethylene (CH$_2$-21: δ_H 5.25 and 4.76; δ_C 70.5) were observed in **5** in place of the signals of one acetyl group in **4**. The oxymethylene protons (H$_2$-21) showed HMBC correlations with C-17, C-20, and one acetoxy carbonyl carbon, suggesting the existence of an acetoxy acetyl group at C-17 in **5**. The resonance due to H-12 of **5** (δ_H 4.35) was up-field shifted as compared with that of **4** (δ_H 6.09), implying that **5** has a hydroxy group at C-12 in place of the acetoxy group in **4**. Therefore, the structure of munropin E (**5**) was concluded as shown in Figure 2.14.

Analysis of the ROESY spectrum of munropin E (**5**) suggested that its relative configuration was the same as **4**. Resemblance of the experimental and TDDFT calculated ECD spectra of **5** suggested the absolute configurations of **5** as shown in Figure 2.15.
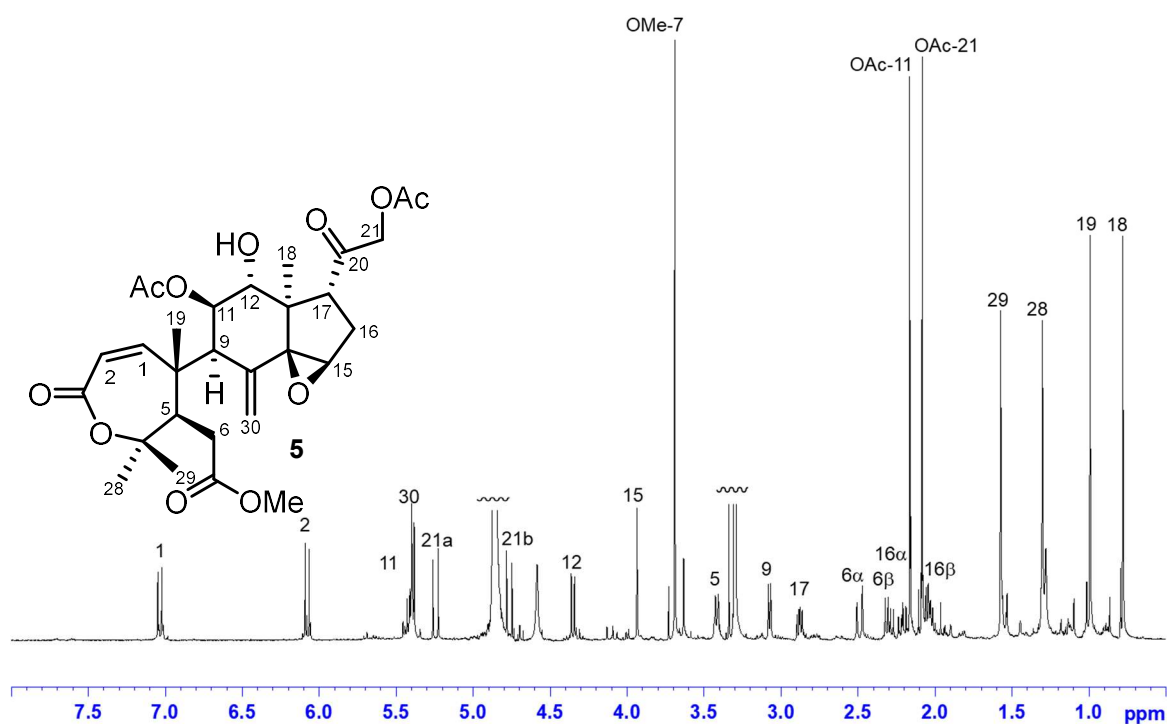
Figure 2.14. ^{1}H NMR spectrum of munropin E (**5**) in CD$_3$OD (500 MHz).
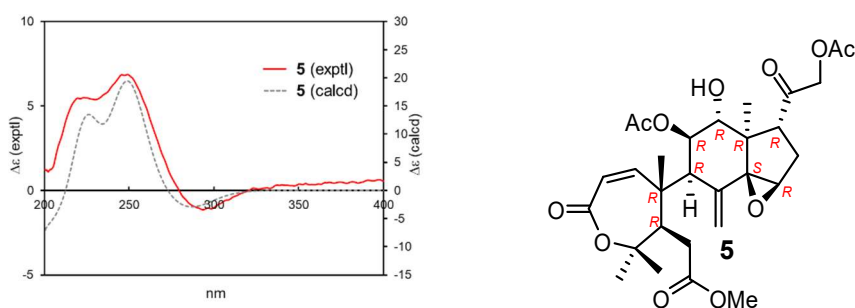
Figure 2.15. Experimental and calculated ECD spectra of munropin E (**5**).

2.3.4 Munropin G (**6**)

The HRESIMS showed the molecular formula of munropin G (**6**) to be C$_{33}$H$_{46}$O$_{14}$ {*m/z* 689.2756 [M+Na]$^+$, −0.9 mmu}. Detailed analyses of the 1D and 2D NMR spectra (Figures 2.16 and 2.17 and Table 2.3) revealed that the structure of **6** was similar to **3**, except for the substituent at C-17. Key HMBC correlations of H-17 with C-20, C-21, and C-22; 21-OMe with

C-21, and 23-OMe with C-23, together with a COSY correlation of H-22 with H-23 allowed the establishment of the substituent to be 3,4-dihydroxy-2,5-dimethoxytetrahydrofuran (Figure 2.17). The chemical shifts of C-20 (δ_C 81.3), C-21 (δ_C 110.5), C-22 (δ_C 79.3), and C-23 (δ_C 110.7) further support this analysis. Thus, the planar structure of **6** was assigned as depicted at Figure 2.16.
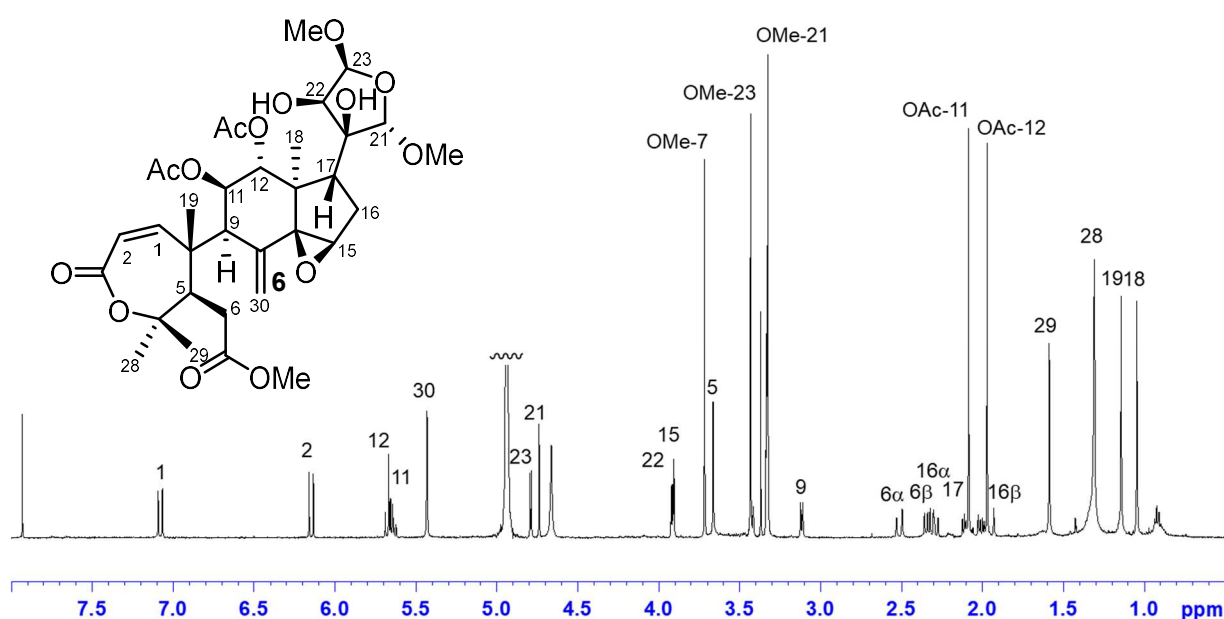
Figure 2.16. ^{1}H NMR spectrum of munropin G (**6**) in CD₃OD (500 MHz).
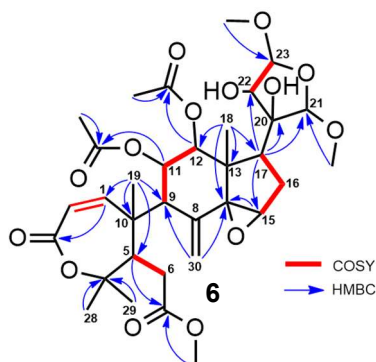
Figure 2.17. Selected ^{1}H-^{1}H COSY and HMBC correlations for munropin G (**6**).

Table 2.3 ^{1}H and ^{13}C NMR data for munropin G (**6**) in CD$_3$OD.

Position	6	
	δ_C	δ_H (*J* in Hz)
1	151.9	7.05 (d, 13.1)
2	122.5	6.11 (d, 13.1)
3	169.3	-
4	86.1	-
5	51.2	3.39 (d, 8.3)
6	35.5	2.30, 2.48 (each, brs)
7	175.7	-
8	137.7	-
9	54.3	3.08 (d, 6.7)
10	47.6	-
11	73.3	5.61 (dd, 10.6, 6.7)
12	76.4	5.64 (d, 10.6)
13	46.9	-
14	72.7	-
15	60.7	3.87 (brs)
16	29.8	2.22 (2H, m)
17	47.8	2.08, 1.99 (dd, 13.1, 6.8)
18	13.9	1.11 (3H, s)
19	23.0	1.02 (3H, s)
20	81.3	-
21	110.5	4.70 (1H, s)
22	79.3	3.89 (d, 4.1)
23	110.7	4.76 (d, 4.1)
28	22.6	1.56 (3H, s)
29	30.6	1.28 (3H, s)
30	122.3	5.40 (2H, brs)
OMe-7	54.2	3.29 (3H, s)
OMe-21	56.6	3.40 (3H, s)
OMe-23	52.8	3.69 (3H, s)
OAc-11	172.2	-
	21.3	1.94 (3H, s)
OAc-12	171.7	-
	20.7	2.05 (3H, s)

The ROESY spectrum of **6** indicated that the relative configurations of C-5, C-9, C-10, C-11, C-12, C-13, C-14, C-15 and C-17 were the same as those of **3** (Figure 2.19). ROESY cross-

peaks of H-17/H-22 and H-22/H-23 suggested that H-17, H-22, and H-23 were oriented to the β face. The α orientation of H-21 was elucidated from a ROESY cross-peak of H-21/H$_3$-18. The ^{1}H and ^{13}C chemical shifts of the 3,4-dihydroxy-2,3-dimethoxy-tetrahydrofuran moiety at C-17 in **6** were similar to those of toonasinemine L (Figure 2.18) [38], indicating that relative configurations of the moiety were the same. Munropin G (**6**) showed Cotton effects similar to those of **1**–**5**. Therefore, the absolute configuration of **6** was assigned as shown in Figure 2.20.
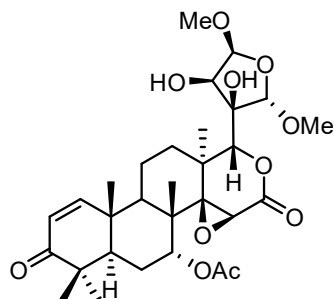

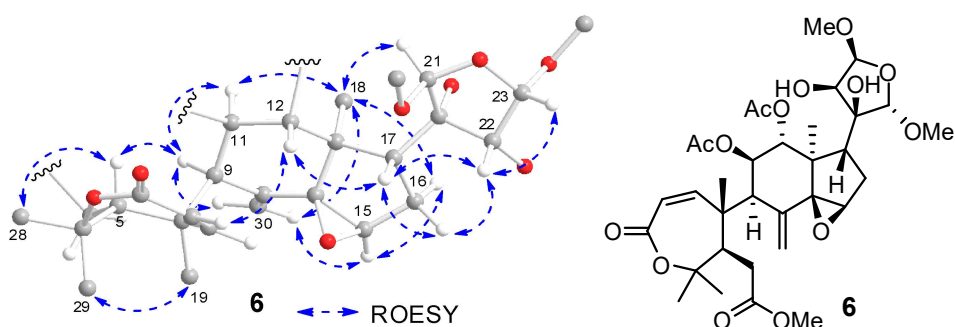**Figure 2.18.** Structure of toonasinemine L

Figure 2.19. Selected NOESY correlations and relative stereochemistry for munropin G (**6**) (protons of hydroxy and methyl groups, and substituents at C-6, C-11, and C-12 are omitted).
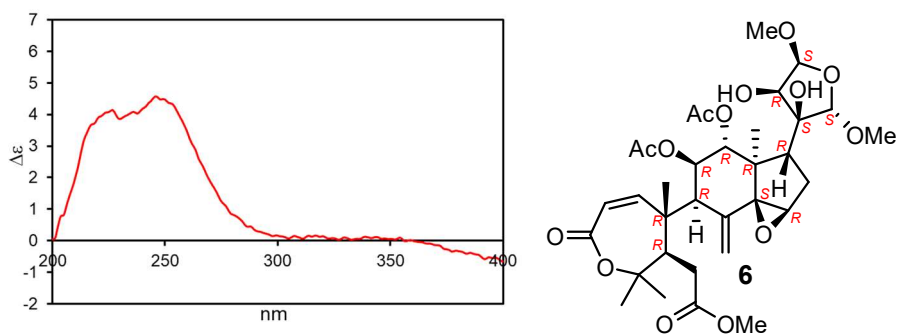
Figure 2.20. Experimental ECD spectrum of munropin G (**6**).

21

2.3.5 Munropins H (7) and I (8)

Munropins H (**7**) and I (**8**) were obtained as optically active colorless amorphous solids {[α]$_D^{21}$ −148 (*c* 0.10, MeOH) for **7**, [α]$_D^{21}$ −127 (*c* 0.10, MeOH) for **8**}. The HRESIMS revealed that they had the same molecular formula of $C_{36}H_{46}O_{15}$ (*m/z* 741.2734 [M+Na]$^+$, Δ −3.1 mmu for **7**; *m/z* 741.2724 [M+Na]$^+$, Δ −1.0 mmu for **8**). Analyses of the 1D and 2D NMR spectra of **7** and **8** implied that they were prieurianin type limonoids similar to **3** with a formyloxy group at C-11 and an acetoxy group at C-29 (Figure 2.20–22 and Table 2.4). HMBC correlations (Figure 2.22) of H-12 with C-1' and H-2' with C-1', C-3', C-4', and C-6', and COSY correlations among H-2'/H-3'/H$_2$-4'/H$_3$-5'/H$_3$-6' allowed the presence of a 3-methyl-2-hydroxy pentanoate (C-1'–C-6') at C-12. The observations of some duplicated signals in the 1D NMR spectra of **7** (H-4'; C-23) and **8** (H-6, H-12, H-21–22, H-2'; C-3, C-6, C-12, C-21–22, C-6') (Table 2.4) indicated that they were two inseparable mixture of epimers. The existence of an α-substituted γ-hydroxy α,β-unsaturated γ-lactone moiety at C-17 in **7** was revealed by HMBC correlations of H-17 with C-20 and H-22 with C-20, C-21, and C-23, while a β-substituted γ-hydroxy α,β-unsaturated γ-lactone moiety at C-17 in **8** was determined by correlations of H-22 with C-20, C-21, and C-23, with COSY correlation of H-22 with H-23. Thus, the planar structures of **7** and **8** were assigned as shown at Figures 2.20 and 21.

Figure 2.20. ^{1}H NMR spectrum of munropin H (**7**) in CD$_3$OD (500 MHz).

Figure 2.21. ^{1}H NMR spectrum of munropin I (**8**) in CD$_3$OD (500 MHz).

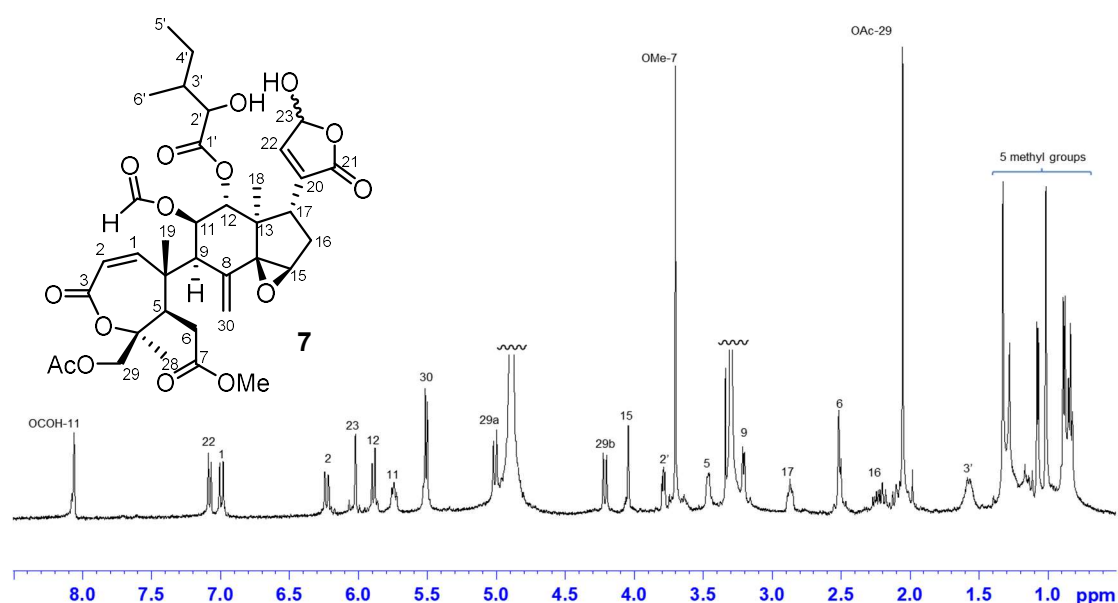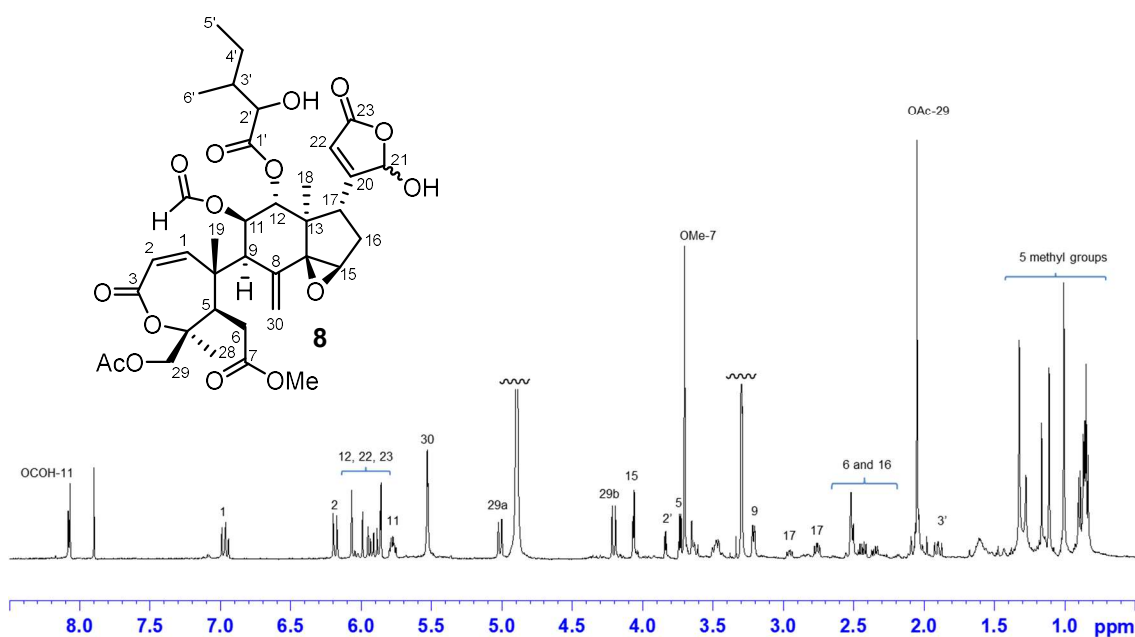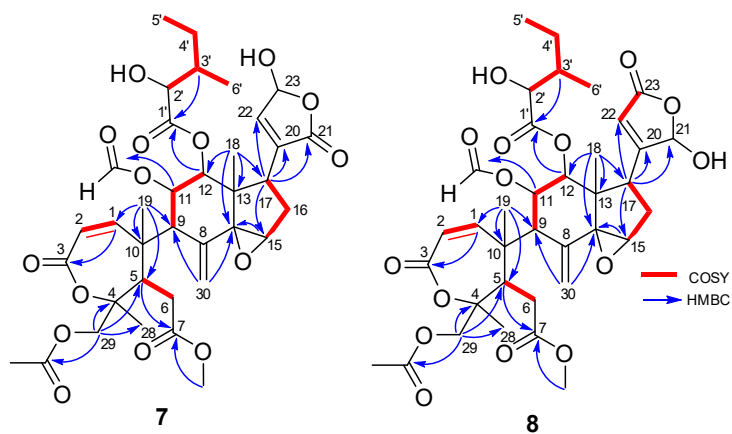
Figure 2.22. Selected ^{1}H-^{1}H COSY and HMBC correlations for **7** and **8**.

Table 2.4 ^{1}H and ^{13}C NMR data for munropins H–I (**7**–**8**) in CD$_3$OD.

Position	7		8	
	δ$_C$	δ$_H$ (*J* in Hz)	δ$_C$	δ$_H$ (*J* in Hz)
1	150.1	6.99 (d, 10.4)	150.0	6.98 (d, 10.7)
2	123.4	6.23 (d, 10.4)	123.4	6.22 (d, 10.7)
3	168.4	-	168.7/168.4	-
4	86.2	-	86.3/86.2	-
5	51.7	3.45 (m)	51.6	3.47 (m)
6	35.3	2.52 (2H, m)	35.2/35.2	2.51/ 2.47 (each, m)
7	175.4	-	174.5	-
8	136.8	-	136.5	-
9	54.3	3.20 (d, 7.2)	54.0	3.21 (dd, 7.0, 2.1)
10	47.3	-	47.2	-
11	71.6	5.74 (dd, 10.6, 7.2)	71.4	5.78 (dd, 10.6, 7.0)
12	76.2	5.89 (d, 10.6)	75.9/76.1	5.92 (d, 11.2)/5.87 (d, 12.1)
13	47.4	-	47.3	-
14	72.1	-	72.1	-
15	61.1	4.05 (brs)	61.0	4.07 (brs)
16	32.4	2.23, 2.15 (each, m)	32.6	2.04, 2.35 (each, m)
17	39.3	2.87 (br)	41.3	2.79 (dd, 10.3, 6.8)
18	13.5	1.08 (3H, s)	13.6	1.15 (3H, s)
19	24.3	1.16 (3H, s)	24.4	1.04 (3H, s)
20	134.6	-	169.3	-
21	173.4	-	101.8/101.0	5.99/5.86 (s)
22	149.5	7.04 (brs)	121.0/119.7	6.07/5.93 (brs)
23	98.5/98.3	6.02 (brs)	172.2	-
28	24.7	1.33 (3H, s)	24.7	1.35 (3H, s)
29	64.4	5.01, 4.21, (each, d, 11.6)	64.4	5.01, 4.21 (each, d, 12.6)
30	123.7	5.52, 5.50 (each, brs)	123.4	5.53, 5.52 (each, brs)
OMe-7	52.8	3.71 (3H, s)	52.8	3.70 (3H, s)
OAc-28	20.5	2.06 (3H, s)	20.5	2.08 (3H, s)
	172.0	-	171.2	-
OCHO-11	161.6	8.06 (1H, s)	161.5	8.07 (1H, s)
1'	174.5	-	173.1	-
2'	76.4	3.80 (dd, 6.8, 3.8)	76.6	3.84/3.77 (d, 4.3)
3'	39.2	1.58 (m)	39.3	1.61 (m)
4'	24.1	1.28/1.16 (m)	24.0	1.17 (m)
5'	15.8	0.84 (3H, t, 8.3)	15.6	0.88 (3H, t, 6.9)
6'	11.7	0.86 (3H, d, 6.9)	11.8/11.5	0.85 (3H, d, 6.8)

Detailed analyses of the NOESY spectra indicated that the relative configurations of the limonoid core of **7** and **8** were the same as **3**, which were further supported by the resemblance of their 1D NMR spectra. The relative configurations of the 3-methyl-2-hydroxy-pentanoyl groups of **7** and **8** remain to be assigned.

Positive Cotton effects around at 200 nm to 250 nm seen in the experimental ECD spectra of **7** and **8** (Figure 2.23) were similar to those of **1−6**, which indicated that their absolute configurations were the same.
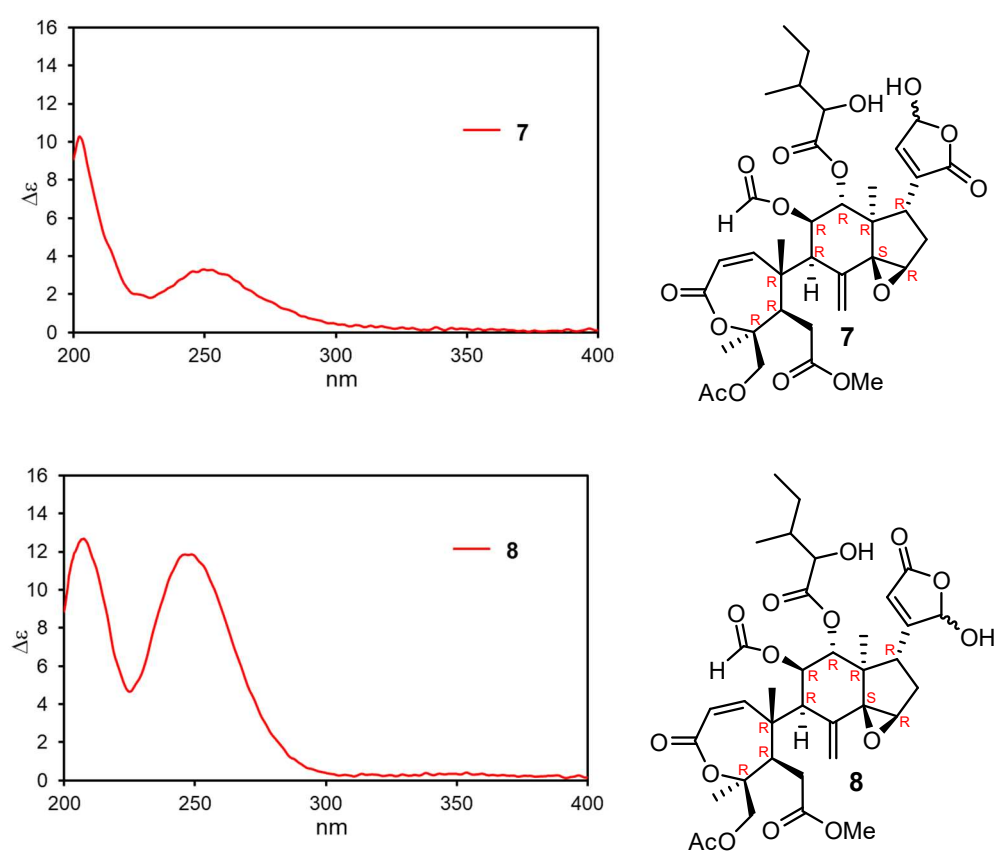
Figure 2.23. Experimental ECD spectrum of munropins H (**7**) and I (**8**).

2.3.6 Munropin F (9)

Munropin F (9) was obtained as an optically active colorless amorphous solid $\{[\alpha]_D^{21} +27 (c$ 0.10, MeOH)$\}$. The molecular formula of 9 was elucidated to be $C_{33}H_{44}O_{11}$ by the HRESIMS $\{m/z$ 639.2766 $[M+Na]^+$ (Δ −1.5 mmu)$\}$. Analysis of the 1D and 2D NMR spectra of 9 (Figure 2.24 and Table 2.5) indicated that 9 was a nimbolinin type limonoid similar to munronin K (Figure 25) [18], but had different substituents at C-12 and C-17. In addition, the observation of some duplicated signals (H-21, H-22; C-14, 15, C-21–23) in the 1D NMR spectra of 9 implied the existence of an equilibrium mixture of epimers. HMBC analysis for the correlations involving these duplicated signals revealed the presence of a γ-hydroxy-α,β-unsaturated γ-lactone moiety (C-21–C-23) at C-17, which underpinned the existence of an equilibrium mixture due to C-21 epimers. In contrast, C-12 was assigned as a hemiacetal carbon by a ^1H-^1H COSY cross-peek of H-11/H-12 and an HMBC correlation for H-15 with C-12 taking the chemical shifts of CH-12 (δ_H 4.57; δ_C 95.4) and the molecular formula of 9 into consideration. Thus, the gross structure of 9 was assigned as depicted in Figure 2.24.
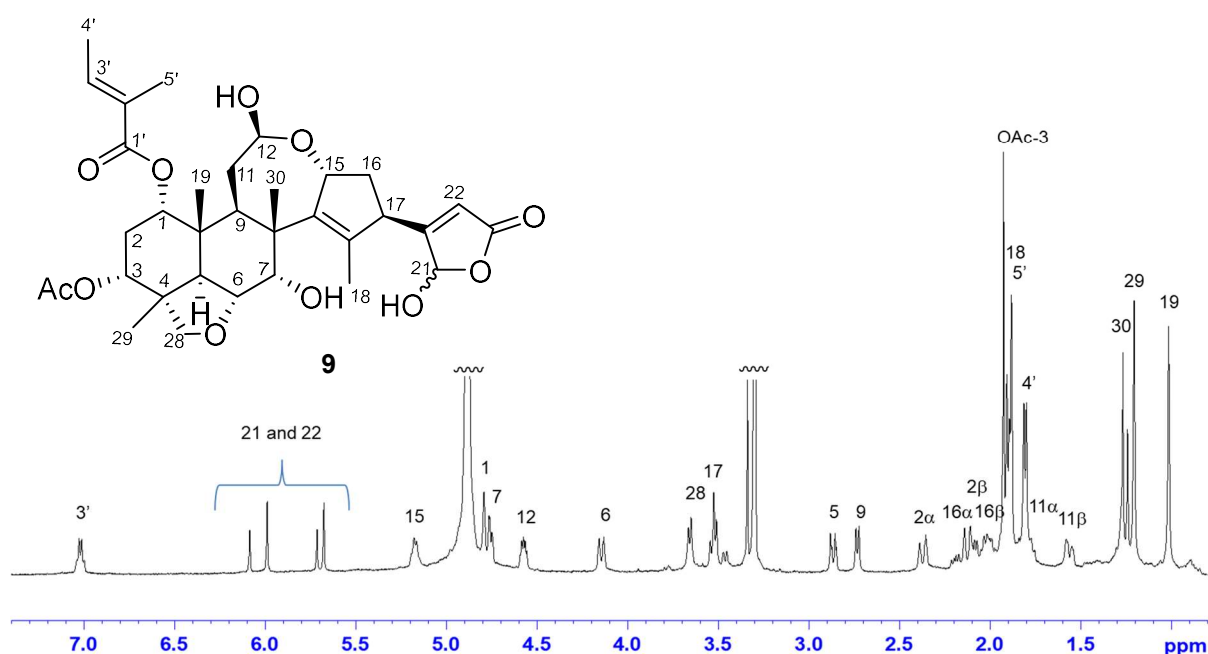
Figure 2.24. ^1H NMR spectrum of munropin F (9) in CD_3OD (500 MHz).

26

Table 2.5 ^{1}H and ^{13}C NMR data for munropin F (**9**) in CD$_3$OD

Position	9	
	δ_C	δ_H (J in Hz)
1	73.4	4.79 (m)
2	28.6	2.37, 2.13 (each, m)
3	73.3	4.87^a
4	43.9	–
5	40.0	2.87 (d, 12.8)
6	75.3	4.15 (d, 12.8)
7	72.0	4.76 (d, 8.3)
8	51.0	–
9	36.7	2.74 (d, 8.3)
10	41.9	–
11	30.5	1.79, 1.57 (each, m)
12	95.4	4.57 (dd, 10.3, 4.6)
13	133.6	–
14	146.9/146.2	–
15	76.2/76.3	5.18 (t, 8.2)
16	36.5	2.09, 2.01 (each, m)
17	48.5	3.53 (t, 10.8)
18	16.8	1.91 (3H, s)
19	17.0	1.02 (3H, s)
20	174.2	–
21	101.5/100.3	6.04/5.99 (s)
22	118.1/117.9	5.71/6.68 (s)
23	173.4/173.3	–
28	78.8	3.66, 3.52 (each, m)
29	19.5	1.21 (3H, s)
30	21.2	1.27 /1.24 (3H, s)
3-OAc	172.3	–
	21.0	1.93 (3H, s)
1'	168.3	–
2'	129.9	–
3'	139.8	7.02 (m)
4'	14.5	1.81 (3H, d, 6.5)
5'	12.2	1.88 (3H, s)

^{a} Overlapped with the signal of HOD.
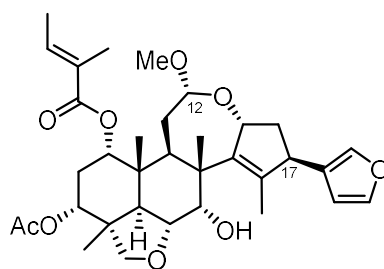
Figure 2.25. Structure of munronin K.
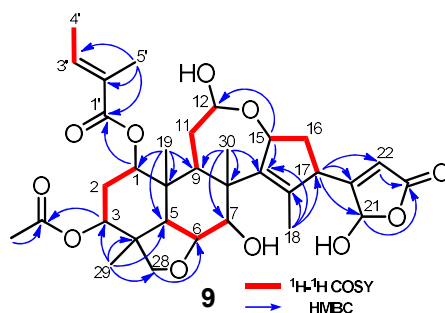
Figure 2.26. Selected ^{1}H-^{1}H COSY and HMBC correlations for munropin F (**9**).

NOESY correlations for H-6/H$_3$-19, H-6/H$_3$-29, and H$_3$-19/H$_3$-30 revealed the axial orientations of H-6, Me-19, Me-29, and Me-30 as well as the *trans*-junction of the decaline ring (C-1−C-10) (Figure 2.27). A NOESY correlation for H-5/H-9 suggested the α-orientations of H-5 and H-9, and supported the *trans*-decaline junction. The H-12α, H-15β, and H-17α orientations were indicated by NOESY correlations for H-9/H-12, and H-15/H$_3$-30. NOESY cross-peaks of H-1/H$_3$-19, H-1/H$_2$-2, H-3/H$_2$-2, H-3/H$_3$-29, and H-7/H$_3$-30 suggested the α-orientations of oxygen functionalities at C-1, C-3, and C-7. Consequently, the relative configuration of munropin F (**9**) was elucidated as shown in Chart 1. The absolute configuration of **9** remains to be assigned.
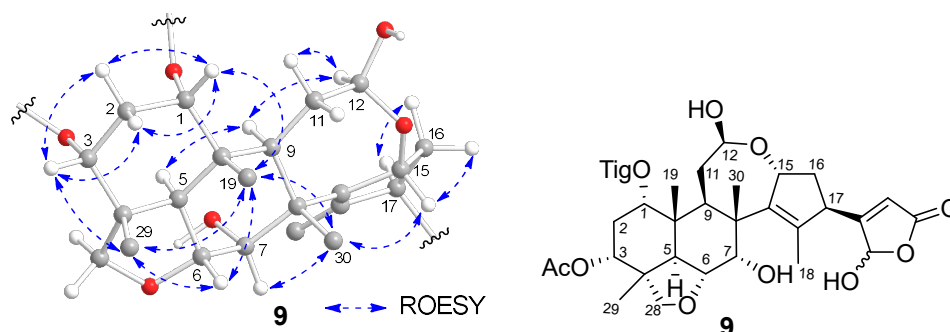
Figure 2.27. Selected NOESY correlations and relative stereochemistry for munropin F (**9**) (protons of methyl groups and substituents at C-1, C-3, and C-17 are omitted).

2.4 Bioassy

Munropins A–F (**1**–**5** and **9**), munronin C (**10**), and munronoid O (**12**) were evaluated for their antiproliferative activity against human cancer cell lines (Hela and A549), showing that no limonoids exhibited cytotoxicity at 100 μM.

2.5 Summary

The aerial parts of a Guangxi medicinal plant, *M. pinnata* were investigated to give nine new limonoids (**1**–**9**), together with 12 known compounds. On the basis of spectroscopic analysis and ECD calculations, the structures of munropins A (**1**) and B (**2**) were assigned to be prieurianin type limonoids with γ-lactam moieties at C-17. Munropins C–E (**3**–**5**) and munropins G–I (**6**–**8**) are limonoids possessing a prieurianin skeleton with either α,β-unsaturated γ-lactone, acetyl, acetoxyacetyl, 3,4-dihydroxy-2,5-dimethoxytetrahydrofuran, α-substituted γ-hydroxy α,β-unsaturated γ-lactone, and β-substituted γ-hydroxy α,β-unsaturated γ-lactone moieties at C-17, respectively. Munropin F (**9**) was assigned as a nimbolinin type limonoid. Munropins A (**1**) and B (**2**) are rare natural products with lactam moieties.
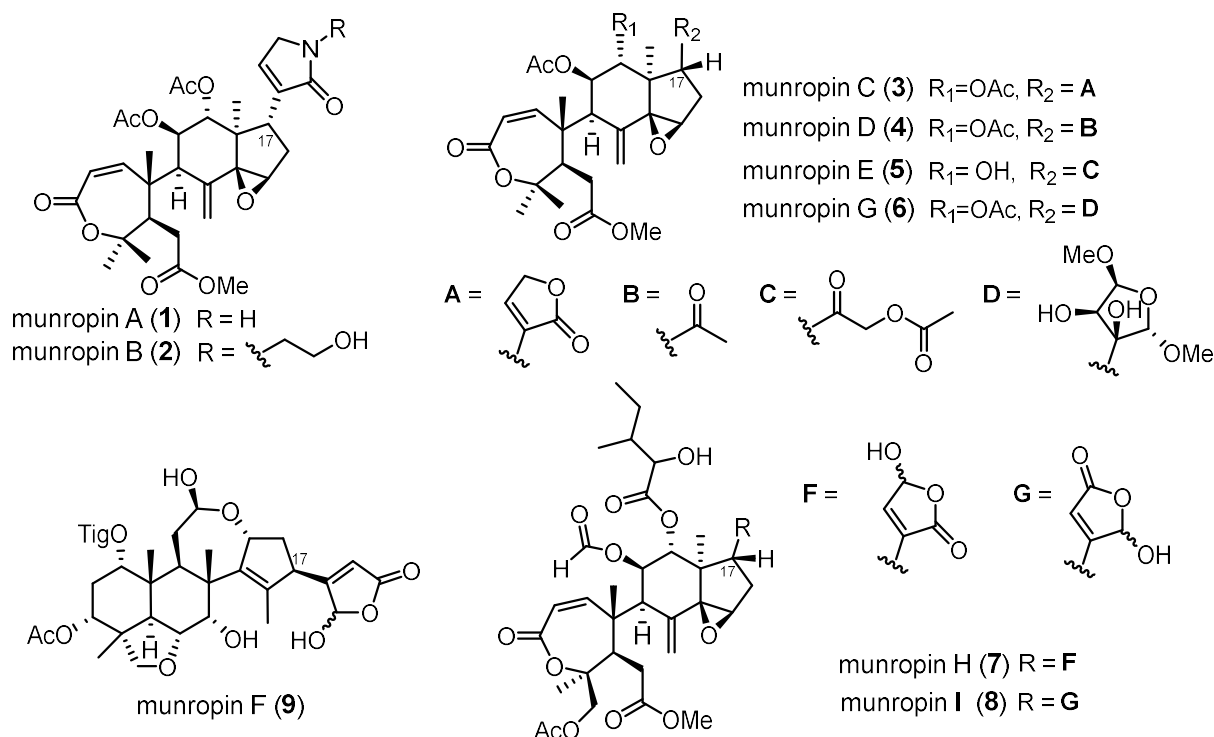
Chart 1. Structures of munropins A–F (**1**–**5**, and **9**) and **G**–**I** (**6**–**8**).

29

Chapter 3 Chemical study on *Sarcandra glabra* (Thunb.) Nakai

3.1 Introduction

The family Chloranthaceae consisting of four genera, *Ascarina*, *Chloranthus*, *Hedyosmum*, and *Sarcandra*, includes around 70 species. Previous phytochemical studies on the Chloranthaceous plants led to the isolation of various specialized metabolites such as flavonoids, sesquiterpenes, sesquiterpene oligomers, diterpenes, triterpenes, and phenylpropanoids [39, 40].

Sarcandra glabra (Thunb.) Nakai (Figure 3.1) is an evergreen shrub widely distributed in south Asia. In Japan, this plant is cultivated as an ornamental [41]. *S. glabra* exhibited various activities such as antibacterial, antiinflammatory, and antitumor activities, and has been used as a traditional herbal medicine for the treatments of bone fracture, arthritis, and cancer in China [42-45]. Up to now, phytochemical studies on this plant have revealed coumarins, sesquiterpenes, flavonoids, triterpene saponins, and phenolic acids to be its constituents [44-46]. Among others, lindenane type sesquiterpenes and their dimers (Figure 3.2) are known as characteristic specialized metabolites of this plant, which have attracted considerable interest due to their diverse structures and interesting biological activities [47,48]. As a part of our study on medicinal plants of Guangxi, specialized metabolites of the aerial parts of *Sarcandra glabra* (Thunb.) Nakai were investigated.

Figure 3.1. *Sarcandra glabra* (Thunb.) Nakai
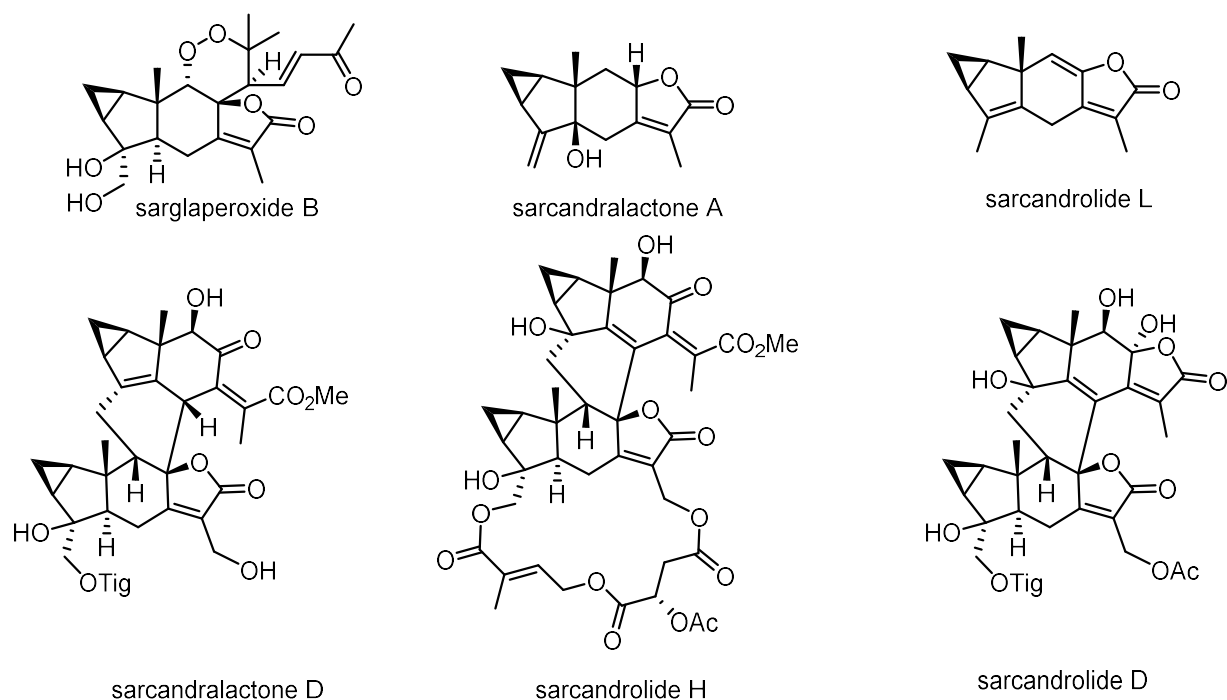
Figure 3.2. Previously isolated sesquiterpenes from *Sarcandra glabra*.

3.2 Extraction and isolation

The air-dried aerial parts of *S. glabra* (3.1 kg) collected at Guangxi were extracted with MeOH in room temperature. The concentrated extract (304.1 g) was then partitioned with H_2O and EtOAc. The EtOAc-soluble materials (93.3 g) were subjected to column chromatographies repeatedly to give fractions containing terpenoids. The fractions were further purified by ODS HPLC to furnish three new terpenes, sarcaglabrins A–C (**22–24**), together with 22 known terpenoids (**25–46**) (Figure 3.3).

the aerial parts of *Sarcandra glabra* (dry, 3.1 kg)

| extracted with MeOH

MeOH ext. (304.1 g)

| partitioned between EtOAc/H_2O

EtOAc (93.3 g) H_2O (210.8 g)

a. MCI gel CHP-20P (MeOH/H_2O)
b. silica gel (*n*-hexane /EtOAc)
c. Sephadex LH-20 (MeOH/H_2O)
d. GPC on HPLC (MeOH)
e. silica gel (CHCl$_3$/MeOH)
f. YMC gel ODC-A (MeOH/H_2O)
g. ODS on HPLC (MeCN/H_2O)

new terpenes

22 (6.2 mg)
23 (5.5 mg)
24 (5.1 mg)

known compounds

25 (1.1 mg)	**36** (30.4 mg)
26 (315.9 mg)	**37** (77.1 mg)
27 (4.6 mg)	**38** (5.6 mg)
28 (3.1 mg)	**39** (21.0 mg)
29 (1.4 mg)	**40** (117.9 mg)
30 (10.4 mg)	**41** (3.6 mg)
31 (250.0 mg)	**42** (14.9 mg)
32 (256.3 mg)	**43** (17.6 mg)
33 (23.0 mg)	**44** (12.0 mg)
34 (29.0 mg)	**45** (2.7 mg)
35 (148.5 mg)	**46** (13.1 mg)

Scheme 2. Isolation procedure for compounds **22**–**46**.

The structures of known compounds **25**–**46** were identified as sarglaperoxide A (**25**) [49], chloranthalactones A (**26**) and B (**27**) [50], chloranthalactone A photodimer (**28**) [51], chlorajapolide F (**29**) [52], 8-*epi*-chlorajapolide F (**30**) [52], chloranthalactone E (**31**) [53], chloranthalactone C (**32**) [54], shizukanolide H (**33**) [55], shizukaols C (**34**) and D (**35**) [56], chlorahololide D (**36**) [57], multistalide B (**37**) [58], shizukaol G (**38**) [59], sarglabolides B (**39**), C (**40**), and E (**41**) [46], spicachlorantin E (**42**) [60], henriol B (**43**) [61], chloramultiol D (**44**) [62], sarcandrolide F (**45**) [46], and chloramultilide A (**46**) [63] by comparison of their spectroscopic data with the literature data.

25

26

27

28

29 R_1=β-OMe, R_2=α-OH
30 R_1=α-OMe, R_2=α-OH
31 R_1=α-OH R_2=β-OH

32 R=H
33 R=OH

34 R_1=Tig, R_2=H. R_3=OH
35 R_1=Ac, R_2=H, R_3=H
36 R_1=Tig, R_2=Ac, R_3=OH
37 R_1=Ac, R_2=H, R_3=OH

38 R_1=α-OH, R_2=H
39 R_1=β-OH, R_2=H
40 R_1=H, R_2=α-OH

41 R=OH
42 R=OOH
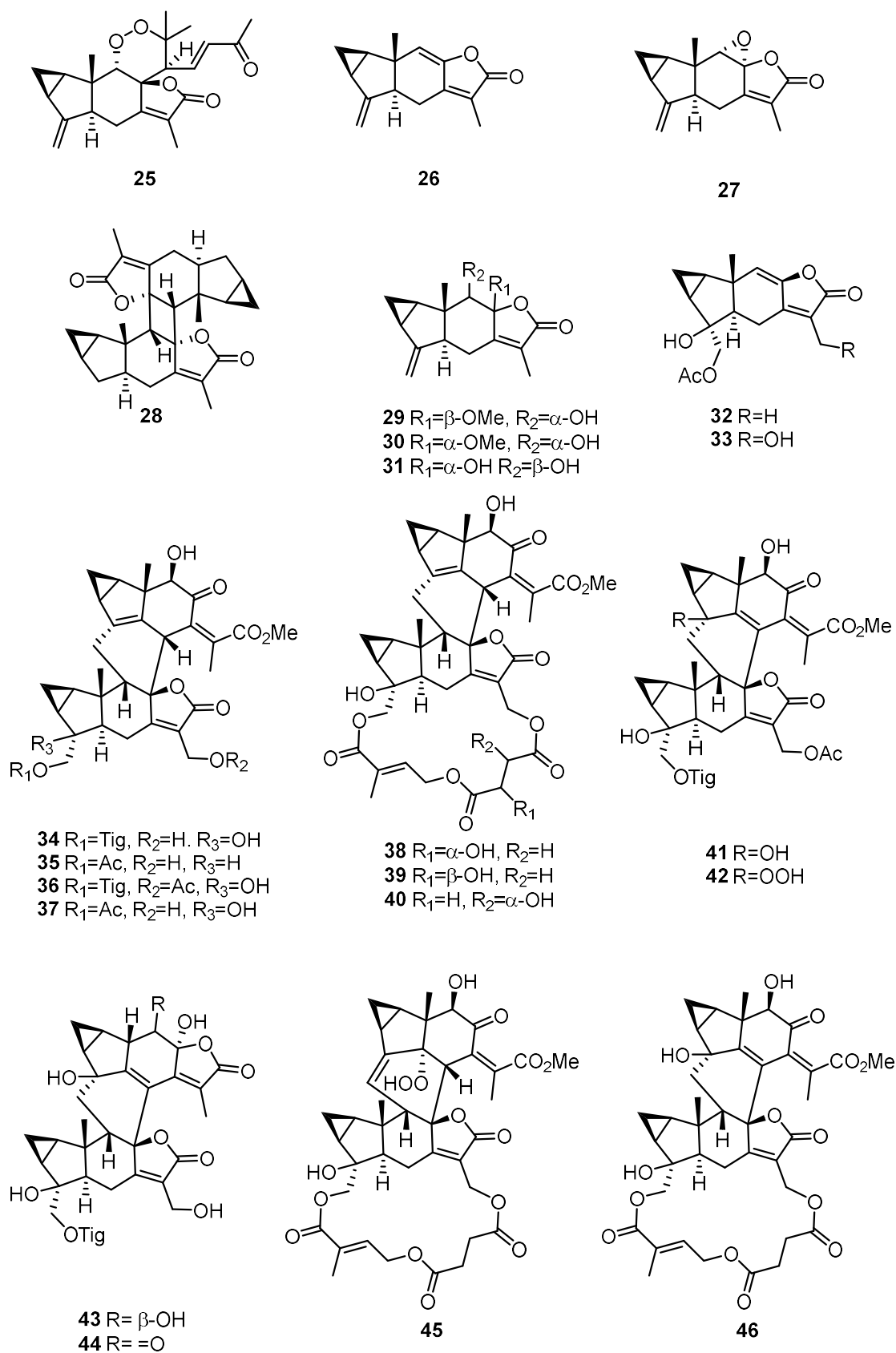
43 R= β-OH
44 R= =O

45

46

Figure 3.3. Known sesquiterpenes (**25–46**) isolated from the aerial parts of *S. glabra* in this study.

3.3 Structure elucidation of new terpenes

3.3.1 Sarcaglabrin A (22)

Sarcaglabrin A (22) was obtained as an optically active colorless amorphous solid {$[\alpha]_D^{24}$ −25 (c 0.10, MeOH)}. The molecular formula of 22 was determined to be $C_{25}H_{32}O_2$ by the HREIMS {m/z 403.2028 ([M+K]$^+$, Δ −1.1 mmu)}. The IR spectrum displayed an absorption at 1749 cm^{-1} due to carbonyl functionality. The ^{1}H NMR spectrum (Figure 3.4 and Table 3.1) showed the resonances due to two trisubstituted olefins, one 1,1-disubstituted olefin, five sp^3 methines, four sp^3 methylenes, and five methyls. The ^{13}C NMR spectrum exhibited 25 signals including one ester carbonyl, eight olefinic, one oxygenated tertiary, and one quaternary carbon signals. The characteristic upfield-shifted chemical shifts of H_2-2 (δ_H 0.81 and 0.71) implied the existence of a cyclopropane ring. The presence of a lindenane sesquiterpene moiety (C-1−C-15) in 22 was revealed by ^{1}H-^{1}H COSY cross-peaks of H-1/H_2-2/H-3 and H-5/H_2-6, along with HMBC correlations for H-5 and H-9 with C-7; H_3-14 with C-1, C-5, C-9, and C-10; H_3-13 with C-7, C-11, and C-12; and H_2-15 with C-3, C-4, and C-5 (Figure 3.5). The structure of a monoterpene moiety (C-16–C-25) was suggested by ^{1}H-^{1}H COSY cross-peaks of H-16/H-17 and H-19/H_2-20/H-21 as well as HMBC correlations for H_3-25 with C-17, C-18, and C-19, and H_3-23 with C-21, C-22, and C-24. The connectivity among the sesquiterpene and monoterpene moieties forming a cyclohexene ring (C-8, C-9, and C-16–C-19) was evident from a ^{1}H-^{1}H COSY correlation of H-9/H_2-16 and an HMBC correlation for H-9 with C-19. Therefore, the planar structure of 22 was assigned as shown in Figure 3.4.

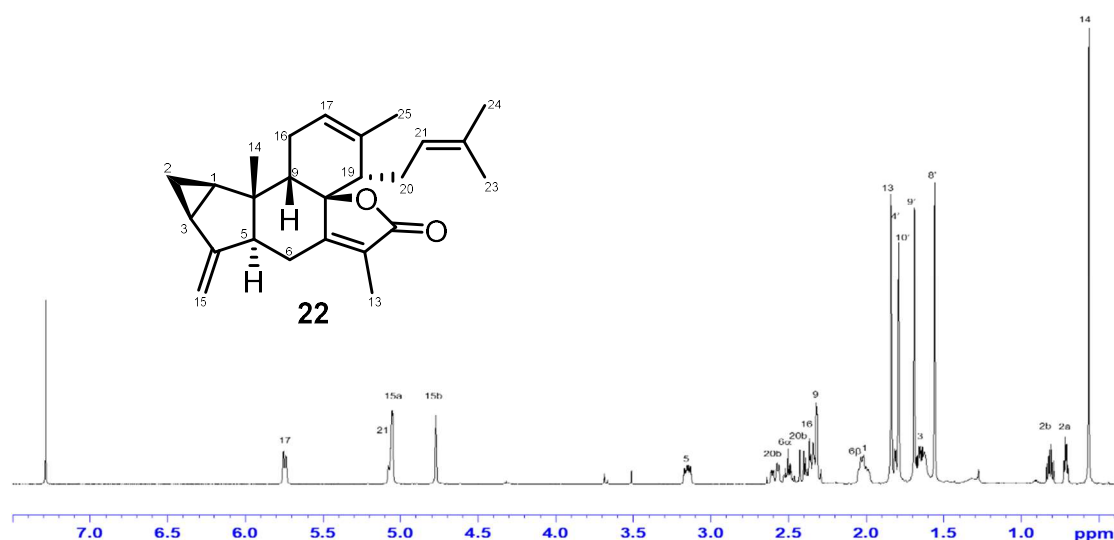**Figure 3.4.** ^{1}H NMR spectrum for sarcaglabrin A (22) in CDCl$_3$.

Table 3.1 ^{1}H and ^{13}C NMR data for sarcaglabrin A (**22**) in CDCl$_3$.

Position	**22**	
	δ_C	δ_H (J in Hz)
1	24.6	2.01 (m)
2	16.3	0.81, 0.71 (each, m)
3	24.2	1.68 (m)
4	152.8	-
5	54.6	3.15 (ddd, 12.0, 9.1, 3.5)
6	28.7	2.34, 2.00 (each, m)
7	166.2	-
8	95.2	-
9	50.0	2.32 (brs)
10	42.3	-
11	125.1	-
12	173.5	-
13	9.1	1.83 (3H, s)
14	22.1	0.56 (3H, s)
15	126.3	5.04, 4.77 (each, brs)
16	23.9	2.02 (2H, brs)
17	120.6	5.75 (d, 7.6)
18	141.6	-
19	57.1	1.81 (d, 3.7)
20	25.6	2.58, 2.40 (each, ddd, 17.7, 6.8, 1.7)
21	134.6	5.06 (dd, 9.3, 6.8)
22	122.4	-
23	17.9	1.56 (3H, s)
24	25.8	1.69 (3H, s)
25	24.5	1.79 (3H, s)

The relative configuration of **22** was elucidated by analysis of the NOESY spectrum (Figure 3.6). The β-orientations of CH$_2$-2, H-6, H-9, and Me-14 were arbitrarily assigned by NOESY cross-peaks of H$_3$-14/H-2β, H$_3$-14/H-6β, and H$_3$-14/H-9, while the α-orientations of H-1, H-3, and H-5 were elucidated by NOESY correlations for H-1/H-3, H-1/H$_2$-16, H-3/H-5, and H-5/H-16α. In addition, the 8R* and 19S* configurations were assigned by correlations for H$_2$-20/H-6α and H-5/H-20a. Thus, the relative configuration of sarcaglabrin A (**22**) was elucidated as shown at Figure 3.6.
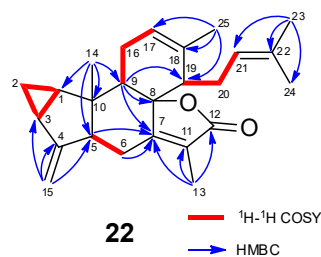
Figure 3.5. Selected ¹H-¹H COSY and HMBC correlations of sarcaglabrin A (**22**).
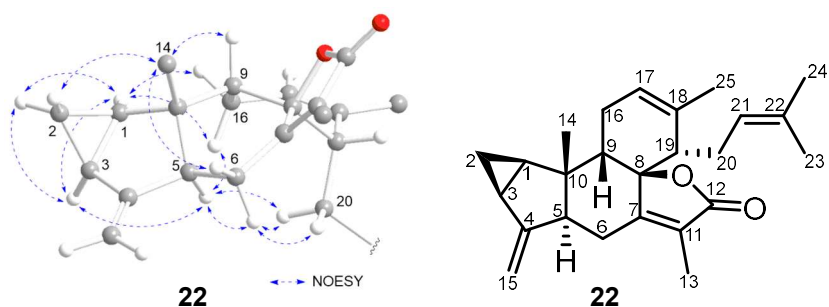
Figure 3.6. Selected NOESY correlations and relative stereochemistry for sarcaglabrin A (**22**) (protons of methyl groups and substituents at C-20 are omitted).

The CD spectrum of **22** measured in methanol exhibited positive Cotton effects at 256 and 202 nm, and a negative Cotton effect at 228 nm. The TDDFT {CAM-B3LYP/6-31G+(d)} calculated ECD spectrum of a (1*R*,3*S*,5*S*,8*R*,9*S*,10*S*,19*S*) enantiomer of **22** was in good agreement with the experimental spectrum (Figure 3.7), suggesting the 1*R*, 3*S*, 5*S*, 8*R*, 9*S*, 10*S*, and 19*S* configurations of sarcaglabrin A (**22**).
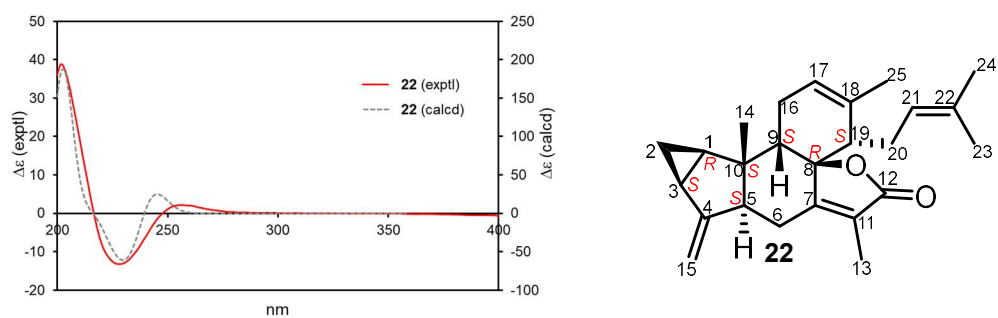
Figure 3.7. Experimental and calculated ECD spectra of sarcaglabrin A (**22**).

3.3.2 Sarcaglabrin B (23)

Sarcaglabrin B (**23**) was obtained as an optically active white amorphous powder $\{[\alpha]_D^{24}$ −69 (*c* 0.10, MeOH)$\}$. The HRESIMS revealed that **23** had the molecular formula of $C_{38}H_{44}O_{12}$ $\{m/z$ 715.2721 ([M+Na]$^+$, Δ −0.9 mmu)$\}$. The IR spectrum displayed absorptions at 3414 and 1752 cm^{-1} due to hydroxy and carbonyl functionalities, respectively. The ^{1}H NMR spectrum of **23** (Figure 3.8 and Table 3.2) showed the presence of one trisubstituted olefin, one 1,1-disubstituted olefin, eight sp^3 methines, six sp^3 methylenes, and six singlet methyls including one acetyl and one methoxy methyls. In addition, the ^{13}C NMR spectrum (Table 3.2) showed 38 carbon resonances, which were categorized into five carbonyl, eight olefinic, three oxygenated tertiary, two quaternary carbons, eight sp^3 methines, six sp^3 methylenes, and six methyls. Although these 1D NMR data were similar to a dimer of lindenane sesquiterpene, multistalide A (Figure 3.9) [58], the additional resonances due to a tigloyl group (C-1″–C-5″) were observed in **23**. In addition, the chemical shifts of H$_2$-13′ (δ_H 4.70, 4.44) of **23** were down-field shifted as compared with those of multistalide A. In the HMBC spectrum of **23** (Figure 3.10), H$_2$-13′ and H$_2$-15′ were correlated with the carbonyl carbons of the acetyl and tigloyl groups, respectively. These observations clearly revealed that **23** had the acetyl group at C-13′ and the tigloyl group at C-15′ in place of acetyl group in multistalide A. Therefore, the gross structure of **23** was concluded as shown in Figure 3.9.

Figure 3.8. ^{1}H NMR spectrum for sarcaglabrin B (**23**) in CDCl$_3$.
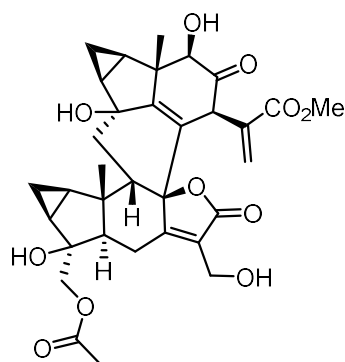
Figure 3.9. Structure of multistalide A.
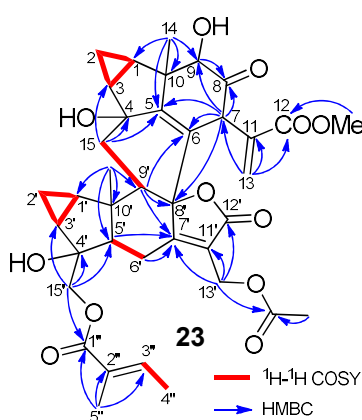
Figure 3.10. Selected ^{1}H-^{1}H COSY and HMBC correlations of sarcaglabrin B (**23**).

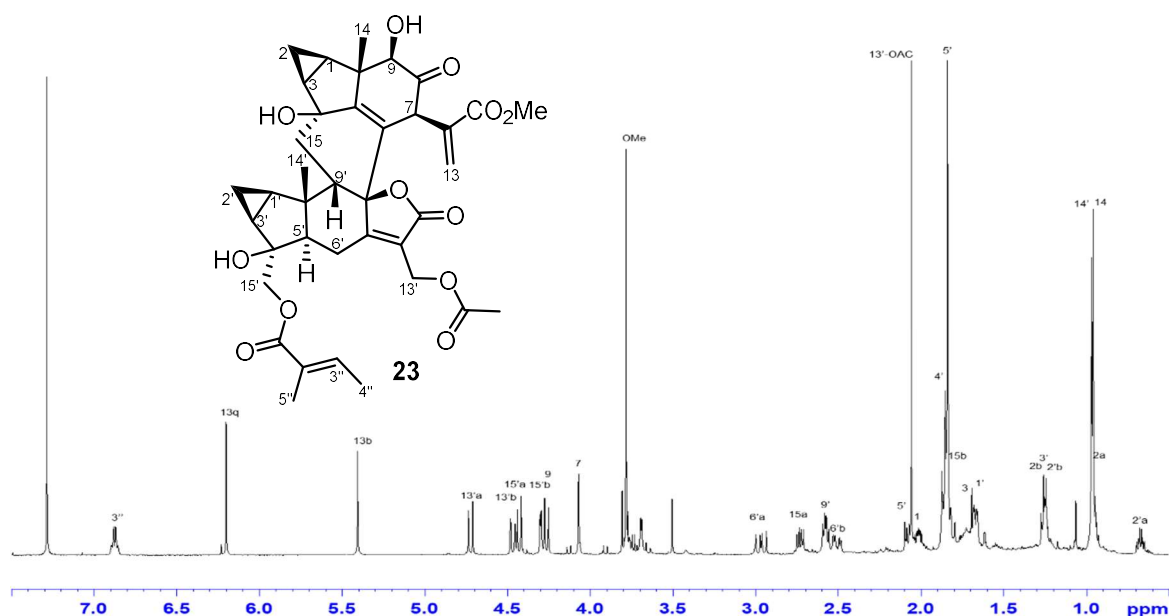The stereochemistry of **23** was determined as follows. The relative configuration of **23** was deduced to be the same as multistalide A by detailed analysis of the NOESY spectrum (Figure 3.11). Key cross-peaks of H-1/H-3, H-1/H-9, H-3/H-15, H-15/H-1', H-3'/H-1', H-1'/H-5', H-7/H-5', H-5'/H$_2$-15', and H-3'/H$_2$-15' implied that they were cofacial and arbitrarily assigned as α-oriented. NOESY correlations of H$_3$-14/H-2β, H$_3$-14/H-13a, H$_3$-14'/H-9', H-6'β/H$_3$-14', and H-2'β/H-14' suggested that they were β-oriented. The CD spectrum of **23** was similar to that of multistalide A [58]. In addition, the TDDFT {CAM-B3LYP/6-31G+(d)} calculated ECD spectrum for a (1*R*,3*S*,4*S*,7*R*,9*R*,10*S*,1'*R*,3'*S*,4'*S*,5'*S*,8'*S*,9'*S*,10'*S*) enantiomer of **23** was in good agreement with the experimental spectrum of **23** (Figure 3.12). Accordingly, the absolute configuration of **23** was established as depicted in Figure 3.12.

Table 3.2 ^{1}H and ^{13}C NMR data for sarcaglabrins B (**23**) and C (**24**) in CDCl$_3$.

| Position	23		24	
	δ_C	δ_H (*J* in Hz)	δ_C	δ_H (*J* in Hz)
1	26.6	1.99 (m)	29.2	1.93 (m)
2	10.1	1.23, 0.93 (each, m)	9.7	1.13, 0.92 (each, m)
3	30.8	1.83 (m)	29.7	1.67 (m)
4	79.4	-	77.4	-
5	160.9	-	164.7	-
6	124.6	-	122.5	-
7	49.1	4.05 (1H, s)	151.5	-
8	208.0	-	105.2	-
9	80.2	4.27 (brs)	75.4	3.81 (1H, s)
10	49.1	-	49.9	-
11	136.3	-	125.1	-
12	166.7	-	170.9	-
13	126.6	6.18, 5.32 (each, s)	10.6	1.59 (3H, s)
14	20.5	0.93 (3H, s)	14.1	0.80 (3H, s)
15	40.8	2.71, 1.78 (each, dd, 13.7, 7.2)	40.2	2.68, 1.68 (each, dd, 14.1, 6.9)
1'	26.6	1.65 (m)	26.6	1.56 (m)
2'	10.3	1.23, 0.65 (each, m)	9.7	1.12, 0.92 (each, m)
3'	29.5	1.66 (m)	29.8	1.80 (m)
4'	78.3	-	77.6	-
5'	54.1	2.06 (dd, 12.8, 6.5)	53.5	1.99 (dd, 11.6, 7.5)
6'	22.9	2.95, 2.48 (each, dd, 20.1, 13.3)	21.6	2.91, 2.30 (each, dd, 17.7, 6.9)
7'	168.3	-	170.8	-
8'	87.7	-	85.2	-
9'	50.4	2.55 (dd, 12.3, 7.8)	51.02	2.68 (dd, 12.2, 6.8)
10'	44.9	-	44.6	-
11'	126.0	-	123.6	-
12'	170.2	-	170.9	-
13'	55.2	4.70, 4.44 (each, d, 13.3)	55.3	4.81, 4.76 (each, d, 13.0)
14'	24.2	0.94 (3H, s)	24.3	0.96 (3H, s)
15'	70.4	4.40, 4.24 (each, d, 11.3)	70.9	4.16, 3.98 (each, d, 11.1)
1"	167.9	-	168.2	-
2"	127.9	-	128.2	-
3"	139.8	6.85 (ddd, 14.4, 6.3, 2.7)	138.6	6.88 (ddd, 15.3, 6.8, 1.1)
4"	14.7	1.82 (3H, d, 6.5)	14.6	1.81 (3H, d, 7.5)
5"	12.2	1.81 (3H, s)	12.3	1.84 (3H, s)
OMe-12	52.6	3.76 (3H, s)		
OMe-8			52.7	3.60 (3H, s)
OAc-15'	170.6	-	170.5	-
	20.6	2.03 (3H, s)	20.7	2.05 (3H,s)
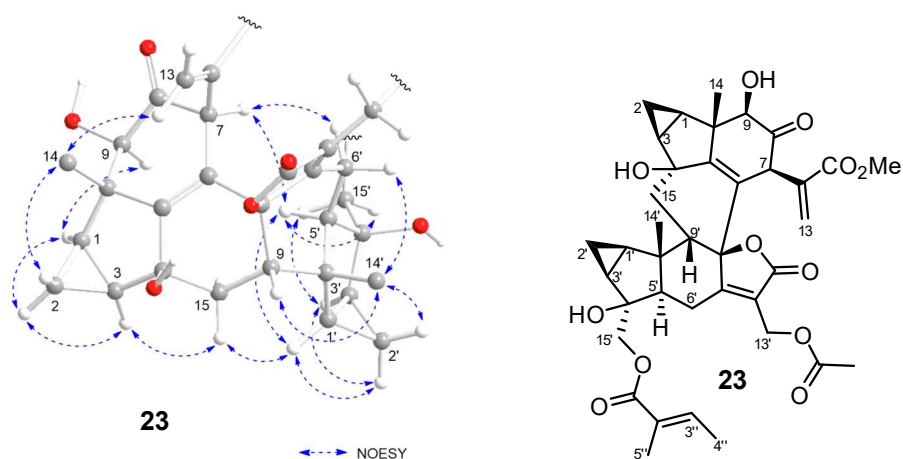
Figure 3.11. Selected NOESY correlations and relative stereochemistry for sarcaglabrin B (**23**) (protons of methyl groups and substituents at C-11, C-13', and C-15' are omitted).
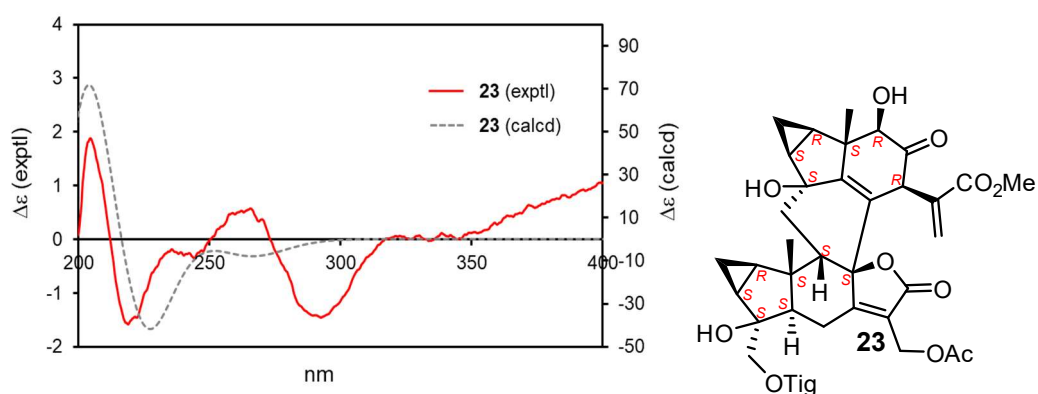
Figure 3.12. Experimental and calculated ECD spectra of sarcaglabrin B (**23**).

3.3.3 Sarcaglabrin C (24)

Sarcaglabrin C (**24**), obtained as an optically active white amorphous powder {$[\alpha]_D^{24}$ −23 (*c* 0.10, MeOH)}, had a molecular formula of $C_{38}H_{44}O_{12}$ as determined by the HREIMS {*m/z* 715.2726 ([M+Na]$^+$, Δ −0.4 mmu)}. The 1D NMR spectra (Table 3.2 and Figure 3.13) displayed the signals similar to those of a lindenane sesquiterpene dimer, sarcandrolide D (Figure 3.1) [45], except for the existence of the methoxy signal in **24**. Key HMBC correlation for methoxy protons with C-8 (Figure 3.14) revealed the position of the methoxy group at C-8 in **24**.
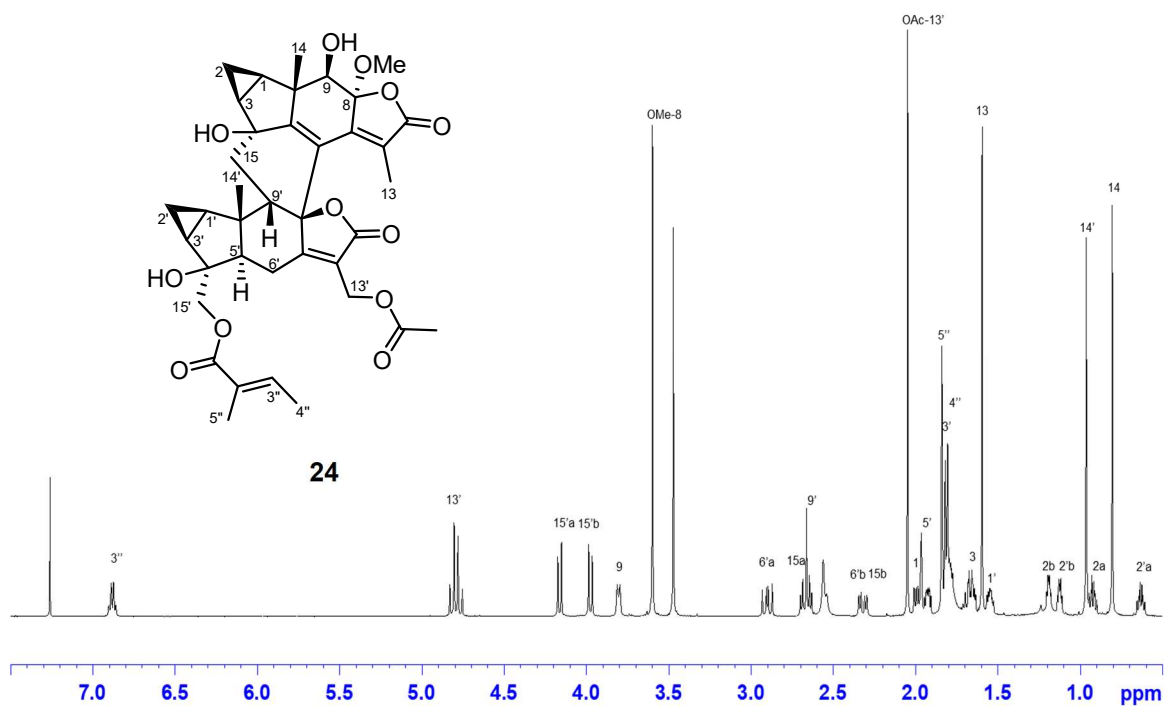
Figure 3.13. ^{1}H NMR spectrum for sarcaglabrin C (**24**) in CDCl3.
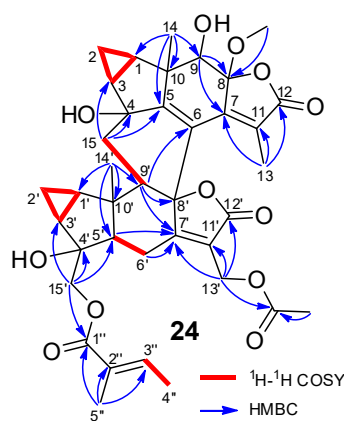
Figure 3.14. Selected ^{1}H-^{1}H COSY and HMBC correlations of sarcaglabrin C (**24**).

The relative configuration of **24** was deduced to be the same as sarcandrolide D by resemblance of their 1D NMR and NOESY data (Figure 3.15). Thus, the relative configuration of **24** was assigned as shown in Figure 3.15.
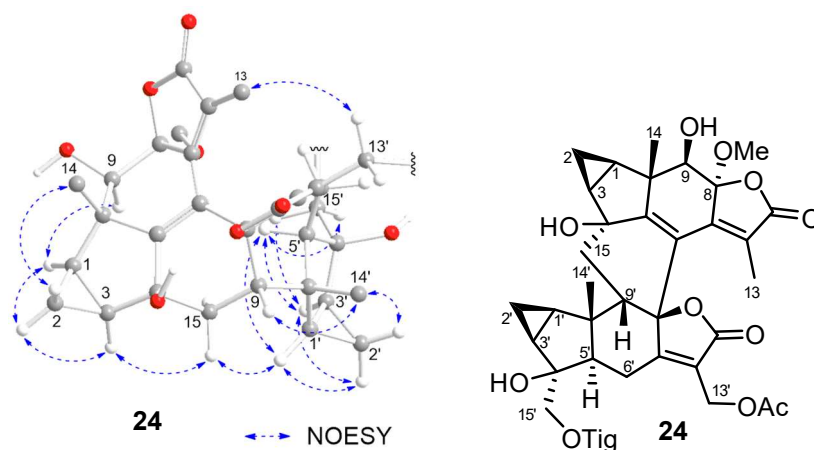
Figure 3.15. Selected NOESY correlations and relative stereochemistry for sarcaglabrin C (**24**) (protons of methyl groups and substituents at C-13' and C-15' are omitted).

The absolute configuration of sarcaglabrin C (**24**) was assigned by application of the ECD exciton chirality method. The split pattern of Cotton effects {246 nm ($\Delta\varepsilon$ +13.08) and 214 nm ($\Delta\varepsilon$ −28.26)} observed in **24** implied the right-handed helicity between two chromophores of α,β-unsaturated γ-lactone and conjugated dinone. Therefore, the absolute configuration of **24** was assigned as shown in Figure 3.16.
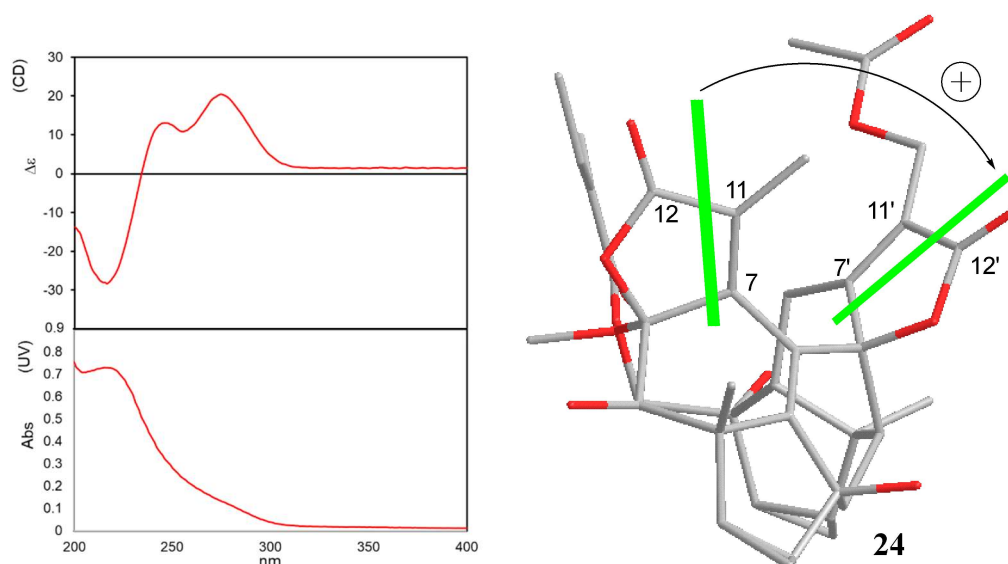
Figure 3.16. CD and UV spectra measured in MeOH and the stereoview of sarcaglabrin C (**24**). Bold lines denote electronic transition dipoles.

3.4 Summary

Phytochemical investigation on the aerial parts of *Sarcandra glabra* resulted in the isolation of 25 terpenoids (**22**–**46**), including three new terpenes, sarcaglabrins A–C (**22**–**24**) (Chart 2). The structures of sarcaglabrins A–C (**22**–**24**) was elucidated by spectroscopic analysis. Sarcaglabrin A (**22**) is a conjugate of lindenane type sesquiterpene and monoterpene, whereas sarcaglabrins B (**23**) and C (**24**) are new lindenane type sesquiterpene dimers. A conjugate biogenetically related to **22**, bolivianine [64], has been isolated from *Hedyosmum angustifolium* (Chloranthaceae). Similar to the proposed biogenetic pathway of bolivianine [65], sarcaglabrin A (**22**) might be generated by intermolecular condensation of chloranthalactone A (**26**) and a monoterpene, β-*E*-ocimene, via Diel-Alder cycloaddition. Moreover, **24** might be also generated from two lindenane sesquiterpenes by Diels−Alder reaction as shown in scheme 3.
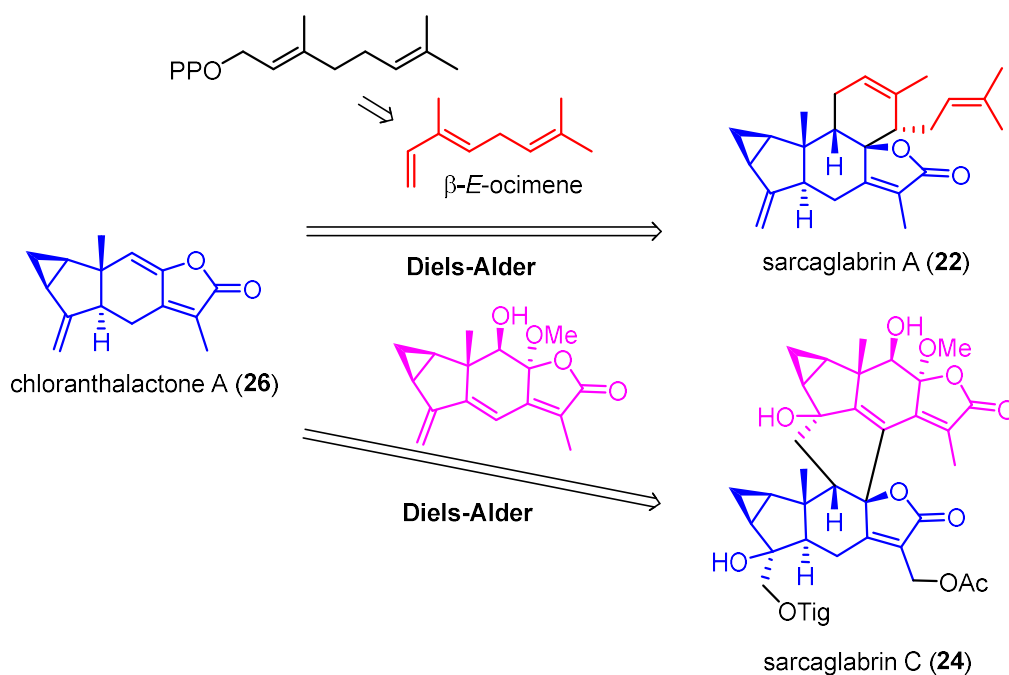
Scheme 3. Possible biogenetic pathway of sarcaglabrins A (**22**) and C (**24**).

43

| sarcaglabrin A (**22**) | sarcaglabrin B (**23**) | sarcaglabrin C (**24**) |
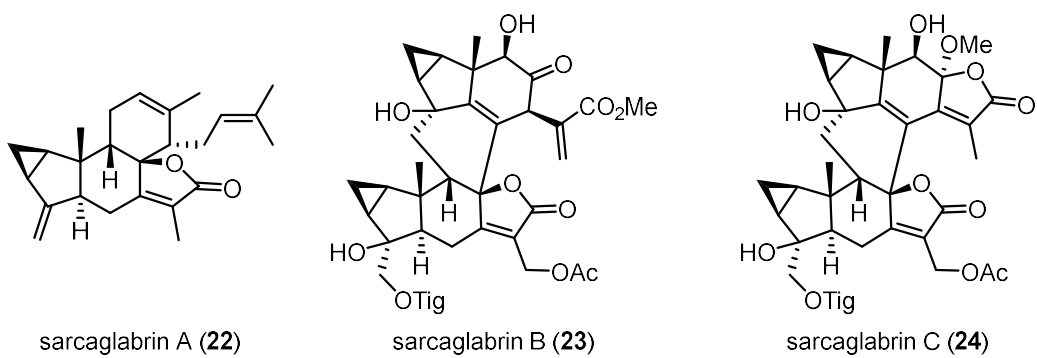
Chart 2. Structures of sarcaglabrins A–C (**22**–**24**).

Chapter 4 Chemical study on *Rhododendron molle* (Blume) G. Don

4.1 Introduction

Plants belonging to the genus *Rhododendron* (Ericaceae), comprising 8 subgenera with over 850 species, are evergreen or less often deciduous shrubs or trees mainly distributed in the Northern hemisphere [66]. Although *Rhododendron* plants cause intoxications, they have been used as herbal medicines for the treatments of inflammation, pain, common cold symptoms, skin ailments, and gastro-intestinal disorders. Previous chemical investigations of *Rhododendron* plants showed hundreds of secondary metabolites, many of which are flavonoids and diterpenes [67].

Rhododendron molle (Blume) G. Don (Figure 4.1), a small undershrub distributed around south China. *R. molle* has been used as a traditional medicinal plant for the treatments of analgesics, antiinflammatory, rheumatoid arthritis, and insecticides [67,68]. Recent study on this plant led to the isolation over 60 specific metabolites, many of which were diterpenes (Figure 4.2) [69–74]. As a part of our investigation on medicinal plants of Guangxi, the stems and leaves of *R. molle* collected in Guangxi was studied to isolate 23 natural products (**47**–**69**).

Figure 4.1. *Rhododendron molle* (Blume) G. Don.

rhodomollein XIX

rhodomollein XIV

rhodomollein F

rhodojaponin II
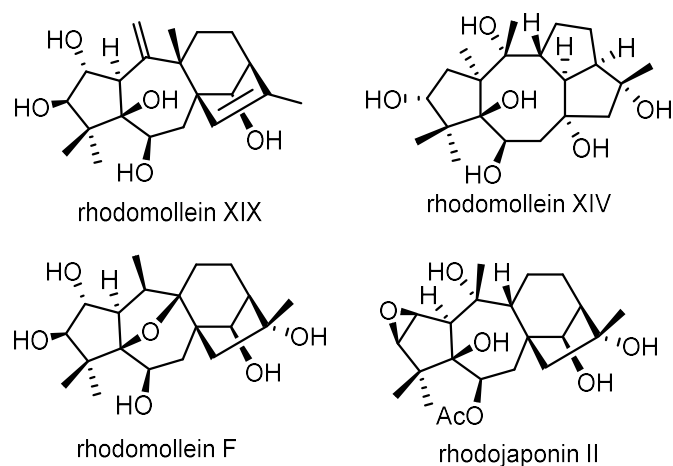
Figure 4.2. Previously isolated diterpenes from *Rhododendron molle.*

4.2 Extraction and isolation

The MeOH in room temperature extract from the stems and leaves (1.7 kg) of *Rhododendron molle* (Blume) G. Don collected at Guangxi was partitioned with EtOAc and H_2O. Repeated chromatographic separations of the EtOAc-soluble material (34.8 g) gave 23 compounds, including two new glycosides of orsellinic acid, compounds **47** and **48** (Scheme 4).

Stems and leaves of *Rhododendron molle* (dry, 1.8 kg)

extracted with MeOH

MeOH ext. (88.3 g)

partitioned between EtOAc/H_2O

EtOAc (34.8) H$_2$O (53.5 g)

a. MCl gel CHP-20P (MeOH/H_2O)
b. YMC gel ODS-A (MeOH/H_2O)
c. Sephadex LH-20 (MeOH/H_2O)
d. silica gel (CHCl$_3$/MeOH)
e. silica gel (*n*-hexane/EtOAc)
f. ODS on HPLC (MeOH/H_2O)

new compounds

47 (4.6 mg)
48 (3.2 mg)

known compounds

49 (2.2 mg)   **56** (10.2 mg)   **63** (6.3 mg)
50 (4.1 mg)   **57** (23.6 mg)   **64** (2.1 mg)
51 (7.5 mg)   **58** (31.2 mg)   **65** (2.3 mg)
52(6.2 mg)   **59** (93.7 mg)   **66** (4.3 mg
53 (3.2 mg)   **60** (12.3 mg)   **67** (4.2 mg)
54 (1.2 mg)   **61** (20.2 mg)   **68** (5.6 mg)
55 (4.2 mg)   **62** (3.2 mg)   **69** (3.2 mg)

Scheme 4. Isolation procedure for compounds **47**–**69**.

Compounds **49–69** (Figure 4.3) were identified as rhodojaponin III (**49**) [74], rhodomollein XVIII (**50**) [75], rhodomollein I (**51**) [76], 2-*O*-methylrhodomollein XI (**52**) [77], grayanotoxin XVIII (**53**) [78], grayanotoxin II (**54**) [79], quercetin-3-*O*-glucoside (**55**) [79], quercitrin (**56**) [81], hyperoside (**57**) [81], (−)-epicatechin (**58**) [82], (+)-catechin (**59**) [82], proanthocyanidin A-2 (**60**) [83], proanthocyanidin A-6 (**61**) [84], colosolic acid (**62**) [85], asiatic acid (**63**) [86], jacoumaric acid (**64**) [87], oleanolic aldehyde acetate (**65**) [88], maslinic acid (**66**) [89], 3-*O*-(*E*)-*p*-coumaroyl oleanolic acid (**67**) [90], 3-*O*-(*E*)-*p*-coumaroyl maslinic acid (**68**) [91], and 3-*O*-(*Z*)-*p*-coumaroyl oleanolic acid (**69**) [92] by comparison of their spectroscopic data with the literature data. Among these, **49–54** are grayanane type diterpenes, **55–58** are flavonoids and its glycosides, **60** and **61** are proanthocyanidins, and **62–67** are triterpenes.
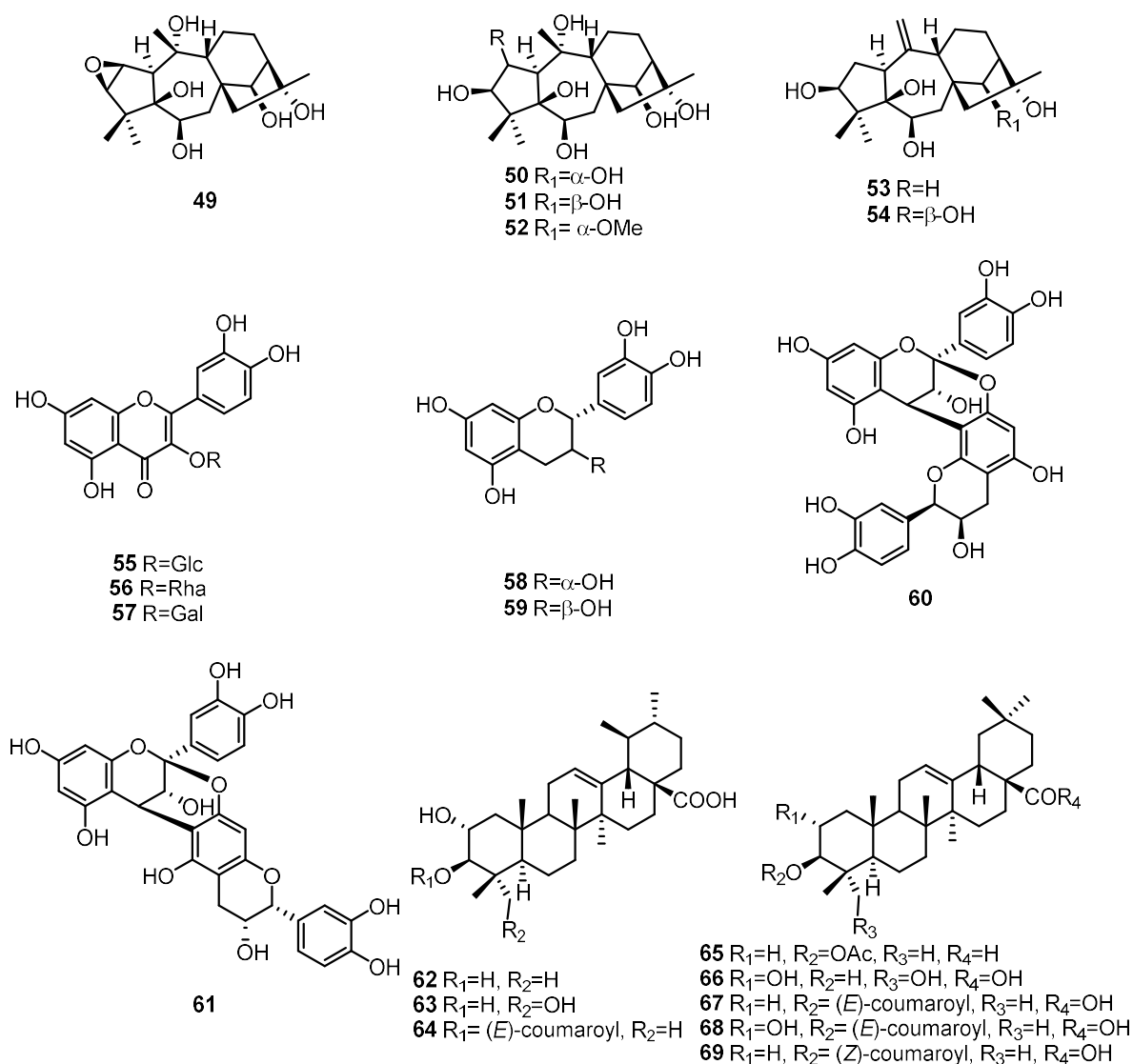

Figure 4.3. Known compounds isolated from *R. molle* in this study.

47

4.3 Structure elucidation of compounds 47 and 48

Compounds **47** and **48** were individually isolated as optical active colorless solids $\{[\alpha]^{24}_D -90\ (c\ 0.10,\ \text{MeOH})$ for **47**; $[\alpha]^{24}_D -24\ (c\ 0.10,\ \text{MeOH})$ for **48**$\}$. Their molecular formulae were assigned to be $C_{16}H_{22}O_9$ in light of HRESIMS data (m/z 381.1199 $[M+Na]^+$, Δ +3.5 mmu for **47**, m/z 381.1119 $[M+Na]^+$, Δ –4.4 mmu for **48**). Detailed analyses of the 1D NMR spectra (Figure 4.4 and Table 4.1) of **47** indicated the existence of an orsellinic acid moiety, two methoxy groups, and a glucosyl moiety. The absolute configuration of the glucosyl moiety was determined to be D according to the literature [93]. HMBC and NOESY analysis confirmed the substitution pattern of the orselllinic acid moiety including the position of the methoxy group at C-4 (Figure 4.5). The β-glycosidic linkage of the D-glucosyl moiety was indicated by the coupling constant of the anomeric proton ($J = 7.4$ Hz). An HMBC correlation for the methoxy proton to C-7 showed the existence of a methoxy carbonyl moiety. Accordingly, the structure of **47** was assigned as shown.
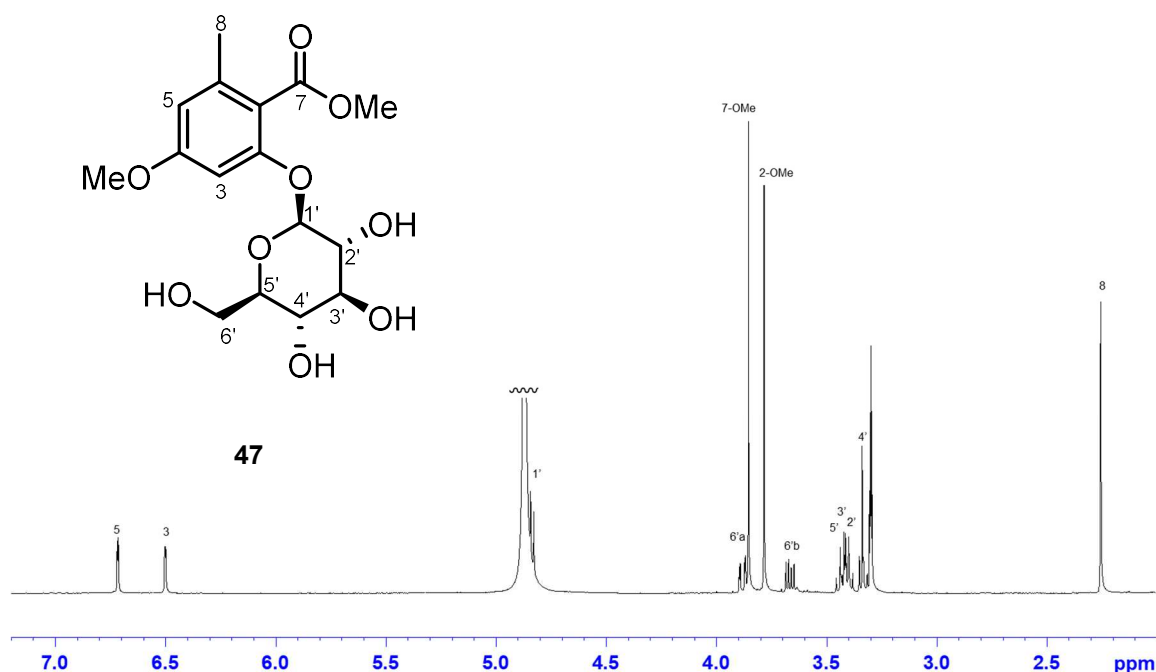
Figure 4.4. ^{1}H NMR spectrum for compound **47** in CD$_3$OD.
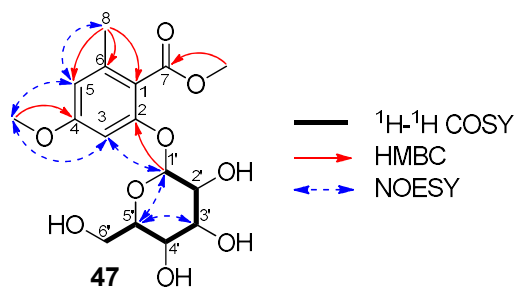
Figure 4.5. Selected 2D NMR spectra for compound **47** in CD₃OD.

Table 4.1. ¹H and ¹³C NMR data for compounds **47** and **48** in CD₃OD.

Position	47		48	
	δ_C	δ_H (*J* in Hz)	δ_C	δ_H (*J* in Hz)
1	118.4	-	118.3	-
2	139.5	-	139.5	-
3	111.3	6.50 (d, 2.1)	111.1	6.49 (d, 2.0)
4	163.1	-	163.1	-
5	101.4	6.72 (d, 2.1)	102.2	6.72 (d, 2.0)
6	157.9	-	158.2	-
7	170.5	-	170.6	-
8	20.1	2.26 (3H, s)	20.1	2.26 (3H, s)
4-OMe	55.9	3.79 (3H, s)	55.9	3.79 (3H, s)
7-OMe	52.6	3.86 (3H, s)	52.6	3.85 (3H, s)
1'	103.6	4.84 (d, 7.4)	101.6	5.17 (d, 6.9)
2'	75.0	3.41 (m)	72.2	3.54 (m)
3'	77.9	3.43 (m)	72.7	4.11 (t, 6.1)
4'	71.4	3.34 (brs)	68.7	3.55 (dd, 5.7, 2.8)
5'	78.4	3.41 (m)	76.1	3.83 (dd, 3.8, 2.8)
6'	62.6	3.88, 3.67 (each, m)	62.9	3.87, 3.65 (each, m)

The ^{1}H and ^{13}C NMR spectral data (Table 4.1 and Figure 4.6) of **48** were similar to those of **47** except for the resonances due to the sugar moiety. The sugar moiety of **48** was elucidated as β-D-allose based on HPLC analysis as well as by the coupling constant of anomeric proton ($J =$ 6.9 Hz). Therefore, **48** was determined as shown.
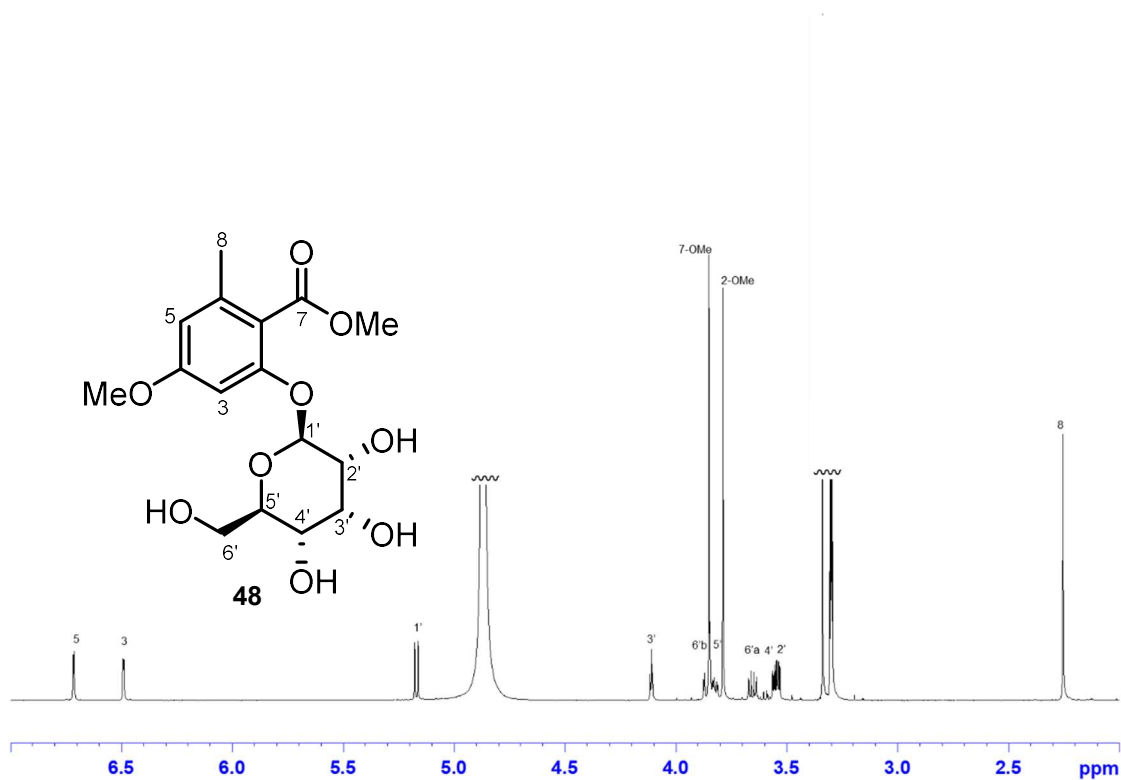
Figure 4.6. ^{1}H NMR spectrum for compound **48** in CD$_3$OD.

4.4 Summary

Phytochemical investigation on the leaves and stems of *R. molle* was carried out to give 23 natural products (**47–69**), including two new glycosides of orsellinic acid (**47** and **48**). **47** and **48** are the first methyl orsellinate with sugar moieties at C-2. Compounds **61–62**, **64–65**, **67–69** were isolated from *R. molle* for the first time. As biological activities of these compounds, an intense deterring oviposition activity of Rodojaponin III (**49**) against various insects [95], high cytotoxicity of rhodomolein XVIII (**50**) [96] and rhodomollein I (**51**) [97].

Chart 3. Structures of compounds **47–48**.

Chapter 5 Chemical studies on *Phyllanthus urinaria* L. and *Macrosolen cochinchinensis* (Lour.) Tiegh.

5.1 Introduction

Phyllanthus, a large genus of the family Phyllanthaceae, includes about 800 species widely distributed in tropical and subtropical areas. More than 20 species of *Phyllanthus* plants have been traditionally used in various countries [98,99]. Among others, 17 species found in Guangxi have been used in Zhuang or Yao medicines for the treatment of jaundice, hepatitis B, and painful disorders [100]. Previous phytochemical investigations on *Phyllanthus* plants resulted in the isolations of triterpenes, limonoids, lignans, tannins, coumarins, flavonoids, alkaloids, saponins, and phenylpropanoids [101,102]. Among others, phainanolide A, phyllanthoid A, and phainanoids A are structurally interesting (Figure 5.2), while englerin A exhibited a selective inhibitory effect on renal cancer cell growth [103−106].

In contrast, *Macrosolen* (Loranthaceae) plants, commonly known as mistletoe, are the aerial hemiparasites, which attach to the stems of trees through their haustoria to derive nutrients and water [107,108].

Macrosolen cochinchinensis (Lour.) Tiegh. grows on various host trees belonging to the families of Fagaceae, Theaceae, and Moraceae in the montane broadleaved evergreen forests. *M. cochinchinensis* has been used as a herbal medicine for muscle swelling and sprains, bone fractures, headaches, postpartum, and cancer in various countries [109,110]. The isolation of some flavonoids and triterpenes from this species have been reported (Figure 5.3).

In our research on the constituents of medicinal plants seen in Guangxi, the aerial parts of *Phyllanthus urinaria* and those of *M. cochinchinensis* (Figure 5.1) collected in Guangxi were investigated.
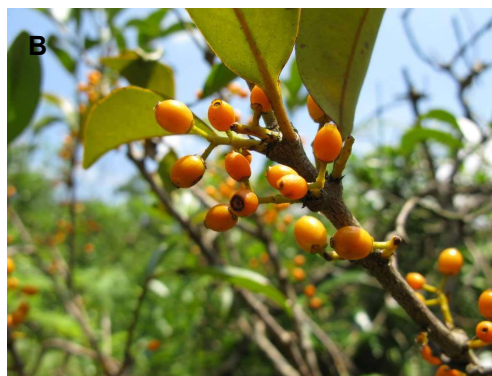
Figure 5.1. *Phyllanthus urinaria* L (**A**) and *Macrosolen cochinchinensis* (Lour.) Tiegh (**B**).

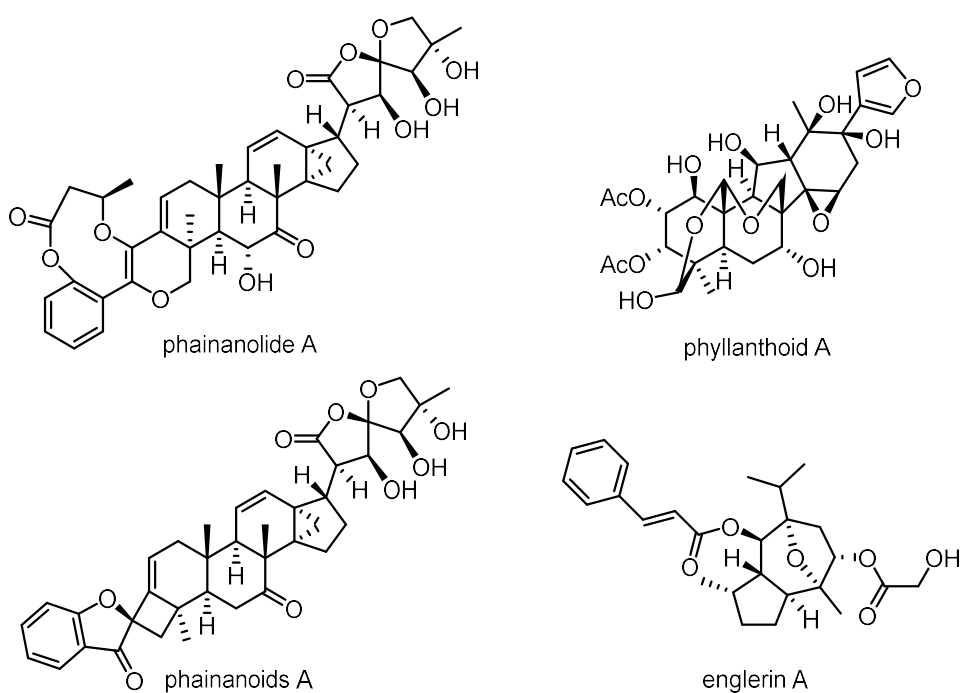phainanolide A

phyllanthoid A

phainanoids A

englerin A

Figure 5.2 Previously isolated compounds from the *Phyllanthus* plants.
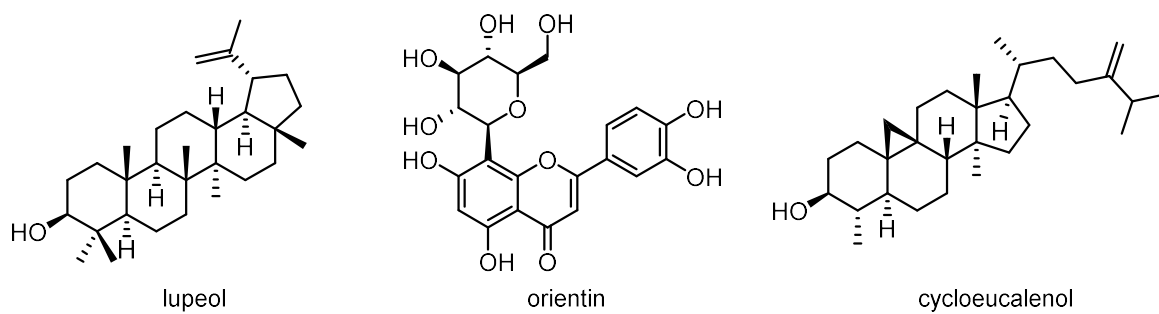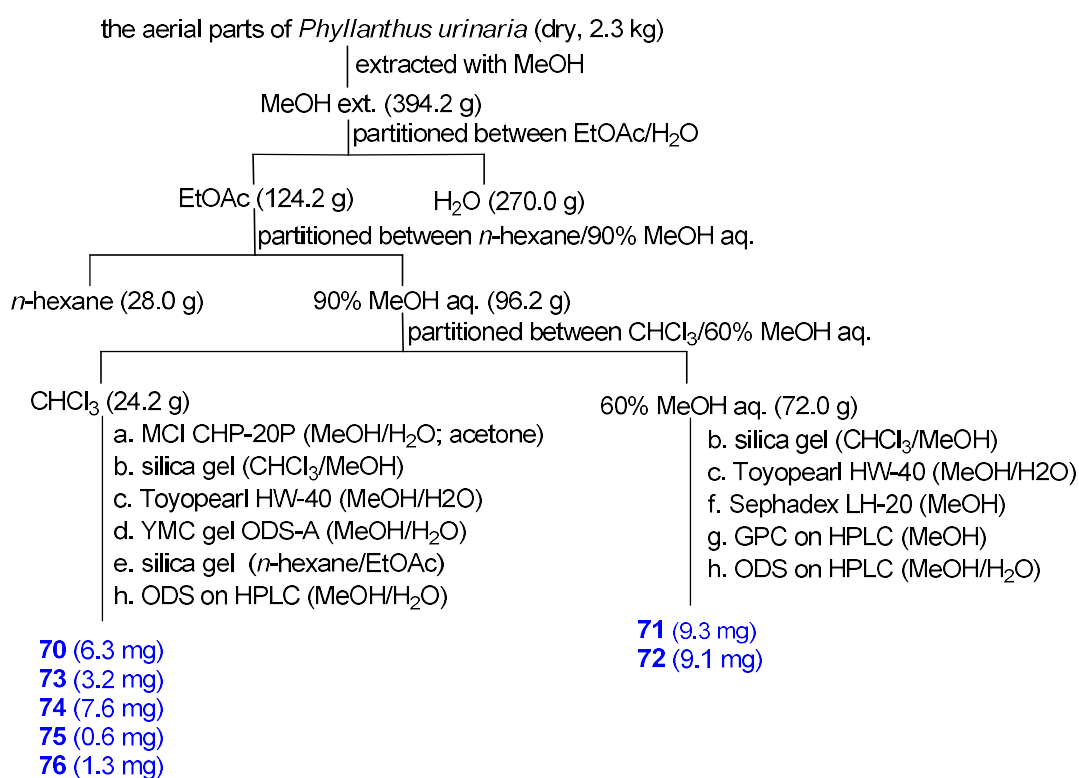

lupeol

orientin

cycloeucalenol

Figure 5.3. Previously isolated compounds from *Macrosolen cochinchinensis*.

5.2 Extraction and isolation

The air-dried aerial parts of *P. urinaria* (2.3 kg) collected in Guangxi were extracted with MeOH in room temperature. The MeOH extract (282.6 g) was partitioned with H_2O and EtOAc. The EtOAc-soluble fraction was further partitioned between *n*-hexane and 90% MeOH aq. The 90% MeOH aq.-soluble fraction was finally partitioned between $CHCl_3$ and 60% MeOH aq. The $CHCl_3$-soluble fraction (24.2 g) were subjected to column chromatographies repeatedly to give seven compounds (**72–76**). Compounds **70** and **71** were isolated from the 60% MeOH aq.-soluble fraction (32.5 g) (Scheme 5.1).

Similarly, the MeOH extract from the aerial parts of *M. cochinchinensis* (dry, 5 kg) was partitioned with EtOAc and water. Repeated chromatographic separations (Scheme 5.2) of the EtOAc-soluble material gave six known compounds (**77–82**) (Figure 5.5).

the aerial parts of *Phyllanthus urinaria* (dry, 2.3 kg)
| extracted with MeOH

MeOH ext. (394.2 g)
| partitioned between EtOAc/H_2O

EtOAc (124.2 g)　　　　H_2O (270.0 g)
| partitioned between *n*-hexane/90% MeOH aq.

n-hexane (28.0 g)　　　90% MeOH aq. (96.2 g)
| partitioned between $CHCl_3$/60% MeOH aq.

$CHCl_3$ (24.2 g)
a. MCI CHP-20P (MeOH/H_2O; acetone)
b. silica gel ($CHCl_3$/MeOH)
c. Toyopearl HW-40 (MeOH/H2O)
d. YMC gel ODS-A (MeOH/H_2O)
e. silica gel (*n*-hexane/EtOAc)
h. ODS on HPLC (MeOH/H_2O)

70 (6.3 mg)
73 (3.2 mg)
74 (7.6 mg)
75 (0.6 mg)
76 (1.3 mg)

60% MeOH aq. (72.0 g)
b. silica gel ($CHCl_3$/MeOH)
c. Toyopearl HW-40 (MeOH/H2O)
f. Sephadex LH-20 (MeOH)
g. GPC on HPLC (MeOH)
h. ODS on HPLC (MeOH/H_2O)

71 (9.3 mg)
72 (9.1 mg)

Scheme 5.1. Isolation procedure for compounds **70–76**.

extracted with MeOH

MeOH ext. (132.7 g)

partitioned between EtOAc/H$_2$O

EtOAc (23.8 g)

a. Sephadex LH-20 (MeOH)
b. MIC gel CHP-20P MeOH/H$_2$O)
c. YMC gel ODS-A (MeOH/H$_2$O)
d. MCI CHP-20P (MeOH/H$_2$O)
e. GPC on HPLC (MeOH)
f. silica gel (*n*-hexane/Acetone)
g. ODS on HPLC (MeCN/H$_2$O)

H$_2$O (43.5 g)

partit between *n*-BuOH/H$_2$O

n-BuOH (64.6 g) H$_2$O (43.5 g) Insoluble (12.9 g)

77 (38.8 mg)
78 (8.7 mg)
79 (26.6 mg)
80 (2.1 mg)
81 (7.2 mg)
82 (1.7 mg)
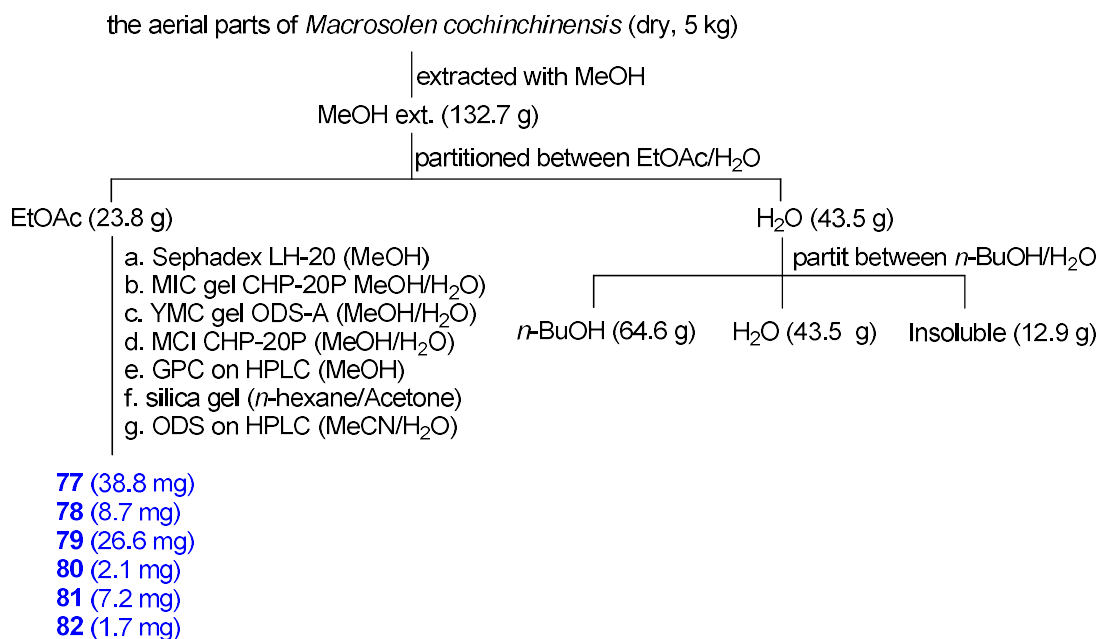
Scheme 5.2. Isolation procedure for compounds **77**–**82**.

Structures of compounds **70–76** (Figure 5.3) isolated from *P. urinaria* were identified as aquilegiolide (**70**) [110], menisdaurilide (**71**) [112], (−)-β-sitosterol glucoside (**72**) [113], aurantiamide (**73**) [114], asperglaucide (**74**) [114], (−)-*O*-methylcubebin (**75**) [115], and jolkinol B (**76**) [116]. Compounds **77–82** isolated from *M. cochinchinensis* were identified to be lyoniresinol (**77**) [117], sandaracopimaric acid (**78**) [118], 3,4-dehydrotheaspirone (**79**) [119], syringic acid (**80**) [120], 2-hydroxy-3-methoxybenzonic acid (**81**) [121], and 3-hydroxy-2-methoxybenzoic acid (**82**) [122] by comparison of the spectroscopic data with the literature data.

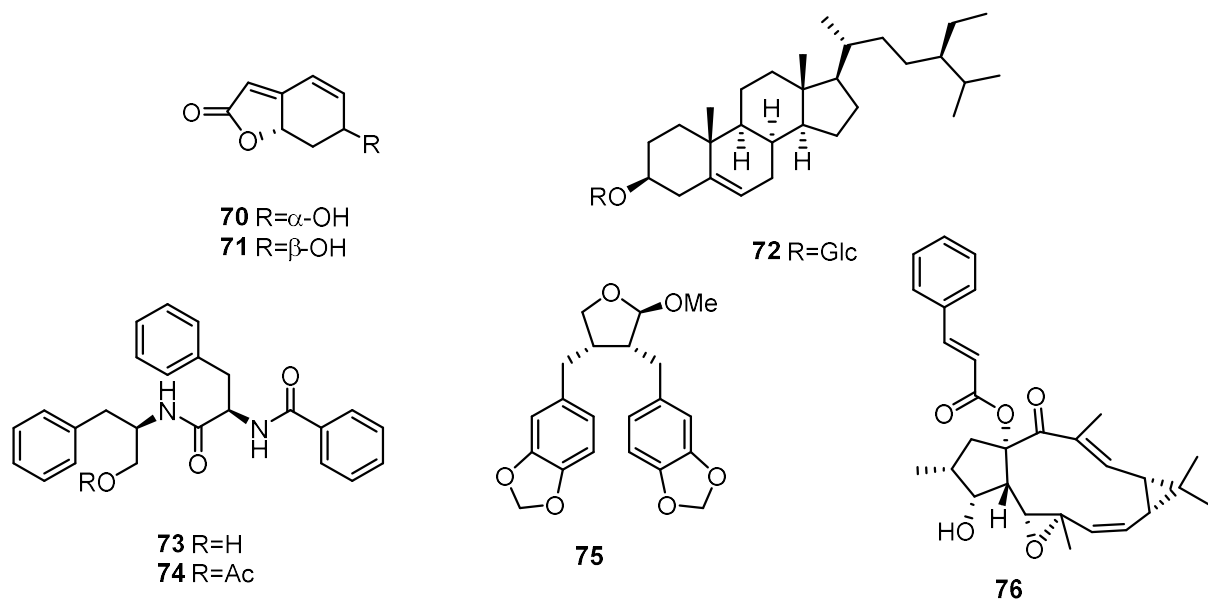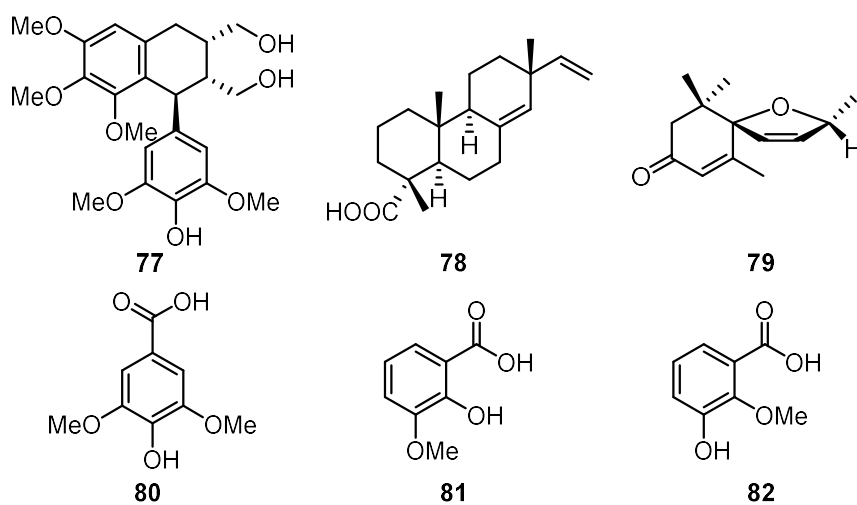**Figure 5.4.** Known compounds (**70–76**) isolated from the aerial parts of *P. urinaria* in this study.

70 R=α-OH
71 R=β-OH
72 R=Glc
73 R=H
74 R=Ac
75
76

77
78
79
80
81
82

Figure 5.5. Known compounds isolated from *M. cochinchinensis* in this study.

5.3 Summary

Seven compounds (**70**–**76**) were isolated from the aerial parts of *Phyllanthus urinaria*. Compounds **70**, **73**–**75** were firstly obtained from this plant. Cytotoxicty of aquilegiolide (**70**) and menisdaurilide (**71**) [123], and antibacterial activity of methylcubebin (**75**) [124] were reported previously.

Investigation of the MeOH extract from the aerial parts of *M. cochinchinensis* afforded six known compounds, lyoniresinol (**77**), sandaracopimaric acid (**78**), 3,4-dehydrotheaspirone (**79**), syringic acid (**80**), 2-hydroxy-3-methoxybenzonic acid (**81**), and 3-hydroxy-2-methoxybenzoic acid (**82**), whose structures were elucidated by comparisons of spectroscopic data with those reported in the references. Amoug others, lyoniresinol (**77**) and 3,4-dehydrotheaspirone (**79**) were firstly isolated from *M. cochinchinensis*. 3,4-Dehydrotheaspirone (**79**) was previously shown to have antiproliferative activity against cancer cells (HeLa, A-549 and MCF-7) [119].

Chapter 6 Conclusion

This research focused on searching new specialized metabolites from medicinal plants of Guangxi Zhuang autonomous region, China. The chemical constituents of five medicinal plants (*Munronia pinnata*, *Sarcandra glabra*, *Rhododendron molle*, *Phyllanthus urinaria*, and *Macrosolen cochinchinensis*) seen in Guangxi were investigated, resulting in the isolation and characterization of nine new limonoids (**1–9**), three terpenes (**22–24**), and two new glycosides of orsellinic acid (**47**, **48**) together with 68 known natural products.

From the MeOH extract of *Munronia pinnata*, nine new limonoids munropins A–I (**1–5**, **9**, and **6–8**). The structures of **1–9** were elucidated by detailed analyses of spectroscopic data. Munropins A (**1**) and B (**2**) are peieurianin type limonoids with novel γ-lactam moieties at C-17. Munropins C–E (**3–5**) and munropins G–I (**6–8**) are limonoids possessing a prieurianin skeleton with either α,β-unsaturated γ-lactone, acetyl, acetoxyacetyl, 3,4-dihydroxy-2,5-dimethoxytetrahydrofuran, α-substituted γ-hydroxy-α,β-unsaturated γ-lactone, and β-substituted γ-hydroxy-α,β-unsaturated γ-butenolactone moieties at C-17, respectively. Munropin F (**9**) was assigned as a nimbolinin limonoid. Munropins A (**1**) and B (**2**) are rare natural products with lactam moieties from plants. Three new terpenoids, sarcaglabrins A–C (**22–24**), were isolated from the aerial parts of *S. glabra*. Sarcaglabrin A (**22**) is a conjugate of lindenane type sesquiterpene and monoterpene possessing a unique 3/5/6/6/5 pentacyclic ring system. Sarcaglabrins B (**23**) and C (**24**) are new lindenane type sesquiterpene dimers. Phytochemical study on the MeOH extract of *Macrosolen cochinchinensis* gave two new glycosides of orsellinic acid (**47** and **48**).

Thus, the medicinal plants of Guangxi Zhuang autonomous region were shown as a rich source of new specialized metabolites. However, huge number of the medicinal plants still remain to be investigated. Further efforts should be continued to clarify their specialized metabolites.

Chapter 7 Experimental Section

7.1 General experimental procedures

Optical rotations were measured by a JASCO P-2200 digital polarimeter. UV, ECD, and IR spectra were recorded on a Hitachi U-3900H, a JASCO J-1500, and a JASCO FT-IR-6200 spectrophotometers, respectively. NMR spectra were measured by a Bruker AVANCE-500 instrument. The resonances of residual chloroform (δ_H 7.26 and δ_C 77.2) and methanol (δ_H 3.30 and δ_C 49.0) were used as internal references for ^{1}H and ^{13}C NMR chemical shifts, respectively. HRESIMS were recorded on a Waters LCT PREMIER 2695. Column chromatography was performed with silica gel 60N (63-210 μm, Kanto Chemical), MCI gel CHP-20P (75-150 μm, Mitsubishi Chemical), YMC gel ODS-A (S-50 μm, YMC Co., Ltd.), and Sephadex LH-20 (25-100 μm, GE Health Care). HPLC was performed on Asahipak GS-310 2G (GPC SHOWA DENKO), COSMOSIL 5C$_{18}$-AR-II (5 μm, 20×250 mm), and COSMOSIL 5C$_{18}$-MS-II (5 μm, 20×250 mm).

7.2 Experimental procedure of chapter 2

7.2.1 Plant material

Aerial parts of *Munronia pinnata* (Wall.) W. Theob. was collected at Jingxi, Guangxi Zhuang Autonomous Region, China, in May, 2017. A voucher specimen (17-JG-001) was deposited at the herbarium of Graduate School of Pharmaceutical Sciences, Tokushima University.

7.2.2 Extraction and isolation

The dried aerial parts of *M. pinnata* (1.64 kg) were extracted with MeOH (3 L) for three times at room temperature to give the extract (111.4 g), which was partitioned with EtOAc and water. The EtOAc-soluble material (34.2 g) was subjected to passage over a silica gel column, eluting with a gradient of *n*-hexane and EtOAc (from 90:10 to 25:75) to yield 12 fractions (frs. 1−12).

Fr. 5 was separated by MCI gel CHP20P column chromatography (MeOH) to give six fractions (frs. 5.1−5.6). Fr. 5.2 was subjected to YMC gel ODS-A column chromatography (H$_2$O/MeOH) to afford seven fractions (frs. 5.2.1−5.2.7). Fr. 5.2.4 was purified by silica gel column (CHCl$_3$/MeOH) to yield methyl-*ent*-4-*epi*-agath-18-oate (**14**, 13.1 mg).

Fr. 7 was separated by MCI gel CHP20P column chromatography (MeOH) to give 11 fractions (frs. 7.1−7.11). Fr. 7.4 was loaded on a silica gel column to afford six fractions (frs. 7.4.1−7.4.6). Fr. 7.4.2 further purified by ODS HPLC (MeCN/H$_2$O) to give piscidinol B (**15**, 11.8 mg), bourjotinolone A (**16**, 3.2 mg), lanost-7-ene-3,24,25-triol (**17**, 25.6 mg), 2β,3β,4β-trihydroxypregna-16-one (**18**, 8.0 mg), and 7-oxo-stigmasterol (**19**, 12.3 mg). Fr. 7.4.5 was purified by ODS HPLC (MeCN/H$_2$O) to give 5α,8α-epidioxy-24ξ-methylcholesta-6,22-dien-3β-ol (**20**, 4.9 mg). Fr. 7.5 was separated by YMC gel ODS-A column (H$_2$O/MeOH) to yield six fractions (frs. 7.5.1−7.5.6). Stigmast-4-ene-3β,6α-diol (**21**, 9.9 mg) was isolated from fr. 7.5.2 by ODS HPLC (MeCN/H$_2$O).

Fr. 11 was separated by MCI gel CHP20P column chromatography (MeOH) to give five fractions (frs. 11.1−11.5). Fr. 11.1 was subjected to GPC on HPLC (MeOH) to afford seven fractions (frs. 11.1.1−11.1.7). Fr. 11.1.1 was purified by ODS HPLC (30% MeCN aq.) to give munropins C (**3**, 1.5 mg), D (**4**, 1.5 mg), and E (**5**, 3.6 mg), together with munronoid O (**12**, 0.8 mg). Fr 11.1.3 was separated by ODS HPLC to give munropin G (**6**, 3.2 mg) and (−)-sandaracopimaradiene (**13**, 22.0 mg). Munropins H (**7**, 2.5 mg) and I (**8**, 2.3 mg) were obtained from fr. 11.1.5 by ODS HPLC (35% MeCN aq.). Fr. 11.1.4 also was purified by ODS HPLC (30% MeCN aq.) to afford munronins C (**10**, 35.6 mg) and F (**11**, 52.3 mg).

Fr. 12 was separated by MCI gel CHP20P column chromatography (MeOH) to give six fractions (frs. 12.1−12.6). Fr. 12.1 was subjected to GPC on HPLC (MeOH) to yield five fractions (frs. 12.1.1−12.1.5). Fr. 12.1.2 was purified by ODS HPLC (20% MeCN aq.) to furnish munropins A (**1**, 8.6 mg) and B (**2**, 8.4 mg). Purification of fr. 12.1.3 by ODS HPLC (20% MeCN aq.) gave munropin F (**9**, 3.9 mg).

7.2.3 Munropin A (1)

Colorless solid; $[\alpha]_D^{21}$ +82 (*c* 0.10, MeOH); UV (MeOH) λ_{max} (log ε) 209 (4.2) nm; IR (KBr) ν_{max} 3430, 2956, 1748, and 1689 cm^{-1}; CD (MeOH) Δε (nm) +8.55 (220) and +6.13

(247); ^1H and ^{13}C NMR data (Table 2.1); HRESIMS m/z 608.2493 [M+Na]$^+$ (calcd for C$_{31}$H$_{39}$NO$_{10}$Na, 608.2472).

7.2.4 Munropin B (2)

Colorless solid; $[\alpha]_D^{21}$ +111 (c 0.10, MeOH); UV (MeOH) λ_{max} (log ε) 210 (4.4) nm; IR (KBr) ν_{max} 3426, 2955, 1747, and 1686 cm^{-1}; CD (MeOH) $\Delta\varepsilon$ (nm) +9.02 (219) and +7.67 (247); ^1H and ^{13}C NMR data (Table 2.1); HRESIMS m/z 652.2722 [M+Na]$^+$ (calcd for C$_{33}$H$_{43}$NO$_{11}$Na, 652.2734).

7.2.5 Munropin C (3)

Colorless solid; $[\alpha]_D^{21}$ +135 (c 0.10, MeOH); UV (MeOH) λ_{max} (log ε) 212 (4.2) nm; IR (KBr) ν_{max} 3430, 2956, 1748, and 1689 cm^{-1}; CD (MeOH) $\Delta\varepsilon$ (nm) +8.36 (220) and +5.62 (246); ^1H and ^{13}C NMR data (Table 2.2); HRESIMS m/z 609.2285 [M+Na]$^+$ (calcd for C$_{31}$H$_{38}$O$_{11}$Na, 609.2312).

7.2.6 Munropin D (4)

Colorless solid; $[\alpha]_D^{21}$ +79 (c 0.10, MeOH); UV (MeOH) λ_{max} (log ε) 211 (4.2) nm; IR (KBr) ν_{max} 3454, 2956, 1750, 1703, and 1639 cm^{-1}; CD (MeOH) $\Delta\varepsilon$ (nm) +7.82 (216) and +6.65 (248); ^1H and ^{13}C NMR data (Table 2.2); HRESIMS m/z 569.2340 [M+Na]$^+$ (calcd for C$_{29}$H$_{38}$O$_{10}$Na, 569.2363).

7.2.7 Munropin E (5)

Colorless solid; $[\alpha]_D^{21}$ +52 (c 0.10, MeOH); UV (MeOH) λ_{max} (log ε) 209 (3.8) nm; IR (KBr) ν_{max} 3443, 2954, 1740, and 1633 cm^{-1}; CD (MeOH) $\Delta\varepsilon$ (nm) +5.48 (220), +6.86 (246), and –1.13 (293); ^1H and ^{13}C NMR data (Table 2.2); HRESIMS m/z 585.2314 [M+Na]$^+$ (calcd for C$_{29}$H$_{38}$O$_{11}$Na, 585.2312).

7.2.8 Munropin G (6)

Colorless solid; $[\alpha]_D^{21}$ +22 (*c* 0.10, MeOH); UV (MeOH) λ_{max} (log ε) 210 (4.1) nm; CD (MeOH) $\Delta\varepsilon$ (nm) +4.13 (226) and +4.56 (246); ^{1}H and ^{13}C NMR data (Table 2.3); HRESIMS *m/z* 689.2756 [M+Na]$^+$ (calcd for $C_{33}H_{46}O_{14}Na$, 689.2785).

7.2.9 Munropin H (7)

Colorless solid; $[\alpha]_D^{21}$ −148 (*c* 0.10, MeOH); UV (MeOH) λ_{max} (log ε) 209 (4.6) nm; CD (MeOH) $\Delta\varepsilon$ (nm) +10.29 (202) and +3.28 (252); ^{1}H and ^{13}C NMR data (Table 2.4); HRESIMS *m/z* 741.2703 [M+Na]$^+$ (calcd for $C_{36}H_{46}O_{15}Na$, 741.2734).

7.2.10 Munropin I (8)

Colorless solid; $[\alpha]_D^{21}$ −127 (*c* 0.10, MeOH); UV (MeOH) λ_{max} (log ε) 210 (4.9) nm; CD (MeOH) $\Delta\varepsilon$ (nm) +12.66 (208) and +11.84 (248); ^{1}H and ^{13}C NMR data (Table 2.4); HRESIMS *m/z* 741.2724 [M+Na]$^+$ (calcd for $C_{36}H_{46}O_{15}Na$, 741.2734).

7.2.11 Munropin F (9)

Colorless solid; $[\alpha]_D^{21}$ +27 (*c* 0.10, MeOH); UV (MeOH) λmax (log ε) 206 (4.3) nm; IR (KBr) ν_{max} 3439, 2955, 1737, and 1642 cm^{-1}; CD (MeOH) $\Delta\varepsilon$ (nm) +8.96 (208) and +2.72 (244); ^{1}H and ^{13}C NMR data (Table 2.5); HRESIMS *m/z* 639.2766 [M+Na]$^+$ (calcd for $C_{33}H_{44}O_{11}Na$, 639.2781).

7.2.12 Calculation of ECD spectra of 1 and 3-5.

Conformational searches and DFT calculations were carried out on Spartan 18 program (Wavefunction Inc., Irvine, CA.) and Gaussian 09 program [125], respectively. A possible enantiomer of munropin A (5*R*,9*R*,10*R*,11*R*,12*R*,13*R*,14*S*,15*R*,17*R*-**1**) was submitted to conformational search at the Molecular Mechanics (MMFF) to give six initial conformers, which were further optimized by DFT calculations at the B3LYP/6-31G(d) level. The stable conformers with Boltzmann distributions over 1% were subjected to TDDFT calculations at the CAM-B3LYP/6-31G+(d) level in the presence of MeOH with a polarizable continuum model.

The resultant rotatory strengths of the lowest 30 excited states for each conformer were converted into Gaussian-type curves with half-bands (0.3 eV) using SpecDis v1.61 [126]. The calculated ECD spectrum of 5*R*,9*R*,10*R*,11*R*,12*R*,13*R*,14*S*,15*R*,17*R*-**1** was composed after correction based on the Boltzmann distribution of the stable conformers. Accordingly, the possible enantiomers (5*R*,9*R*,10*R*,11*R*,12*R*,13*R*,14*S*,15*R*,17*R*) of munropin C–E (**3**–**5**) were calculated in the same manner as **1**.

7.2.13 Evaluation of cytotoxicity

The human cancer cell lines (HeLa and A549) were cultured in DMEM supplemented with 5% FBS. All cells were incubated at 37 °C in a humidified atmosphere with 5% CO_2–95% air. Cells were seeded at 1 x 10^4 cells/well in a 96-well plate and preincubated for 24 h. Test samples were dissolved in small amounts of DMSO and diluted in the appropriate culture medium (final concentration of DMSO <1%). After removal of preincubated culture medium, 100 μL of medium containing various concentrations of test compound was added and further incubated for 48h. A cell proliferation assay was performed with the Cell Counting Kit-8 (WST-8; Dojindo, Japan) according to the manufacturer's instruction. Briefly, the WST-8 reagent solution (10 μL) was added to each well of a 96 well microplate containing 100 μL of cells in the culture medium at various densities, and the plate incubated for 2 h at 37°C. Absorbance was measured at 450 nm using a microplate reader.

7.3 Experimental procedure of chapter 3

7.3.1 Plant material

Aerial parts of *Sarcandra glabra* (Thunb.) Nakai were collected at Gongcheng, Guangxi Zhuang Autonomous Region, China in September 2018. A voucher specimen (18-JG-014) was deposited on the herbarium of Graduate School of Pharmaceutical Sciences, Tokushima University.

7.3.2 Extraction and isolation

The air-dried aerial parts of *S. glabra* (3.1 kg) were extracted with MeOH to give the extract (304.1 g), which was partitioned between EtOAc and H_2O. The EtOAc-soluble material (93.3 g) was subjected to MCI gel CHP-20P (MeOH/H_2O) to give 8 fractions.

Fr. 3 was separated by a silica gel column (CHCl$_3$/MeOH) to afford seven fractions (frs. 3.1–3.7). Fr. 3.2 was subjected to silica gel (*n*-hexane /EtOAc) column chromatography to give chloranthalactone E (**31**, 250 mg) and five fractions (fr. 3.2.1–fr. 3.2.5). Fr. 3.2.4 was purified by ODS HPLC (45% MeCN aq.) to yield sarcaglabrins B (**23**, 5.5 mg), and C (**24**, 5.1 mg), together with sarglabolide E (**41**, 3.6 mg). Fr. 3.6 was separated by ODS HPLC (31% MeCN aq.) to afford chlorahololide D (**36**, 30.4 mg) and henriol B (**43**, 17.6 mg).

Fractionation of fr. 4 by Sephadex LH-20 (MeOH/H_2O) column chromatography gave ten fractions (frs. 4.1–4.10). Purifications of fr. 4.3, and fr. 4.6–4.7 by ODS HPLC (35-65% MeCN aq.) afforded shizukanolide H (**33**, 23.0 mg), shizukaol C (**34**, 29.0 mg), chloramultiol D (**44**, 12.0 mg), multistalide B (**37**, 77.1 mg), shizukaol G (**38**, 5.6 mg), sarglabolide B (**39**, 21.0 mg), and sarglabolide C (**40**, 117.9 mg).

Fr. 5 was separated by a silica column (*n*-hexane/EtOAc) to afford seven fractions (fr. 5.1–5.7). Fr. 5.3 was further subjected to GPC on HPLC to give chloranthalactone A (**26**, 315.9 mg) as well as seven fractons (fr. 5.3.1–5.3.7). Fr. 5.3.3 was purified by ODS HPLC (35% MeCN aq.) to afford chloranthalactone B (**27**, 4.6 mg), chloranthalactone A photodimer (**28**, 3.1 mg), chlorajapolide F (**29**, 1.4 mg), and 8-*epi*-chlorajapolide F (**30**, 10.1 mg). Fr. 5.5 was loaded to YMC gel ODS-A column chromatography (MeOH/H_2O) to yield six fractions (fr. 5.5.1–5.5.6). Fr. 5.5.3 was purified by ODS HPLC (65% MeCN aq.) to give sarglaperoxide A (**25**, 1.1 mg) and chloranthalactone C (**32**, 256.3 mg). Fr. 5.6 was separated by a silica gel column (CHCl$_3$/MeOH) to afford five fractions (fr. 5.6.1–5.6.5). Fr. 5.6.4 was subjected to GPC on HPLC (MeOH) to give four fractions (fr. 5.6.4.1–5.6.4.4). Fr. 5.6.4.3 was purified by ODS HPLC (30% MeCN aq.) to give shizukaol D (**35**, 148.5 mg), spicachlorantin E (**42**, 14.9 mg), sarcandrolide F (**45**, 2.7 mg), and chloramultilide A (**46**, 13.1 mg).

Fr. 6 was separated by silica gel column chromatography (CHCl$_3$/MeOH) to give five fractions (frs. 6.1–6.5). Fr. 6.2 was purified by ODS HPLC (70% MeCN aq.) to yield sarcaglabrin A (**22**, 4.2 mg)

7.3.3 Sarcaglabrin A (22)

Colorless solid; $[\alpha]_D^{24}$ −26 (*c* 0.10, MeOH); UV (MeOH) λ_{max} (log ε) 210 (4.4) nm; IR (KBr) ν_{max} 2924, 1749, and 1591 cm^{-1}; CD (MeOH) Δε (nm) +38.83 (202), −13.18 (228), and +2.17 (256); ^{1}H and ^{13}C NMR data (Table 3.1); HRESIMS *m/z* 403.2028 [M+K]$^+$ (calcd for $C_{25}H_{32}O_2K$, 403.2039).

7.3.4 Sarcaglabrin B (23)

Colorless solid; $[\alpha]_D^{24}$ −68 (*c* 0.10, MeOH); UV (MeOH) λ_{max} (log ε) 210 (4.4) nm; IR (KBr) ν_{max} 3414, 2923, 1752, and 1594 cm^{-1}; CD (MeOH) Δε (nm) +1.89 (204), −1.58 (219), +0.56 (265), and −1.45 (292); ^{1}H and ^{13}C NMR data (Table 3.2); HRESIMS *m/z* 715.2721 [M+Na]$^+$ (calcd for $C_{38}H_{44}O_{12}Na$, 715.2730).

7.3.5 Sarcaglabrin C (24)

Colorless solid; $[\alpha]_D^{24}$ −23 (*c* 0.10, MeOH); UV (MeOH) λ_{max} (log ε) 220 (4.3) nm; IR (KBr) ν_{max} 3418, 2925, 1758, 1735 and 1593 cm^{-1};CD (MeOH) Δε (nm) −28.26 (214), +13.08 (246), and +20.49 (274); ^{1}H and ^{13}C NMR data (Table 3.2); HRESIMS *m/z* 715.2726 [M+Na]$^+$ (calcd for $C_{38}H_{44}O_{12}Na$, 715.2730).

7.3.6 Calculation of ECD sarcaglabrins A (22) and B (23)

The ECD spectrum of a possible enantiomers of sarcaglabrin A (1*R*,3*S*,5*S*,8*R*,9*S*,10*S*,19*S*-**22**) and sarcaglabrin B (1*R*,3*S*,4*S*,7*R*,9*R*,10*S*,1'*R*,3'*S*,4'*S*,5'*S*,8'*S*,9'*S*,10'*S*-**23**) were calculated in the same manner as described as **1**.

### 7.4 Experimental procedure of chapter 4

7.4.1 Plant material

The stems and leaves of *Rhododendron molle* (Blume) G. Don were collected at Gongcheng, Guangxi Zhuang Autonomous Region, China in June 2018. A voucher specimen (18-JG-013)

was deposited on the herbarium of Graduate School of Pharmaceutical Sciences, Tokushima University.

7.4.2 Extraction and isolation

The stems of *R. molle* (1.1 kg) were extracted with MeOH at room temperature to give the extract (49.1 g), which was partitioned between EtOAc and H_2O. The EtOAc-soluble-material (17.7 g) was subjected to repeated column chromatographies as shown in Scheme 8.1, resulting in the isolation of 15 compounds (**47−49**, **51**, **54−61**, **65**, **67**, **69**). In contrast, the leaves of *R. molle* (1.1 kg) were preformed same as the isolation scheme of the stems to afford 8 compounds (**50**, **52**, **53**, **62−64**, **66**, **68**) (Scheme 8.2).
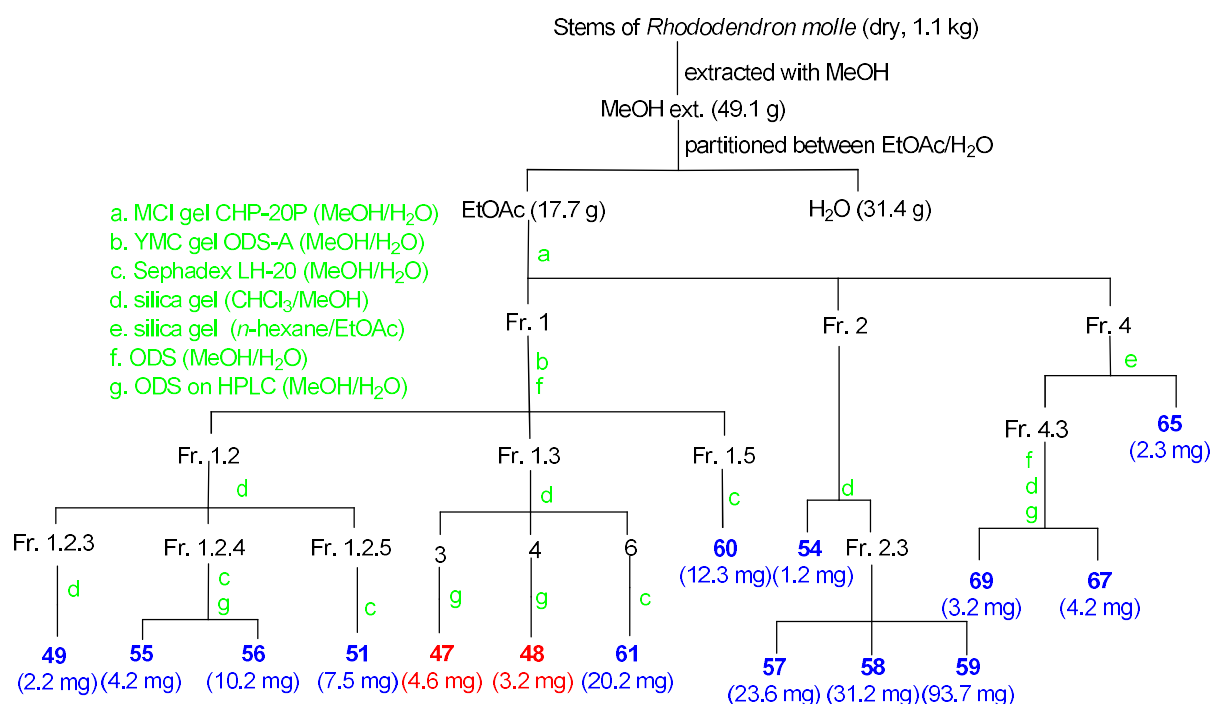
Scheme 8.1. Isolation scheme for the stems of *R. molle*.
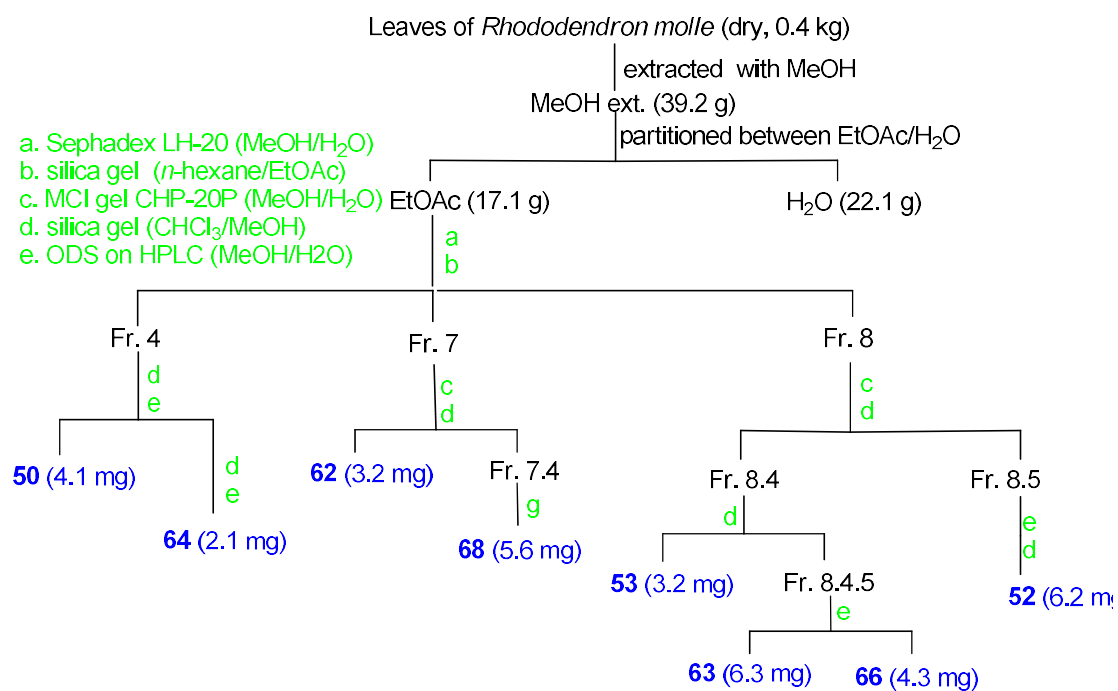
Scheme 8.2. Isolation scheme for the leaves of *R. molle*.

7.4.3 Compound 47

Colorless solid; $[\alpha]_D^{21}$ −90 (*c* 0.10, MeOH); UV (MeOH) λ_{max} (log ε) 246 (4.14) nm; ^{1}H and ^{13}C NMR data (Table 4.1); HRESIMS *m/z* 381.1199 [M+Na]$^+$ (calcd for $C_{16}H_{22}O_9Na$, 381.1162).

7.4.4 Compound 48

Colorless solid; $[\alpha]_D^{21}$ −24 (*c* 0.10, MeOH); UV (MeOH) λ_{max} (log ε) 246 (3.73) nm; ^{1}H and ^{13}C NMR data (Table 4.1); HRESIMS *m/z* 381.1118 [M+Na]$^+$ (calcd for $C_{16}H_{22}O_9Na$, 381.1162).

7.4.5 Identification of sugar moieties of 47 and 48

Compound **47** (0.5 mg) was treated with 1M HCl (2.5 mL) at 80 °C for 2 h. The reaction mixture was neutralized by 1M NaOH and evaporated to afford a residue. The residue and L-cysteine methyl ester hydrochloride (2.5 mg) was dissolved in pyridine (0.5 mL) and heated at 60 °C for 1 h, and then *o*-tolylisothiocyanate (50 μL) was added to the mixture and heated at

60 °C for 1 h. HPLC analysis of the reaction mixture [COSMOSIL 5C$_{18}$-AR-II (4.6 i.d. × 250 mm); CH$_3$CN/50 mM H$_3$PO$_4$ aq. (25:75), flow rate 1 mL/min, UV dection 254 nm, column temperature 35 °C] gave a peak at t$_R$ 17.1 min, which was identical to that of the derivative from authentic D-glucose prepared by the same procedure. In similar manner described above, the sugar moiety of **48** was confirmed to be D-allose (t$_R$ 65.5 min).
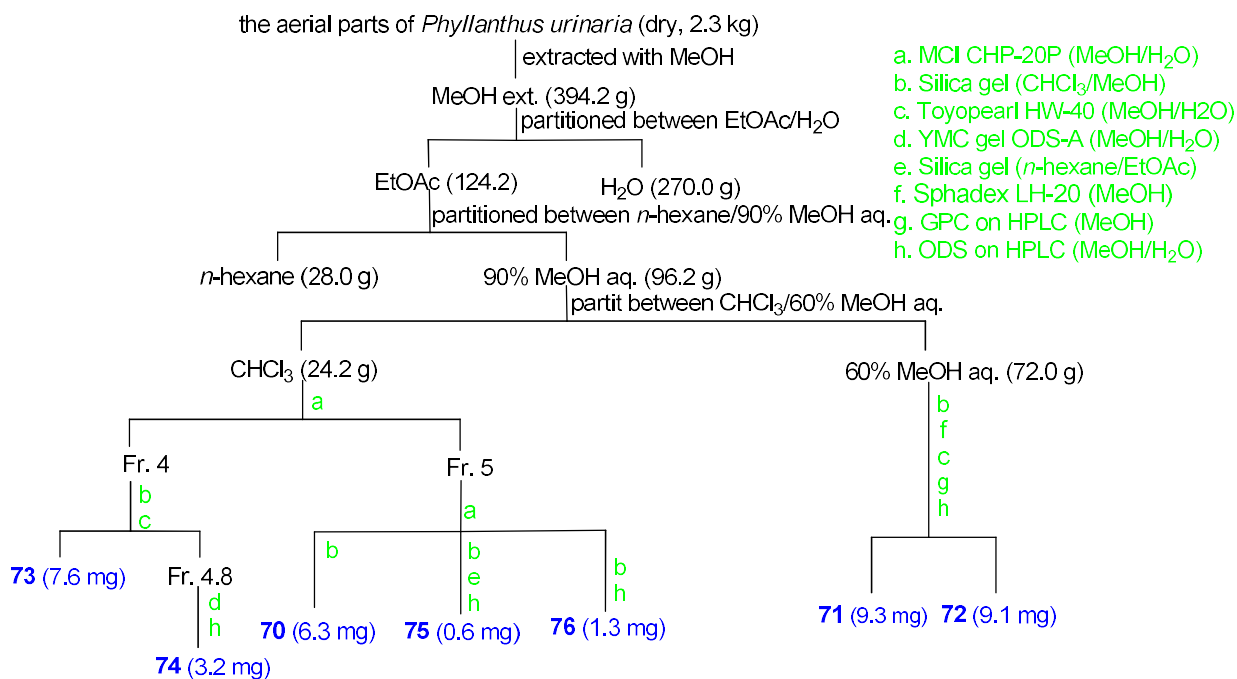
7.5 Experimental procedure of chapter 5

7.5.1 Plant materials

Aerial parts of *Phyllanthus urinaria* L. and *Macrosolen cochinchinensis* (Lour.) Tiegh were collected at Guilin, Guangxi Zhuang Autonomous Region, China, in February, 2017. the voucher specimen (17-JG-010 and 17-JG-011) was deposited at the herbarium of Graduate School of Pharmaceutical Sciences, Tokushima University.
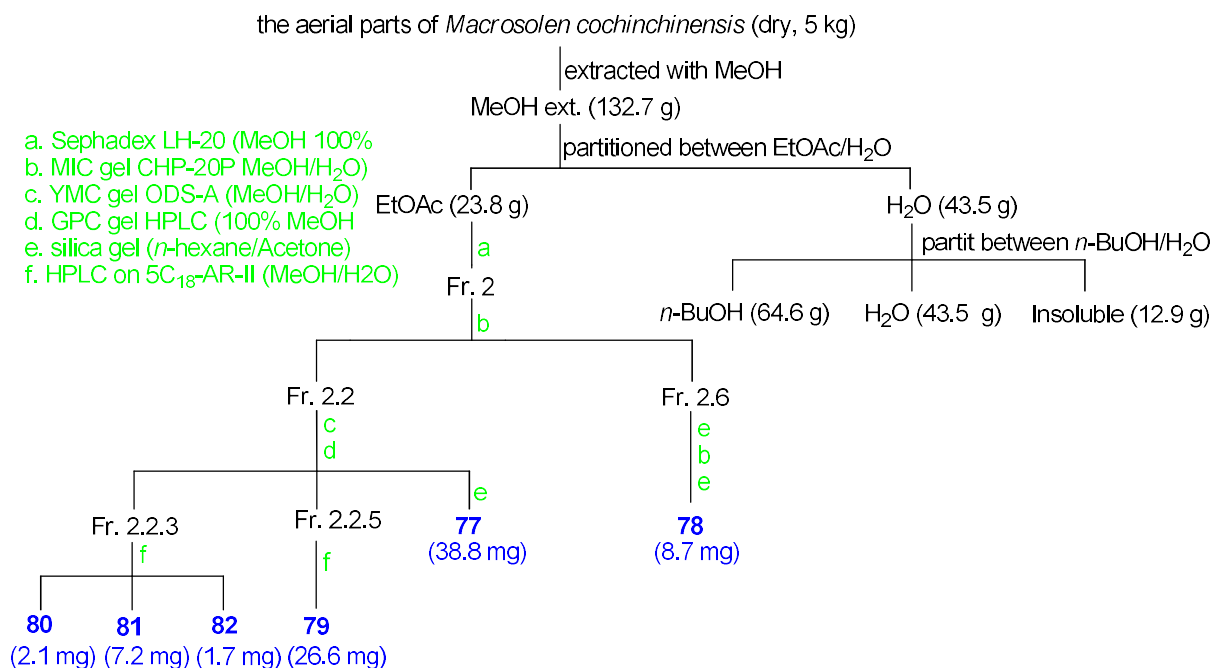
7.5.2 Extraction and isolation

The air-dried aerial parts of *P. urinaria* (2.3 kg) were extracted with MeOH (5 L) for three times at room temperature to give the extract (394.2 g), which was partitioned with *n*-hexane and 90% MeOH aq. The 90% MeOH-soluble material (34.2 g) was partitioned with CHCl$_3$ and 60% MeOH aq. The CHCl$_3$-soluble material (24.2 g) was subjected to column chromatographies to give known compounds **70**, **73-76**, while compounds **71** and **72** were isolated from the 60% MeOH-soluble material (72 g) (Scheme 9.1).

Similarly, the air-dried aerial parts (5.0 kg) of *M. cochinchinensis* were extracted with methanol at room temperature to give the extract (132.7 g), which was partitioned with EtOAc and water. The H$_2$O-soluble material (43.5 g) was partitioned with *n*-BuOH and H$_2$O. The EtOAc-soluble material (23.8 g) was subjected to column chromatographies to give six known compounds (**77**–**82**) (Scheme 9.2).

the aerial parts of *Phyllanthus urinaria* (dry, 2.3 kg)

extracted with MeOH

MeOH ext. (394.2 g)

partitioned between EtOAc/H₂O

EtOAc (124.2)   H₂O (270.0 g)

partitioned between *n*-hexane/90% MeOH aq.

n-hexane (28.0 g)   90% MeOH aq. (96.2 g)

partit between CHCl₃/60% MeOH aq.

CHCl₃ (24.2 g)   60% MeOH aq. (72.0 g)

a. MCI CHP-20P (MeOH/H₂O)
b. Silica gel (CHCl₃/MeOH)
c. Toyopearl HW-40 (MeOH/H2O)
d. YMC gel ODS-A (MeOH/H₂O)
e. Silica gel (*n*-hexane/EtOAc)
f. Sphadex LH-20 (MeOH)
g. GPC on HPLC (MeOH)
h. ODS on HPLC (MeOH/H₂O)

a

Fr. 4   Fr. 5

b
c

b   a

73 (7.6 mg)   Fr. 4.8

d
h

74 (3.2 mg)

b   b
e   h
h

70 (6.3 mg)   75 (0.6 mg)   76 (1.3 mg)

b
f
c
g
h

71 (9.3 mg)   72 (9.1 mg)

Scheme 9.1. Isolation scheme for the aerial parts of *P. urinaria*.

the aerial parts of *Macrosolen cochinchinensis* (dry, 5 kg)

extracted with MeOH

MeOH ext. (132.7 g)

partitioned between EtOAc/H₂O

a. Sephadex LH-20 (MeOH 100%
b. MIC gel CHP-20P MeOH/H₂O)
c. YMC gel ODS-A (MeOH/H₂O)
d. GPC gel HPLC (100% MeOH
e. silica gel (*n*-hexane/Acetone)
f. HPLC on 5C₁₈-AR-II (MeOH/H2O)

EtOAc (23.8 g)   H₂O (43.5 g)

a   partit between *n*-BuOH/H₂O

Fr. 2   *n*-BuOH (64.6 g)   H₂O (43.5 g)   Insoluble (12.9 g)

b

Fr. 2.2   Fr. 2.6

c   e
d   b
e

Fr. 2.2.3   Fr. 2.2.5   77   78
                        (38.8 mg)   (8.7 mg)

f   f

80   81   82   79
(2.1 mg)   (7.2 mg)   (1.7 mg)   (26.6 mg)

Scheme 9.2. Isolation scheme for the aerial parts of *M. cochinchinensis*.

Acknowledgments

March 2020

Xue-Rong Yang

References

[1] Wangchuk, P. *J. Biol. Active Prod. Nat.* **2018**, *8*, 1−20.

[2] Li, J.; Sang, Z. *World J. Acup. Moxi.* **2017**, *27*, 21−56.

[3] Jung, B.; Bae, S.; Kim, S. *Evid. Based Complement Alternat. Med.* **2017**, *2017*, 2038095.

[4] Weathers, J.P.; Towler, M.; Hassanali, A.; Lutgen P.; Engeu, O.P. *World J. Pharmacol.* **2014**, *4*, 39−55.

[5] Liu, W. X.; Liu, Y. *Cardiovasc. Diagn. Ther.* **2016**, *6*, 1−2.

[6] Moskaleva, V. E.; Goncharova, E. V. *Rastitel'nye Resursy* **1969**, *5*, 286−293.

[7] Odaguchi, H.; Hyuga, S.; Sekine, M.; Nakamori, S.; Takemoto, H.; Huang, X.; Oshima, N.; Shimada, N.; Yang, J.; Amakura, Y.; Hyuga, M.; Uchiyama, N.; Kobayashi, Y.; Hakamatsuka, T.; Goda, Y.; Hanawa, T. *Yakugaku Zasshi* **2019**, *139*, 1417−1425.

[8] Amin, A.; Gali-Muhtasib, H.; Ocker, M.; Schneider-Stock, R. *Int. J. Biomed. Sci.* **2009**, *5*, 1−11.

[9] Gong, D. H.; Zheng, W.H.; Luo, N.; Tang, G. C. *Chin. J. Chin. Pharmacol. Ther*. **2014**, *19*, 743−746.

[10] Wani, M. C.; Horwitz, S.B. *Anticancer Drug.* **2014**, *25*, 482−487.

[11] Phillipson, J. D. *Phytochemistry* **2001**, *56*, 237−243.

[12] Qin, H. N.; Liu, Y. *A checklist of vascular plants of Guangxi* **2010**, 625.

[13] Hong, L.; Guo, Z.; Huang, K.; Wei, S. J.; Liu, B.; Meng, S. W. *J. Ethnobiol. Ethnomed.* **2015**, *11*, 32.

[14] Miao, J. H. *J. Guangxi Acad. Sci.* **2007**, *23*, 113−116.

[15] Lin, C. R.; Lu, Z. C.; Liu, J. Huang, Y. S.; Xu, W. B.; Liu, Y. *Mod. Chin. Med.* **2016**, *6*, 730−736.

[16] Lin, C. R.; Liu, Y.; Xu, W. B.; Liang, Y.Y. *Lishizhen Med. Mater. Med. Res.* **2010**, *21*, 3286−3288.

[17] Qi, S. H.; Wu, D. G.; Chen, L.; Ma, Y. B.; Luo, X. D. *J. Agric. Food Chem.* **2003**, *51*, 6949−6952.

[18] Yan, Y.; Zhang, J. X.; Huang, T.; Mao, X. Y.; Gu, W.; He, H. P.; Di, Y. T.; Li, S. L.; Chen, D. Z.; Zhang, Y. Hao, X. J. *J. Nat. Prod.* **2015**, *78*, 811−821.

[19] Ge, Y. H.; Zhang, J. X.; Mu, S. Z.; Chen, Y.; Yan, F. M. Lű, Y.; Hao, X. J. *Tetrahedron* **2012**, *68*, 566−572.

[20] Li, X. L.; He, Q. X.; Zhang, F. L.; Zhao, Y. L.; Liu, K. C.; Jiang, S. P. *Nat. Prod. Bioprospect.* **2012**, 76−80.

[21] Zhang, H. P.; Bao, G. H.; Wang, H. B.; Qin, G. W. *Nat. Prod. Res.* **2004**, *18*, 415–419.

[22] Yan, Y.; Yuan, C.M.; Di, Y. T.; Huang, T.; Fan, Y. M.; Ma, Y.; Zhang, J. X.; Hao, X. J. *Fitoterapia* **2015**, *107*, 29–35.

[23] Yan, Y.; Tang, L.; Hu, J.; Wang, J.; Adelakun, T. A.; Yang, D.; Di, Y.; Zhang, Y.; Hao, X. J. *Pestic. Biochem. Physiol.* **2018**, *146*, 13–18.

[24] Abdelgaleil, S. A. M.; Iwagawa, T.; Doe, M.; Nakatani, M. *Fitoterapia* **2004**, *75*, 566–572.

[25] Qi, S. H.; Chen, L.; Wu, D. G.; Ma, Y. B.; Luo, X. D. *Tetrahedron* **2003**, *59*, 4193–4199.

[26] Huang, M. H.; Zhang, Y. M.; Li, J.; Shao, F.; Yang, M.; Zhang, P. Z. *Chin. Tradit. Herbal Drugs* **2017**, *48*, 1240–1249.

[27] Ge, Y. H.; Liu, K. X.; Zhang, J. X.; Mu, S. Z.; Hao, X. J.; *J. Agric. Food Chem.* **2012**, *60*, 4289–4295.

[28] Kenmoku, H.; Tanaka, M.; Ogiyama, K.; Kato, N.; Sassa, T. *Biosci. Biotechnol. Biochem.* **2004**, 68, 1574–1577.

[29] Zdero, C.; Bohlmann, F.; Niemeyer, H. M. *Phytochemistry* **1990**, *29*, 326–329.

[30] Govindachari, T. R.; Kumari, G. N.; Krishna, S. G. *Phytochemistry* **1995**, *39*, 167–170.

[31] Mitsui, K.; Saito, H.; Yamamura, R.; Fukaya, H.; Hitotsuyanagi, Y.; Takeya, K. *Chem. Pharm. Bull.* **2007**, *55*, 1442–1447.

[32] Sherman, M. M.; Borris, R. P.; Ogura, M.; Cordell, G. A.; Farnsworth, N. R. *Phytochemistry* **1980**, *19*, 1499–1501.

[33]. Tinto, Winston F.; Jagessar, P. K.; Ketwaru, P.; Reynolds, W. F.; McLean, S. *J. Nat. Prod.* **1991**, *54*, 972–977.

[34] Katsui, N.; Matsue, H.; Hirata, T.; Masamune, T. *Bull. Chem. Soc. Jpn.* **1972**, *45*, 223–226.

[35] Gunatilaka, A. A. L.; Gopichand, Y.; Schmitz, F. J.; Djerassi, C. *J. Org. Chem.* **1981**, 46, 3860–3866.

[36] Chaudhuri, P. *Phytochemistry* **1987**, *26*, 3361–3362.

[37] Zhu, G. Y.; Chen, G.; Liu, L.; Bai, L. P.; Jiang, Z. H. *J. Nat. Prod.* **2014**, *77*, 983–989.

[38] Li, J. H.; Li, Y.; An, F. L.; Zhou, M. M. Luo, J.; Jian, K. L.; Luo, J.; Kong, L.Y. *Tetrahedron* **2016**, *72*, 7481–7487.

[39] Zhang, M. L.; Liu, D.; Fan, G. Q.; Wang, R. X.; Lu, X. H.; Gu, Y. C.; Shi, Q. W. *Heterocycl. Commun.* **2016**, *22*, 175–220.

[40] Radice, M.; Tasambay, A.; Perez, A.; Dieguez, S. K.; Sacchetti, G.; Buso, P.; Buzzi, R.; Vertuani, S.; Manfredini, S.; Baldisserotto, A. *J. Ethnopharmacol.* **2019**, *244*, 111932.

[41] Li, Y.; Zhang, D. M.; Li, J. B.; Yu, S. S.; Li, Y.; Luo, Y.M. *J. Nat. Prod.* **2006**, *69*, 616–620.

[42] Feng, S.; Xu, L.; Wu, M.; Hao, J.; Qiu, S. X.; Wei, X. *Fitoterapia* **2010**, *81*, 472–474.

[43] Hu, X. R.; Yang, J. S.; Xu, X. D.; *Chem. Pharm. Bull.* **2009**, *57*, 418–420.

[44] Wu, H.; Hu, X.; hang, X.; Chen, S.; Yang, J.; Xu, X. *Molecules* **2012**, *17*, 5212–5218.

[45] He, X. F.; Yin, S.; Ji, Y. C.; Su, Z. S.; Geng, M. Y.; Yue, J. M. *J. Nat. Prod.* **2010**, *73*, 45–50.

[46] Huang, M.; Zeng, G.; Tan, J.; Li, Y.; Tan, G.; Zhou, Y. *Zhongguo Zhongyao Zazhi* **2008**, *33*, 1700–1702.

[47] Wang, P.; Luo, J.; Zhang, Y. M.; Kong, L. Y. *Tetrahedron* **2015,** *71*, 5362–5370.

[48] Ni, G.; Zhang, H.; Liu, H. C.; Yang, S. P.; Geng, M. Y.; Yue, J. M. *Tetrahedron* **2013**, *69*, 564–569.

[49] Wang, P.; Li, R. J.; Liu, R. H.; Jian, K. L.; Yang, M. H.; Yang, L.; Kong, L. Y.; Luo, J. *Org. Lett.* **2016**, *18*, 832−835.

[50] Uchida, M.; Kusano, G.; Kondo, Y.; Nozoe, S.; Takemoto, T. *Heterocycles* **1978**, *9*, 139–144.

[51] Okamura, H.; Iwagawa, T., Nakatani, M. *Bull. Chem. Soc. Jpn*. **1995**, *68*, 3465–3467.

[52] Zhang, M.; Wang, J. S.; Wang, P. R.; Oyama, M.; Luo, J.; Ito, T.; Iinuma, M.; Kong, L.Y. *Fitoterapia* **2012**, *83*, 1604–1609.

[53] Zhu, L. P.; Li Y.; Yang J. Z.; Zuo, L.; Zhang, D. M. *J. Asian Nat. Prod. Res.* **2008**, *10*, 541–545.

[54] Tahara, S.; Fukushi, Y.; Kawabata, J.; Mizutani, J. *Agric. Biol. Chem.* **1981**, *45*, 1511–1512.

[55] Fang, P. L.; Liu, H. Y.; Zhong, H. M. *Chin. J. nat. med.* **2012**, *10*, 24–27.

[56] Kawabata, J.; Mizutani, J. *Phytochemistry* **1992**, *31*, 1293–1296

[57] Yang, S. P.; Gao, Z. B.; Wu, Y.; Hu, G. Y.; Yue, J. M. *Tetrahedron* **2008**, *64,* 2027–2034.

[58] Zhang, S.; Yang, S. P.; Yuan, T.; Lin, B. D.; Wu, Y.; Yue, J. M. *Tetrahedron Lett.* **2010**, *51*, 764–766.

[59] Kawabata, J.; Fukushi, E.; Mizutani, J. *Phytochemistry* **1995**, *39*, 121–125.

[60] Kim, S. Y.; Kashiwada, Y.; Kawazoe, K.; Murakami, K.; Sun, H. D.; Li, S. L.; Takaishi, Yoshihisa. *Tetrahedron Lett.* **2009**, *50*, 6032–6035.

[61] Li, C. J.; Zhang, D. M.; Luo, Y. M.; Yu, S. S.; Li, Y.; Lu, Y. *Phytochemistry* **2008**, *69*, 2867–2874.

[62] Ran, X. H.; Teng, F.; Chen, C. X.; Wei, G.; Hao, X. J.; Liu, H. Y. *J. Nat. Prod.* **2010**, *73*, 972–975.

[63] Yang, S. P.; Yue, J. M. *Tetrahedron Lett.* **2006**, *47*, 1129–1132.

[64] Acebey, L.; Sauvain, M.; Beck, S.; Moulis, C.; Gimenez, A.; Jullian, V. *Org. Lett.* **2007**, *9*, 4693–4696.

[65] Yuan, C. C.; Du, B.; Yang, L., Liu, Bo. *J. Am. Chem. Soc.* **2013**, *135*, 9291–9294.

[66] Popescu, R.; Kopp, B. *J. Ethnopharmacol.* **2013**, *147*, 42–62.

[67] Cai, Y. Q.; Hu, J. H.; Qin, J.; Sun, T.; Li, X. L. *Chin. J. nat. med.* **2018**, *16*, 401–410.

[68] Zhi, X.; Xiao, L.; Liang, S.; Yi, F.; Ruan, K. F. J. *Chem. Nat. Compd.* **2013**, *49*, 454–456.

[69] Wang, S.; Lin, S.; Zhu, C.; Yang, Y.; Li, S.; Zhang, J.; Chen, X.; Shi, J. *Org. Lett.* **2010**, *12*, 1560–1563.

[70] Zhou, J.; Liu, J.; Dang, T.; Zhou, H.; Zhang, H.; Yao, G. *Org. Lett.* **2018**, *20*, 2063–2066.

[71] Li, Y.; Liu, Y.B.; Liu, Y. L.; Wang, C.; Wu, L. Q.; Li, L.; Ma, S. G.; Qu, J.; Yu, S.S. *Org. Lett.* **2014**, *16*, 4320–4323.

[72] Li, Y.; Liu, Y. B.; Zhang, J. J.; Li, Y. H.; Jiang, J. D.; Yu, S. S.; Ma, S. G.; Qu, J.; Lv, H. N. *Org. Lett.* **2013**, *15*, 3074–3077.

[73] Zhou, J.; Sun, N.; Zhang, H.; Zheng, G.; Liu, J.; Yao, G. *Org. Lett.* **2017**, *19*, 5352–5355.

[74] Zhou, J.; Zhan, G.; Zhang, H.; Zhang, Q.; Li, Y.; Xue, Y.; Yao, G. *Org. Lett.* **2017**, *19*, 3935–3938.

[75] Hikino, H.; Ito, K.; Ohta, T.; Takemoto, T. *Chem. Pharm. Bull.* **1969**, *17*, 1078–1079.

[76] Li, C.; Wang, L. Q; Chen, S. N; Qin, G. W. *J. Nat. Prod.* **2000**, *63*, 1214–1217.

[77] Chen, S. N.; Zhang, H. P.; Wang, L. Q.; Bao, G. H.; Qin, G. W. *J. Nat. Prod.* **2004**, *67*, 1903–1906.

[78] Zhou, S. Z.; Yao, S.; Tang, C. P.; Ke C. Q.; Li, L.; Lin, G.; Ye, Y. *J. Nat. Prod.* **2014**, *77*, 1185–1192.

[79] Sakakibara, J.; Shirai, N.; Kaiya, T.; Nakata, H. *Phytochemistry* **1979**, *18*, 135–137.

[80] Kashiwada, Y.; *Chem. Pharm. Bull.* **1990**, *38*, 888–893.

[81] Saleh, N. A. M.; Bohm, B. A.; Ornduff, R. *Phytochemistry* **1971**, *10*, 611–614.

[82] Miyajima, S.; Takei, S. *Nippon Nogei Kagaku Kaishi* **1936**, *12*, 497–502.

[83] Liu, Y. Q.; Kong, L. Y. *Chin. Trad. Herb. Drug.* **2009**, *40*, 199–201.

[84] Ezaki, F. E.; Nonaka, G.; Nishioka, I.; Hayashi, K. *Agric. Biol. Chem.* **1986**, *50*, 2061–2067.

[85] Kamiya, K.; Watanabe, C.; Endang, H.; Umar, M.; Satake, T. *Chem. Pharm. Bull.* **2001**, *49*, 551–557.

[86] Murakami, C.; Myoga, K.; Kasai, R.; Ohtani, K.; Kurokawa, T.; Ishibashi, S.; Dayrit, F.; Padolina, W. G.; Yamasaki, K. *Chem. Pharm. Bull.* **1993**, *41*, 2129–2131.

[87] Boiteau, P.; Buzas, A.; Lederer, E.; Polonsky, J. *Bull. Soc. Chim. Biol.* **1949**, *31*, 46–51.

[88] Ogura, M.; Cordell, G. A.; Farnsworth, N.R. *Phytochemistry* **1977**, *16*, 286–287.

[89] Kim, M. R.; Lee, H. H.; Hahm, K. S.; Moon, Y. H.; Woo, E. R. *Arch. Pharmacal. Res.* **2004**, *27*, 283–286.

[90] Ontsi, D.; Sondengam, B. L.; Ayafor, J.F. *J. Nat. Prod.* **1989**, *52*, 52–56.

[91] Liao, C. R.; Kuo, Y. H.; Wang, C. Y.; Yang, C. S.; Chang, Y. S.; Ho, Y. L.; Lin, C. W. *Molecules* **2014**, *19*, 9515–9534.

[92] Numata, A.; Yang, P.; Takahashi, C.; Fujiki, R.; Nabae, M.; Fujita, E. *Chem. Pharm. Bull.*

1989, *37*, 648–651.

[93] Tanaka, T.; Nakashima, T.; Ueda, T.; Tomii, K.; Kouno, I. *Chem. Pharmaceut. Bull.* **2007**, *55*, 899–901.

[94] Ravindranath, N.; Ravinder, R. M.; Ramesh, C.; Ramu, R.; Prabhakar, A.; Jagadeesh, B.; Das, B. *Chem. Pharm. Bull.* **2004**, *52*, 608–611.

[95] Yi, X.; Liu, J. X.; Wang, P. D.; Hu, M. Y.; Zhong, G. H. *Arch. Insect. Biochem. Physiol.* **2014**, *86*, 122–136.

[96] Zhong, G.; Hu, M.; Lin, J. T.; Liu, H. M.; Xie, J. J.; Liu, J. X. *Huazhong Nongye Daxue Xuebao* **2004**, *23*, 620–625.

[97] Zhong, G. H.; Hu, M. Y.; Wei, X. Y.; Weng, Q. F.; Xie, J. J.; Liu, J. X.; Wang, W. X. *J. Nat. Prod.* **2005**, *68*, 924–926.

[98] Mao, X.; Wu, L. F.; Guo, H. L.; Chen, W. J.; Cui, Y. P.; Qi, Q.; Li, S.; Liang, W. Y.; Yang, G. H.; Shao, Y. Y.; Zhu, D.; She, G. M.; You, Y.; Zhang, L. Z. *Evid. Based. Complement. Alternat. Med.* **2016**, *2016*, 7584952.

[99] Ahmed, B.; Verma, A. *Natural Products: An Indian Journal* **2008**, *4*, 5–21.

[100] Calixto, J.; Santos, A; Filho, V; Yunes, R.; *Med. Res. Rev.* **1998**, *18*, 225–258.

[101] Ahmed, B, Verma, A. *Nat. Prod. Ind. J.* **2008**, *4*, 5–21.

[102] Wei, W. X.; Pan Y. J.; Chen, Y. Z.; Lin, C. W.; Wei T. Y.; Zhao, S. K. *Chem. Nat. Compd.* **2005**, *41*, 17–21.

[103] Fan, Y. Y.; Gan, L. S.; Liu, H. C.; Li, H.; Xu, C. H.; Zuo, J. P.; Ding, J.; Yue, J. M.; *Org. Lett.* **2017**, *19*, 4580–4583.

[104] Zhao, J. Q.; Wang, Y. M.; He, H. P.; Li, S. H.; Li, X. N.; Yang, C. R.; Wang, D.; Zhu, H. T.; Xu, M.; Zhang Y. J. *Org. Lett.* **2013**, *15*, 2414–2417.

[105] Fan, Y. Y.; Zhang, H.; Zhou, Y.; Liu, H. B.; Tang, W.; Zhou, B.; Zuo, J. P.; Yue, J. M. *J. Am. Chem. Soc.* **2015**, *137*, 138–141.

[106] Ratnayake, R.; Covell, D.; Ransom, T. T.; Gustafson, K. R.; Beutler, J. A. *Org. Lett.* **2008**, *11*, 57–60.

[107] Lim, Y. C.; Rajabalaya, R.; David, S. R. *Phcog. Rev.* **2017**, *11*, 153–157.

[108] Kunwar, R. M.; Adhikari, N.; Devkota, M.P. *Nepal J. Online.* **2005**, *15*, 38–42.

[109] Lu, G. T.; Lu, W. J.; Chen, J. Y.; Tan, X.; Huang, J. Y.; Huang, Z. F. *Chin. J. Exp. Med. Formul.* **2015**, *21*, 44–46.

[110] Wang, Q.; Li, L. Q.; Li, M. R. *Chin. Tradit. Herb. Drug.* **1996**, *09*, 18–21.

[111] Guerriero, A.; Pietra, F. *Phytochemistry* **1984**, *23*, 2394–2396.

[112] Kato, N.; Inada, M.; Sato, H.; Miyatake, R.; Kumagai, T.; Ueda, M. *Tetrahedron* **2006**, *62*, 7307–7318.

[113] Zaman, M. K. *J. Saudi Chem. Soc.* **2005**, *9*, 161−169.

[114] Anerji, A.; Das, R. *Indian J. Chem.* **1975**, *13*, 1234−1236.

[115] Shen, C. C.; Ni, C. L.; Huang, Y. L.; Huang, R. L.; Chen, C. C. *J. Nat. Prod.* **2004**, *67*, 1947−1949.

[116] Uemura, D.; Nobuhara, K.; Nakayama, Y.; Shizuri, Y.; Hirata, Y. *Tetrahedron Lett.* **1976**, *50*, 4593−4596.

[117] Yasue, M.; Kato, Y. *Yakugaku Zasshi* **1960**, *80*, 1013−1014.

[118] Muto, N.; *Biosci. Biotechnol. Biochem.* **2008**, *72*, 477−484.

[119] Moujir, L. M.; Seca, A. M. L.; Araujo, L.; Silva A. M. S. Barreto, M. *Fitoterapia* **2011**, *82*, 225−229.

[120] Pan, S. M.; *Chin. Pharm. J.* **2006**, *58*, 35−40.

[121] Nguyen, T. H.; Chau, N. T. T.; Castanet, A. S.; Nguyen, K. P. P.; Mortier, J. *J. Org. Chem.* **2007**, *72*, 3419−3429.

[122] Santucci, L. *J. Am. Chem. Soc.* **1958**, *80*, 4537−4539.

[123] McNulty, J.; Poloczek, J.; Larichev, V.; Werstiuk, N. H.; Griffin, C.; Pandey, S. *Planta Med.* **2007**, *73*, 1543−1547.

[124] Rezende, K. C. S.; Lucarini, R.; Simaro, G. V.; Pauletti, P. M.; Januario, A. H.; Esperandim, V. R.; Martins, C. H. G.; Silva, Mi. A.; Cunha, W. R.; Bastos, J. K. *Rev. bras. farmacogn.* **2016**, *26*, 296−303.

[125] Frisch, M. J.; Trucks, G. W.; Schlegel, H. B. Gausian 09, Revision C. 01. Wallingford, CT: Gaussian; **2010**.

[126] Schaumloffel, T.; Hemberger, A.; Bringmann, Y. SpecDis Version 1.61. Germany: University of Wuerzburg; **2013**.